Characterisation of Enaptin and Sun1, two novel mammalian nuclear envelope proteins

INAUGURAL-DISSERTATION
zur
Erlangung des Doktorgrades
der Mathematisch-Naturwissenschaftlichen Fakultät
der Universität zü Köln

vorgelegt von
Padmakumar Velayuthan Chellammal
aus
Peruvilai, Indien

Köln, 2004

Referees/Berichterstatter: Prof. Dr. Angelika A. Noegel
Prof. Dr. Karin Schnetz

Date of oral examination: 02.07.2004
Tag der mündlichen Prüfung

The present research work was carried out under the supervision of Prof. Dr. Angelika A. Noegel, in the Institute of Biochemistry I, Medical Faculty, University of Cologne, Cologne, Germany. From August 2001 to July 2004.

Diese Arbeit wurde von August 2001 bis Juli 2004 am Biochemischen Institut I der Medizinischen Fakultät der Universität zu Köln unter der Leitung von Prof. Dr. Angelika A. Noegel durchgeführt.

To my parents

Acknowledgements

First of all, I would like to express my heartiest gratitude to Prof.Dr.Noegel for giving me an opportunity to work in her group with Enaptin. Her positive attitude, constant encouragement and sustained interest in my project proved essential for my successful PhD work.

I would like to thank Dr.Iakowos Karakesisoglou (Akis), our group leader for the excellent advice with my work, plentiful of encouragement and lots of motivation. He offered a hospitable environment in the lab with his friendly mannerisms and of course not to forget his sense of humour.

I would also like to thank Dr.Elena Korenbaum with whom I started my PhD in the first year. It was a wonderful first year with her.

It would be unfair if I don't convey my thanks to Dr.Franciso Rivero, who helped me learn Confocal Microscopy and not the least, Spanish (all bad words).

I would also like to thank Jan Melichar and Martina Munck who helped me in the beginning with the administrative work and special thanks to Martina for teaching me many laboratory techniques, Cell Cuture to name one.

I would also like to thank Bettina Lauss, our secretary who made our life in Köln easy with her excellent administrative skills and promptness and Budi, our system administrator to lend his helping hand whenever I had a problem with my computer.

I would like to acknowledge my father, Velayuthan and mother, Chellammal who made enough sacrifices for me to be here today and also bear to be away from me for a long time.

It would be appropriate to note that it can't be coincidental that the majority of successes in my PhD and my friendship with Yogi came in the final year.

My former and current lab mates, Thorsten Olski, who helped me understand more about the culture of the city of cologne, Sabu Abraham, who provided a pleasant and humorous atmosphere in the lab and whose friendship is invaluable, Thorsten Libotte and Hafida Zaim made my three years in the lab totally unforgettable. I would also like to convey my

special thanks to Wenschu Lu, who helped me in the Cell Culture with my knock-in experiments.

I would like to let Dhamu, Sunil, Bharathi, Soraya, Henning, Hameeda, Deen, Maria M, Michael, Sonia, Maria S, Rosi, Nandhu, Christoph, Berthold, Kathrin, Alex, Jessica, Patrick, Vasily, Carola and all the other members of the lab know that I am simply happy and privileged to have been one among all of you.

I would also like to take this opportunity to thank Dr.R. Schröder, University hospital, Bonn for provoding me muscle section, Dr.Karin Niessen for giving $\propto_6\beta_4$ antibody, Dr.Mauch, Department of Dermatology, University of Cologne for offering me human skin sections, Dr. Josef Gotzmann, Biocenter, Vienna for giving Sun1 antibodies.

TABLE OF CONTENTS

1 Introduction

1.1 The cytoskeleton 1

1.2 The actin cytoskleleton 1

1.3 Actin binding proteins 2

1.4 Actin binding proteins related diseases 3

1.5 The nucleus and the nuclear envelope 4

1.6 Proteins of the nuclear envelope 6

1.7 Actin binding proteins in the nucleus and nuclear membrane 8

1.8 Nuclear migration and the involvement of actin binding proteins 9

1.9 Aim of the work 10

2 Materials and Methods

2.1 Materials

2.1.1 Enzymes, inhibitors and antibodies 12

2.1.2 Reagents 13

2.1.3 Kits 14

2.1.4 Bacterial host strains 15

2.1.5 Eukaryotic cells 15

2.1.6 Vectors 15

2.1.7 Oligonucleotides 15

2.1.8 Buffers and other solutions 16

2.1.9 Materials 17

2.1.10 Instruments 17

2.1.11 Computer programs 18

2.2 Molecular biological methods

2.2.1 Plasmid-DNA isolation from *E. coli* by alkaline lysis miniprep 18

2.2.2 Plasmid-DNA isolation with a kit from Macherey-Nagel 19

2.2.3 DNA agarose gel electrophoresis 19

2.2.4 Isolation of total RNA from mouse tissue with RNeasy mini/

midi kit 20
2.2.5 RNA agarose gel electrophoresis and northern blotting 20
2.2.6 Labelling of DNA probes 20
2.2.7 Hybridisation of labelled probes 21
2.2.8 Elution of DNA fragments from agarose gels 21
2.2.9 Measurement of DNA and RNA concentrations 21
2.2.10 Restriction digestion of DNA 21
2.2.11 Dephosphorylation of 5'-ends of linearised vectors 22
2.2.12 Creation of blunt ends 22
2.2.13 Ligation of vector and DNA-fragments 22
2.2.14 Polymerase chain reaction 22
2.2.15 Transformation of E.Coli cells with plasmid DNA 23
2.2.16 Correction of deletion in enaptin-165 by site directed mutagenesis 23
2.3 Protein methods and immunofluorescence
2.3.1 Cloning of GFP fusion protein and yeast two hybrid cloning 24
2.3.2 Expression and purification of recombinant 6x-His tag protein 24
2.3.2.1 Expression 24
2.3.2.2 Purification by affinity chromatography 25
2.3.3 Affinity purification of polyclonal antibody 25
2.3.4 Extraction of protein homogenates from mouse tissues and cell cultures 26
2.3.5 SDS-polyacrylamide electrophoresis (SDS-PAGE) 26
2.3.6 Western blotting 27
2.3.7 Cell fractionation 28
2.3.8 Cell culture methods 28
2.3.9 Immunofluorescence 28
2.3.10 Immunohistochemical staining of formalin-fixed paraffin-embedded sections 29
2.3 Yeast two hybrid and GST pull down
2.4.1 Construction of yeast two hybrid and GST fusion proteins of Sun1 29
2.4.2 Yeast transformation 31
2.4.3 Yeast plasmid rescue 32

2.4.4 X-gal colony-lift filter assay 32
2.4.5 GST-pull down 32
2.5 Construction of GFP fusion proteins and transfection´ 33
2.6 Generation of knock in mouse
2.6.1 Target vector construction 34
2.6.2 Transfection and colony picking 35
2.6.3 Genomic DNA isolation 36
2.6.4 Southern blotting (Southern, 1975) 36
2.6.5 Labeling of DNA probes and hybridization 37

3 Results

3 Characterisation, tissue distribution and subcellular localisation of Enaptin

3.1 Analysis of the *Enaptin* gene sequence 38
3.2 Isoform diversity and domain analysis of Enaptin 38
3.3 Multiple alignment of the actin binding domain of Enaptin with other related ABDs 40
3.4 Analysis of the C-terminal transmembrane domain of Enaptin 42
3.5 Analysis of the spectrin repeats of Enaptin 42
3.6 Generation of polyclonal antibodies 43
3.7 Expression of Enaptin in various cell lines and in brain 45
3.8 Immunofluorescence studies of Enaptin in various cell lines 46
3.9 Cell fractionation studies of fibroblasts cell lysates 48
3.10 Generation of various Enaptin GFP fusion proteins 49
3.11 Enaptin localisation in mouse skeletal muscle 51
3.12 Enaptin localisation in human skin 53
3.13 Influence of cytoskeletal drugs on the subcellular distribution of Enaptin 55

4 Characterisation, localisation and functional analysis of Sun1

4.1 The perinuclear region of Enaptin is highly conserved 56
4.2 SUN domain containing proteins 56
4.3 Sequence and domain analysis of Sun1 58
4.4 The perinuclear segment of Enaptin binds to the C-terminus of Sun1 *in vivo* and the SUN domain is not required for this association 60
4.5 The perinuclear Enaptin amino acids bind to the C-terminus of Sun1 also *in vitro* 61
4.6 A full-length GFP fusion protein of Sun1 localises to the nuclear membrane 62

4.7 Endogenous Sun1 is present in the nuclear membrane in HEK cells 62
4.8 Expression profile of Sun1 in COS7 and HEK cells 63
4.9 N- and C-terminal segments of Sun1 localise independently to the nuclear membrane 64
4.10 Sun1 dimerises *in vivo* 67
4.11 The SUN domain is not required for the NE localisation of Sun1 68
4.12 Western blotting confirms the expression of all the GFP fusion proteins 71
4.13 GFP-CT+3TM behaves like a dominant negative of Sun1 and displaces endogenous Sun1, NUANCE and emerin from the nuclear membrane 72
4.14 Overexpression of GFP-CT+3TM has no effect on lamin A/C or Lap2 localisation 74
4.15 Sun1 is an inner nuclear membrane protein 75
4.16 Sun1 localises to the nuclear envelope in a lamin A/C dependent manner 77

5 Generation of a knock-in mouse expressing GFP-tagged full-length Enaptin without the transmembrane domain

5.1 Aim of the project 79
5.2 The knock out strategy 79
5.3 transfection and screening 81

6 Discussion

6.1 Enaptin, a novel NUANCE-like protein 83
6.2 Isoform diversity of *Enaptin* 84
6.3 Subcellular localisation of Enaptin 85
6.4 Tissue distribution of Enaptin 86
6.5 Sun1 is a novel nuclear envelope protein and binds to Enaptin 87
6.6 The N- and C-termini of Sun1 localise to the nuclear envelope independently 89
6.7 Sun1 is essential for the NE localisation Enaptin and NUANCE 90
6.8 Sun1 dimerises *in vivo* 90
5.9 Sun1 is an element of inner nuclear envelope and its localisation is lamin A/C dependent 91
6.10 Enaptin, NUANCE, Sun1 and laminopathies 91
6.11 A model depicting the various interactions and findings 92
6.12 A hypothetical model depicting the involvement of Enaptin, NUANCE and

Sun1 in nuclear positioning and migration 93
6.13 Future perspectives 94
Summary 96
Zusammenfassung 97
7 Bibliography 98
Erklärung
Curriculum Vitae
Lebenslauf

ABBREVIATIONS

Ade	Adenine
AD	Activating domain
AP	Alkaline phosphatase
APS	Ammonium persulphate
3-AT	3-amino 1,2,4-triazole
BD	Binding domain
BSA	Bovine serum albumin
CH	Calponin homology
DEPC	Diethylpyrocarbonate
DMSO	Dimethylsulfoxide
dNTP	Deoxyribonucleotide triphosphate
DTT	1,4-dithiothreitol
EDTA	Ethylenediaminetetraacetic acid
EGTA	Ethyleneglycol-bis (2-amino-ethylene) N,N,N,N-tetraacetic acid
FITC	Fluorescein-5-isothiocyanate
GFP	Green Fluorescence Protein
GST	Glutathione S-transferase
His	Histidine
HRP	Horse radish peroxidase
HEPES	N- (2-hydroxyethyl) piperazine-N-2-ethanesulphonic acid
IPTG	Iso-propylthio-galactopyranoside
IgG	Immunoglobulin G
Kb	Kilobase pairs
kDa	KiloDalton
Leu	Leucine
MOPS	Morpholinopropanesulphonic acid
Neo	Neomycin cassette
mRNA	messenger ribonucleic acid
mAb	Monoclonal Antibody
NP-40	Nonylphenylpolyethyleneglycol
OD	Optical density
PIPES	Piperazine-N,N.-bis(2-ethanesulphonic acid)
PMSF	Phenylmethylsulphonylfluoride
PAGE	Polyacrylamide gel electrophoresis
rpm	Rotations per minute
SDS	Sodium dodecyl sulphate
TRITC	Tetramethylrhodamine β isothiocyanate
TAE	Tris borate EDTA
Trp	Tryptophan
WT	Wild type allele
X-gal	5-bromo-4-chloro-3-indolyl-D-galactopyranoside

Introduction

1 INTRODUCTION

1.1 The Cytoskeleton

The cytoskeleton is composed mainly of three types of filaments, microfilaments, microtubules and intermediate filaments. Microfilaments are fine, thread-like protein fibers, 7-9 nm in diameter. They are composed of a protein called actin, which is the most abundant cellular protein, often accounting 10 to 20 percent of the total cytoplasmic protein content. Actin exists either as a globular monomer (called G-actin) or as a filament (designated F-actin), the latter formed by head-to-tail polymerisation of asymmetric monomers. Microfilaments in association with the protein myosin are responsible for muscle contraction. They can also carry out cellular movements including gliding, contraction, and cytokinesis.

Microtubules are cylindrical tubes, 20-25 nm in diameter. They are composed of alpha and beta tubulin. Microtubules act as a scaffold to determine cell shape and provide a set of "tracks" for cell organelles and vesicles to move on. Microtubules also form the spindle fibers for separating chromosomes during mitosis. When arranged in geometric patterns inside flagella and cilia they are used for locomotion.

The intermediate filaments average 10 nm in diameter and thus are "intermediate" in size between actin filaments (8 nm) and microtubules (25 nm). There are five major types of intermediate filaments each constructed from one or more proteins characteristic of it. Despite their chemical diversity, intermediate filaments play similar roles in the cell, providing a supporting framework within the cell. For example, in epithelia the nucleus is held within the cell by a basketlike network of cytoplasmic intermediate filaments made of proteins called keratins, whereas lamins are nuclear proteins that line the nuclear membrane. Intermediate filaments (desmin) also anchor the thick and thin filaments of muscle cells in a fixed position and provide mechanical strength to the long axons found in some neurons (neurofilaments).

1.2 The Actin Cytoskeleton

Actin is a moderate sized protein consisting of approximately 375 residues, which is encoded by a large, highly conserved gene family. Some single-celled eukaryotes like yeasts have a single actin gene, whereas most organisms contain many actin genes. For example, mammals have six distinct actin isotypes (Vandekerckhove and Weber). Each actin molecule contains a Mg^{2+} ion complexed with either ATP or ADP. Thus there are four states of actin: ATP-G-actin, ADP-G-actin, ATP-F-actin and ADP-F-actin. Two of these forms, ATP-G-actin

and ADP-F-actin predominate in a cell. The addition of ions, Mg^{2+}, K^{+} or Na^{+} to a solution of G-actin will induce the polymerisation of G-actin into actin filaments. The process is also reversible: F-actin depolymerises into G-actin when the ionic strength of the solution is lowered. All subunits in a filament point towards the same end. Consequently, at one end of the filament, by convention designated plus or barbed end, the ATP-binding cleft of an actin subunit is exposed to the surrounding solution and at the opposite end, the minus or pointed end, the cleft contacts the neighbouring actin subunit. The actin cytoskeleton is organised into bundles and networks of filaments, which are the most common arrangements of actin filaments in a cell. Functionally, bundles and networks have identical roles in a cell: both provide a framework that supports the plasma membrane and, therefore, determines a cell's shape. Structurally, bundles differ from networks mainly in the organisation of actin filaments. In bundles the actin filaments are closely packed in parallel arrays, whereas in a network the actin filaments crisscross, often at right angles, and are loosely packed. In all bundles and networks, the filaments are held together by actin cross-linking proteins. The length and flexibility of a cross-linking protein determine whether bundles or networks are formed.

1.3 Actin Binding Proteins

Actin binding proteins are classified according to their actin binding function. Actin filament severing proteins fragment filaments by mechanisms that do not require the hydrolysis of ATP. The purpose of this severing activity is probably to introduce a device whereby existing actin filament structures may be removed or remodeled to form other structures within the cell. So far, two major groups of actin severing proteins have been identified. The gelsolin group is the archetype of the group of actin binding proteins that sever and cap the fast growing barbed end of actin filaments and that initiate the polymerisation of new filaments by forming a nucleus (Yin et al., 1988; Weeds et al., 1993). The second group, the Actin depolymerising factor (ADF)/Cofilin group comprises low molecular weight actin filament severing proteins which in addition possess actin monomer binding activity.

Actin binding proteins grow by monomer addition exclusively at their ends, particularly barbed ends. Filament capping proteins like radixin (Funayama et al., 1991) and tensin (Davis et al., 1991) bind to the barbed ends of filaments in cells and are therefore essential for the control of actin polymerisation within cells or within local regions of individual cells. DNaseI (Podolski et al., 1988) and tropomodulin (Fowler et al., 1993) are actin binding proteins that bind to the pointed ends.

There is a well-documented abundance of non-filamentous actin in cells despite the intracellular conditions greatly favoring the formation of F-actin. A number of low molecular weight actin binding proteins have been identified that are thought to bind G-actin and thus directly sequester monomers from the filamentous pool. This pool of monomers is possibly drawn upon to support polymerisation when cells are stimulated, for examples by chemoattractants. Profilin (Southwick et al., 1990) is an example of an actin monomer binding protein, which has sequestering activity.

Actin bundling proteins are proteins, which are required to bundle actin filaments in two different ways. Any protein that binds actin at a site exposed on the filament, and also has the ability to self-associate, should bundle actin filaments. These proteins fall into a family sharing a common actin-binding domain (ABD) of the α-actinin type (Matsudaira, 1991). Sequence analysis revealed that these proteins share a 250-residue sequence, which can be divided into two homologous parts, each of them showing a significant similarity to the N-terminal part of the calponins, a family of proteins mainly involved in the regulation of smooth muscle contraction (Castresana & Saraste, 1995). The ABD composed of two calponin homology domains (CH domains) is found in proteins of the α-actinin superfamily with proteins such as β-spectrin, α-actinin, dystrophin, utrophin and filamin. Alternatively bundling proteins like fimbrin (T-plastin) (Namba et al., 1992) and ABP-50 (Demma et al., 1990) have two actin binding domains by which they bundle actin filaments. The monomeric bundling protein synapsin I has three actin binding sites (Südhof et al., 1989).

A distinct group of proteins is formed by the plakins, which have been shown to function as cytoskeleton linkers (Ruhrberg & Watt, 1997). These proteins are thought to crosslink the microfilaments with the microtubule and intermediate filament systems. Some of the plakins like the bullous phemphigoid antigen 1 (BPAG-1/dystonin), plectin and microtubule actin crosslinking factor (MACF) share an α-actinin type actin-binding domain at their N-terminus with the α-actinin superfamily. Plectin and BPAG-1/dystonin contain an additional intermediate-filament-binding domain (Wiche, 1998), and MACF has been shown to connect the actin cytoskeleton with the microtubule filaments (Leung *et al*., 1999).

1.4 Actin binding proteins related diseases

The critical role of actin-crosslinking proteins in maintaining cell structure and function was uncovered in studies on the Duchenne muscular dystrophy (DMD), a X-linked degenerative disorder of muscle. DMD affects about 1 in 3500 live born males. The progressive weakness of the striated muscles also leads to respiratory complications, which

mark the final stage of the disease before the end of the third decade of life (Moser, 1984). Patients with DMD have a defect in the gene encoding the actin-crosslinking protein dystrophin (Ahn & Kunkel, 1993). Dystrophin crosslinks actin filaments into a supportive cortical network and attaches this network to a glycoprotein complex in the muscle cell membrane. The membrane complex is also connected with extracellular proteins. In patients lacking a functional dystrophin, the membrane of muscle cells is not supported by cortical actin and is easily damaged by stress of repeated muscle contraction. The actin-crosslinking protein spectrin mediates important structural properties of erythrocytes to make them robust in deformation so that they can squeeze through the small capillaries and sinusoids of the spleen. In spectrin-deficient erythrocytes deformability is reduced, which results in a spherical shape, lacking the central pallor associated with the biconcave cells. Hereditary spherocytosis, elliptocytosis and pyropoikilocytosis represent a group of disorders that are due to deficiency or dysfunction of spectrin and other proteins involved in the linkage of the cytoskeleton to the plasma membrane in red blood cells (Palek, 1987). Plectin and BPAG-1/dystonin have been shown to be important in the maintenance of the cytoskeletal integrity in several cell types (Brown *et al*., 1995; Dalpe *et al*., 1998). Mutations in the mouse BPAG-1/dystonin gene are responsible for the *dystonia musculorum (dt)* mutant phenotype, which is first recognizable between 7 and 10 days after birth and displays a progressive loss of limb coordination. The *dt* mice suffer from neurological, myelination and muscle abnormalities caused by intrinsic defects in sensory neurons, Schwann cells and skeletal muscle cells, respectively (Bernier *et al*., 1998). Similarly, targeted inactivation of the plectin gene in mice resulted in lethality two to three days after birth, probably a result of severe skin blistering caused by degeneration of keratinocytes (Andrä *et al*., 1997). Mutations in human plectin cause *epidermolysis bullosa simplex* which is associated with muscular dystrophy, an epidermal blister disease which is associated with a myopathy(McLean *et al*., 1996).

1.5 The nucleus and the nuclear envelope

The nucleus is the control center and the hallmark of a eukaryotic cell. Usually the nucleus is round and is the largest organelle in the cell. It is surrounded by a membrane structure called nuclear envelope, which is similar to the cell membrane that encloses the entire cell. The nuclear envelope has a complex structure, consisting of two nuclear membranes, an underlying nuclear lamina and the nuclear pore complexes. The outer nuclear membrane is continuous with the endoplasmic reticulum, so the space between the inner and outer nuclear membranes is directly connected with the lumen of the endoplasmic reticulum.

In addition, the outer nuclear membrane is functionally similar to the membranes of the endoplasmic reticulum and has ribosomes bound to its cytoplasmic surface. In contrast, the inner nuclear membrane carries unique proteins that are specific to the nucleus.

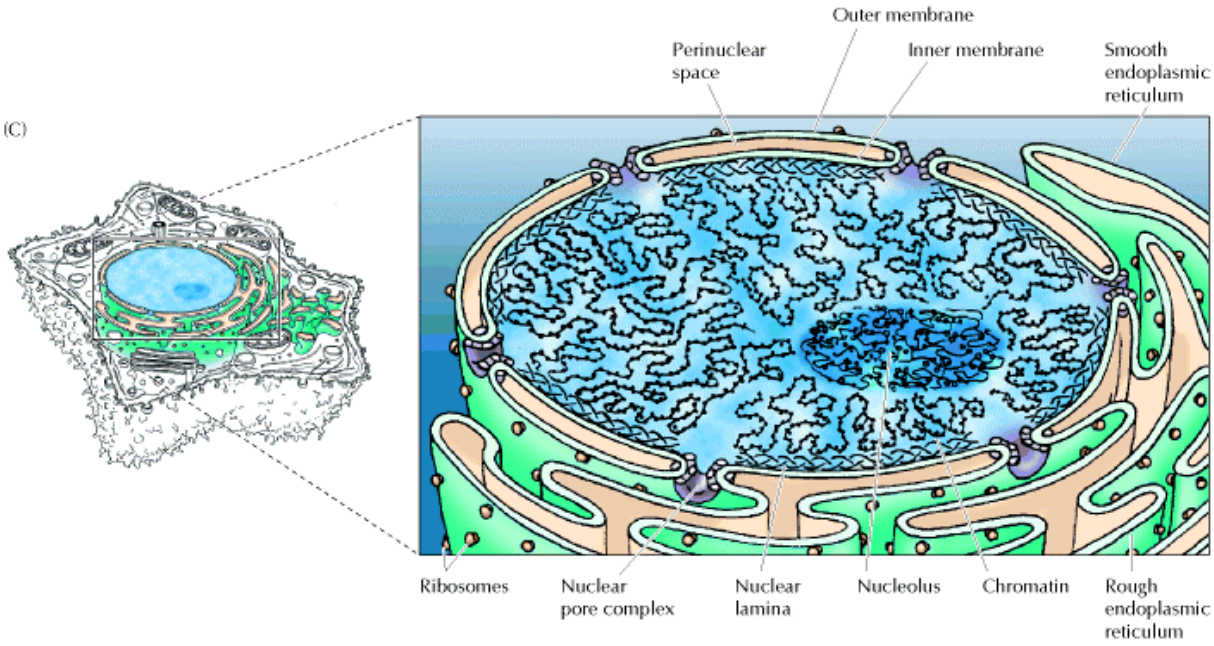

Figure 1.1: A schematic diagram of the nucleus. The picture is taken from "The Cell, A molecular approach", Geoffrey M. Cooper., Second edition.

The critical function of the nuclear membranes is to act as a barrier that separates the contents of the nucleus from the cytoplasm. Like other cell membranes, the nuclear membranes are phospholipid bilayers, which are permeable only to small nonpolar molecules. Other molecules are unable to diffuse through the phospholipid bilayer. The inner and outer nuclear membranes are joined at nuclear pore complexes, the sole channels through which small polar molecules and macromolecules are able to travel through the nuclear envelope. The nuclear pore complex is a complicated structure that is responsible for the selective traffic of proteins and RNAs between the nucleus and the cytoplasm (Figure 1.1).

A unique feature of the nucleus is that in most eukaryotic organisms it disassembles and re-forms each time the cell divides. At the beginning of mitosis, the chromosomes condense, the nucleolus disappears, and the nuclear envelope breaks down, resulting in the release of most of the contents of the nucleus into the cytoplasm. At the end of mitosis, the process is reversed: The chromosomes decondense, and the nuclear envelopes re-form around the separated sets of daughter chromosomes and eventually fuse. Nuclear envelope

breakdown (NEBD) involves the depolymerisation of the lamina, the fragmentation and removal of the nuclear membranes from the chromatin, and the disassembly of the NPCs. The lamina in metazoans is composed of the intermediate filament-like proteins, called lamins, which connect with the NPCs and inner nuclear membrane to form a network underlying the nuclear envelope and extending into the nuclear interior. Here, the lamina can help to organize chromatin into functional domains and provide structure to the nucleus (Liu et al., 2000 and Wilson et al., 2001). The lamina, and by extension, chromatin, are attached to integral inner nuclear membrane proteins which, along with the integral pore membrane proteins, define the unique composition of the nuclear membranes (Worman and Courvalin, 2000).

There is a large body of evidence that many nuclear envelope-associated proteins are reversibly phosphorylated during mitosis, concomitant with their dramatic redistribution away from the vicinity of the nucleus. Initially, it was thought that these phosphorylation events promote NEBD, leading to the dispersal of the inner nuclear membrane into a discrete population of vesicles (Vigers and Lohka, 1991), but recent work has indicated that the nuclear envelope is not fated to vesiculate. Rather, mitosis involves the redistribution of the nuclear envelope membrane proteins into the ER. Although the ER-nuclear envelope membrane system is continuous, all membrane proteins do not normally freely diffuse within it. Instead, once synthesized, inner nuclear membrane proteins diffuse from the ER through the pores to the inner nuclear membrane where they become trapped, presumably by their interactions with the lamina, chromatin, and each other (Worman and Courvalin, 2000).

1.6 Proteins of the nuclear envelope

The major structural framework at the nuclear periphery is the nuclear lamina, whose core structure is formed by type V intermediate filament proteins, the lamins (Stuurman et al., 1998). Lamins assemble into a meshwork of tetragonally organised 10-nm filaments underneath the INM. The attachment of the lamins to the membrane involves several mechanisms, and depends also on the type of lamins. B type lamins, which are constitutively expressed in all somatic cells, contain a stable C-terminal farnesyl modification, which is important but not sufficient for targeting and anchoring B-type lamins to the membrane (Moir et al., 1995). Thus, interactions of B-type lamins with integral membrane proteins must also contribute to the assembly and stable association of lamin B filaments at the membrane (Hutchison et al., 2001). The best-known binding partners for B-type lamins in the INM are the lamin B receptor (LBR) (Worman et al., 1990) and LAP2 β (Furukawa et al., 1995). LBR

contains eight transmembrane domains, and interacts with B-type lamins both in vivo and in vitro (Simos et al., 1992; Ye et al., 1994). LAP2 β is the best-characterized membrane protein of the LAP2 family, which comprises up to six alternatively spliced mammalian isoforms named LAP2∝, β, γ, δ, ε and ζ (Harris et al., 1994 and Berger et al., 1996) and three *Xenopus* LAP2 isoforms (Lang et al., 1999; Gant et al., 1999). Except for LAP2 ∝ and LAP2 ζ, all mammalian LAP2 isoforms have a closely related N-terminal nucleoplasmic domain of variable length, plus a single membrane-spanning region and a short lumenal domain at their C-terminus (Dechat et al., 2000). LAP2 β has the longest nucleoplasmic N-terminal domain (408 residues). Due to alternative messenger RNA (mRNA) splicing, LAP2 ε, δ and γ lack stretches of 40, 72 and 109 amino acids, respectively, but are otherwise identical to LAP2 β. LAP2 ζ is the smallest isoform of LAP2 β, and is missing ~ 190 residues of the nucleoplasmic domain as well as the transmembrane and lumenal regions. LAP2 ∝ is structurally and functionally a unique isoform; it shares only the N-terminal 187 residue 'constant' domain with all other LAP2 isoforms, and then contains a unique C-terminal domain of 506 residues with no transmembrane domain. LAP2 β, but not LAP2 ∝, interacts with lamin B in vitro (Foisner et al., 1993). The lamin B binding domain maps to 73 residues in the nucleoplasmic region (Furukawa et al., 1998), which are also present in the smaller isoforms LAP2 ε and δ, and are partly con-served in LAP2 γ. However, the lamin-binding activities of the smaller isoforms have not yet been demonstrated.

The most-studied A-type lamins are lamin A and its smaller splice variant, lamin C. A-type lamins are only expressed in later stages of development (Moir et al., 1995; Cohen et al., 2001). Lamin A is transiently farnesylated, and lamin C is never farnesylated. Perhaps due to their lack of fatty acid modification, lamins A and C do not associate stably with membranes during mitosis. A-type lamin structures may also be less stable during interphase, or organized differently, because ectopic expression of headless lamin mutants in mammalian cells selectively mislocalises A-type lamins into intranuclear aggregates, whereas lamin B remains unchanged (Izumi et al., 2000; Dechat et al., 2000). The incorporation of mature, non-farnesylated lamins A and C into the lamina after mitosis might depend on B-type lamins (Stuurman et al., 1998) and specific interactions with membrane proteins at the INM. Integral membrane proteins that might link A-type lamins to the INM include three LAP1 proteins (A, B and C), which are alternatively spliced products of a gene unrelated to LAP2 (Martin et al., 1995), and emerin (Manilal et al., 1996), which shares an ~40 residue domain (LEM domain) with the LAP2 isoforms (Dechat et al., 2000; Lin et al., 2000). LAP1-A, LAP1-B and emerin all bind A-type lamins in vitro (Foisner et al., 1993; Clements et al., 2000), and the

localization of LAP1-C and emerin at the INM depends on A-type lamins (Powell et al., 1990; Sullivan et al., 1999). Thus, multiple interactions between lamins and INM proteins are probably required to form a stable peripheral lamina (Figure 1.2).

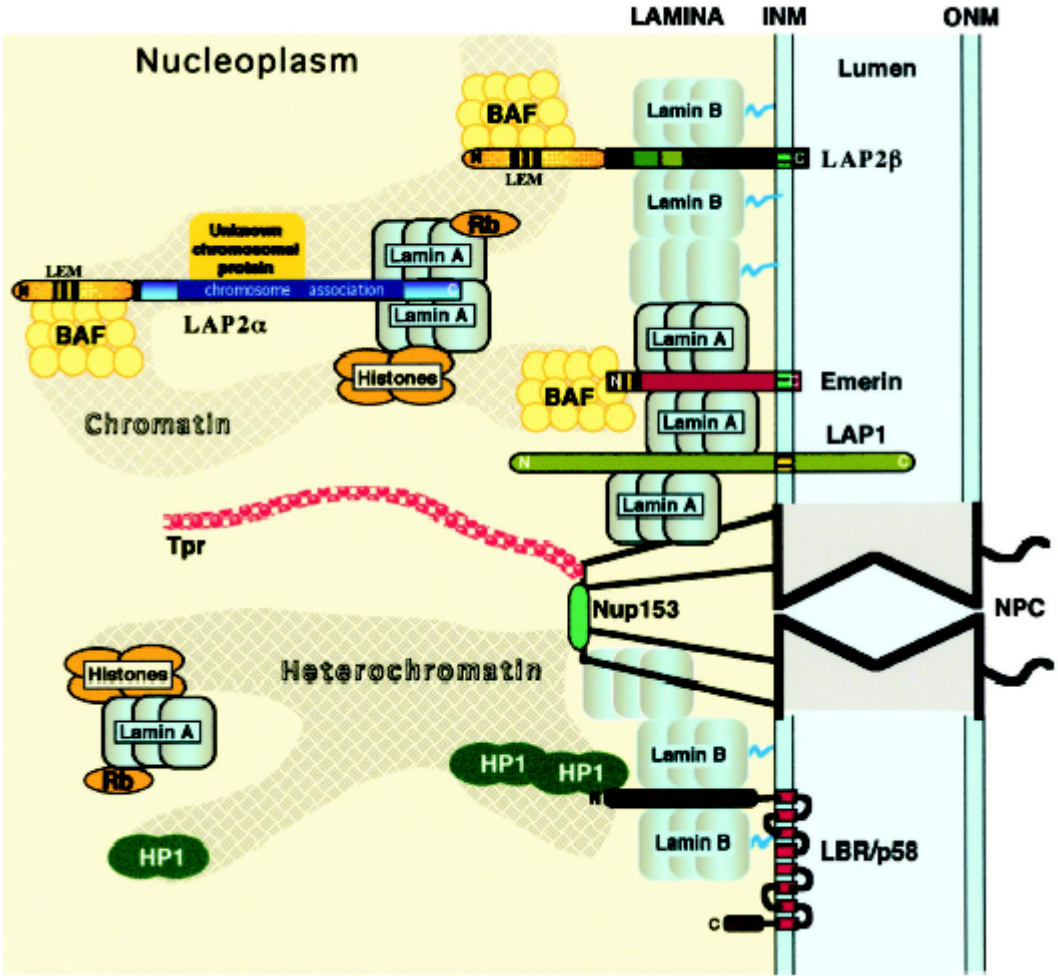

Figure 1.2: Proposed molecular interactions between components of the peripheral lamina, the nucleoskeleton and chromatin. INM, inner nuclear membrane, ONM, outer nuclear membrane and NPC, nuclear pore complex (taken from Vlcek et al., 2001).

1.7 Actin binding proteins in the nucleus and nuclear membrane

The discovery of actin and of numerous actin binding in the nucleus argues that not only is actin present in the nucleus but its polymerisation is controlled. The presence of some of the actin binding proteins in the nucleus might be irrelevant as many of them are small enough to enter the nucleus passively. Thymosin, a 5 kDa sequesterin protein and profilin, a 12 kDa actin sequestering and nucleotide exchange protein could be examples for this kind of passive diffusion into the nucleus. In the light of this objection, two types of nuclear actin binding proteins are of particular interest. The first class comprises proteins like c-Abl, a

tyrosine kinase involved in the cellular response to DNA damage, which was found to have both F- and G-actin binding domains and actin binding activity in vitro (Van Etten et al., 1994). The second class of protein comprises established actin binding proteins that are associated with the nucleus. An example of this class of proteins is the erythrocyte protein 4.1, which in red blood cells is thought to help to anchor the cytoskeleton to the membrane by promoting the interaction of spectrin with actin. In nucleated cells such as HeLa and MDCK cells, protein 4.1 has been reported as a component of the nuclear matrix (De Carcer et al., 1995; Correas et al., 1991). Spectrin has also been reported to be present in the nucleus (Bachs et al., 1990). The function of these proteins in the nucleus is not well understood, but recent data suggest that protein 4.1 plays a role in RNA splicing (Lallena et al., 1998). Recently, a giant actin binding protein of 800 kDa called NUANCE (NUcleus and ActiN Connectind Element) was found to be associated with the nuclear membrane (Zhen et al., 2002).

1.8 Nuclear migration and the involvement of actin binding proteins

The nucleus and other organelles are in fact quite dynamic. They often migrate through the cytoplasm and then occupy specific locales, often far from the center of the cell. For example, in a newly fertilized zygote, pronuclei must first migrate towards one another, and then they migrate to a species-specific location before undergoing the first mitosis. Nuclear positioning is also essential to a variety of polarized cells, such as intestinal brush-border cells and many secreting endocrine cells. In other cases, nuclear migration events reposition nuclei to distant regions of the cell. Examples include growing plant pollen tube cells (Hepler et al., 2001) and developing *C. elegans* hypodermal cells (Sulston et al., 1983). Disruption of nuclear migration in the cell bodies of the developing cerebral cortex leads to the human neurodevelopmental disease lissencephaly (Lambert de Rouvroit and Goffinet, 2001). Even in single celled organisms, such as budding and fission yeast, tight controls exist to position the nucleus correctly prior to cell division (Morris, 2000; Tran et al., 2001).

Nuclei must be carefully positioned throughout oogenesis and embryogenesis of *Drosophila*. During the cytoplasmic dumping stage of oogenesis, when the 15 nurse cells rapidly squeeze their cytoplasm into the oocyte through narrow ring canals, nuclei must remain anchored away from the ring canals. Normally, an array of striated actin bundles extends from the plasma membrane to nurse cell nuclei. These bundles shorten as dumping progresses and the nurse cells shrink (Guild et al., 1997). Mutations in the actin-monomer-binding protein profilin or in the actin-filament-bundling proteins villin and fascin disrupt

these filaments, generating free-floating nuclei (Robinson and Cooley, 1997). These mutations block oocyte development because, as cytoplasmic dumping from the nurse cells begins, nuclei become physically stuck in ring canals. A second example is the early embryonic nuclear migrations towards the periphery of the syncytial blastoderm. The actin gel-like network around migrating nuclei depolymerizes. This has been hypothesized to contribute to the force required for migration as nuclei passively `surf' the depolymerizing front (von Dassow and Schubiger, 1994).

Actin networks can also function actively to reposition nuclei. Chytilova et al. (2000) recently described a dramatic example. Actin depolymerising drugs completely abolished rapid, long-distance intracellular nuclear migration in *Arabidopsis* root hairs, whereas drugs that disrupted microtubules had no effect. Because of the speed and distance of the nuclear migrations in these cells, the actin network must be functioning actively to move nuclei, in contrast to the above examples of passive mechanisms. Budding yeast provides another example: both actin filaments and microtubules are required for proper localization of the nucleus and spindle at the bud neck to ensure normal cell division (Palmer et al., 1992; Bloom, 2001).

ANC-1 is the *C. elegans* orthologue of the mammalian Enaptin, NUANCE proteins and mutations in *anc-1* (nuclear anchorage defective) disrupt the positioning of nuclei and mitochondria in *Caenorhabditis elegans* (Starr et al., 2001). NUANCE is a huge human spectrin repeat containing protein having a functional ABD at its N-terminus and a single transmembrane domain at its C-terminus and is localised to the nuclear envelope (Zhen et al., 2000).

1.9 Aim of the work

The presence of Enaptin-165 and CPG2 (Nedivi et al., 1996), which are highly homologous to the N-terminus of NUANCE and are homologous to human Nesprin-1α, human Nesprin-1β, mouse Syne-1A, Syne-1B and human Myne-1 (Apel et al., 2000; Mislow et al., 2000; Zhang et al., 2000) which themselves are highly homologous to the C-terminus of NUANCE (Zhen et al., 2002) signalled the possible existence of *Enaptin* being a larger gene like *NUANCE*, with Enaptin-165, CPG2, Syne-1A, Syne-1B, Myne-1 and Nesprins being short alternatively spliced isoforms. To address this issue, antibodies for the ABD of Enaptin should be generated and used for immunofluorescence experiments to study the presence of Enaptin at the nuclear envelope in western blots and to detect the biggest transcript of Enaptin. The

antibodies will also be used to follow the distribution of Enaptin in various tissues. Yeast two hybrid and GST-pull down experiments will be used to study the binding partners of Enaptin especially to the evolutionally conserved regions like the region after the transmembrane domain. Mouse knock out targeting the transmembrane domain of Enaptin will be carried out to study the role of Enaptin in muscular dystrophy given the fact that Enaptin was shown to lamin A/C (Mislow et al., 2002), mutations in lamin A/C is known to cause muscular dystrophy.

Materials and Methods

MATERIALS AND METHODS

2.1 Materials

2.1.1 Enzymes, inhibitors and antibodies

Enzymes for molecular biology

alkaline phosphatase	Roche
DNase I (Desoxyribonuclease)	Sigma
lysozyme	Sigma
M-MLV reverse transcriptase	Promega
restriction endonucleases	Life Technologies
ribonuclease A	Sigma
T4-DNA-ligase	Life Technologies
Taq-DNA-polymerase	Roche

Antibodies

primary antibodies:

mouse-anti-α-actinin	Sigma
mouse-anti-desmin	Sigma
mouse-anti-skeletal (Fast) myosin	Sigma
mouse-anti-lamin A/C	CHEMICON
mouse-anti-emerin	NOVO Castra
mouse-anti-LAP2	Transduction
rabbit-anti-PDI	Stressgen

secondary antibodies:

goat-anti-mouse-IgG, peroxidase-conjugated	Sigma
goat-anti-mouse-IgG, Cy3-conjugated	Sigma
goat-anti-mouse-IgG, alkaline phosphatase conjugated	Sigma
goat-anti-mouse-IgG, Alexa 488 conjugated	Molecular Probes
goat-anti-rabbit-IgG,Alexa 568 conjugated	Molecular Probes

Inhibitors

benzamidine	Sigma
DEPC (Diethylpyrocarbonate)	Sigma
PMSF (Phenylmethylsulfonylfluoride)	Sigma
ribonuclease-inhibitor (RNAsin)	Promega
Complete Inhibitor-Cocktail	Roche

Antibiotics

ampicillin	Grünenthal
kanamycin	Biochrom
penicillin/streptomycin	Biochrom

2.1.2 Reagents

acrylamide	National Diagnostics
agarose (electrophoresis grade)	Life Technologies
acetone	Riedel-de-Haen
Bacto-Agar, Bacto-Pepton, Bacto-Trypton	Difco
BSA (bovine serum albumin)	Roth
chloroform	Riedel-de-Haen
calcium chloride	Sigma
Coomassie-brilliant-blue R 250	Serva
p-cumaric acid	Fluka
DMEM (Dulbecco´s Modified Eagle´s Medium)	Biochrom
DMF (dimethylformamide)	Riedel-de Haen
DMSO (dimethyl sulfoxide)	Merck
DTT (1,4-dithiothreitol)	Gerbu
EDTA ([ethylenedinitrilo]tetraacetic acid)	Merck
EGTA (ethylene-bis(oxyethylenenitrilo)tetraacetic acid)	Sigma
ethanol	Riedel-de-Haen
ethidium bromide	Sigma
FCS (fetal calf serum)	Biochrom,
fish gelatine	Sigma
formamide	Merck

formaldehyde	Sigma
glycine	Degussa
IPTG (isopropyl β-D-thiogalactopyranoside)	Sigma
isopropanol	Merck
β-mercaptoethanol	Sigma
methanol	Riedel-de-Haen
methylbenzoate	Fluka
mineral oil	Pharmacia
MOPS ([morpholino]propanesulfonic acid)	Gerbu
Ni-NTA-agarose	Qiagen
paraformaldehyde	Sigma
RNase A	Sigma
SDS (sodium dodecylsulfate)	Serva
sodium azide	Merck
TEMED (tetramethylethylenediamine)	Merck
Tris (hydroxymethyl)aminomethane	Sigma
Triton X-100 (t-octylphenoxypolyethoxyethanol)	Merck
X-Gal(5-bromo-4-chloro-3-indolyl-β-D-galactopyranoside)	Roth
xylol	Fluka
yeast extract	Oxoid

Radionuclides

α-^{32}P-desoxyadenosine-5‘-triphosphate (10 mCi/ml)	Amersham
α-^{32}P-desoxycytosine-5‘-triphosphate (10 mCi/ml)	Amersham

Reagents not listed above were purchased from Clontech, Fluka, Merck, Roth, Serva, Sigma, Promega and Riedel-de-Haen, respectively.

2.1.3 Kits

Nucleobond PC 500	Macherey-Nagel
NucleoSpin Extract 2 in 1	Macherey-Nagel
NucleoSpin Plus	Macherey-Nagel

RNeasy midi kit	Qiagen
pGEMT easy Cloning Kit	Promega
Zero Blunt TOPO PCR Cloning Kit	Invitrogen
EndoFree Plasmid Maxi kit	Qiagen

2.1.4 Bacterial host strains

***E. coli* M15**
E. coli DH5α

2.1.5 Eukaryotic cells

C3H/10T1/2 mouse fibroblasts
N2A mouse neuroblastoma cell line

COS-7 monkey SV40 transformed kidney cell line

human primary keratinocytes (kindly provided by Dr. I. Haase, Clinic of Dermatology, University of Cologne)

C2F3 mouse myoblasts

MB50 human myoblast primary cell line

2.1.6 Vectors

pQE-30	Qiagen
pGEM-T Easy	Promega
pCR-Blunt II-TOPO	Invitrogen
pEGFP-C2	Clontech
pGBKT7	Clontech
pGADT7	Clontech
pBluescript	Stratagen
pGEX4T1	Pharmacia

2.1.7 Oligonucleotides

Oligonucleotides for PCR (polymerase chain reaction) were purchased from MWG-Biotech AG (Ebersberg), Roth GmbH (Karlsruhe), Germany and metabion (Martinsried).

Oligonucleotides used to clone Enaptin-165 in pGEMTeasy vector

624fullGFP5'end
GGAATTCATGGCAACCTCCAGAGCATCTTC

624fullGFPC2-3'end

ACGCGTCGACTTAGAAGTGGTGAAGCACATACTCTTCTTCAAG

Oligonucleotides to correct the deletion after the ABD in the small isoform of Enaptin in the pGEMTeasy vetcor

del.for

5' ATTTTGAAGG AAACAAAAGT TTGGATAGAA C 3'

del.rev

GTTCTATCCA AACTTTTGTT TCCTTCAAAA T

Oligonucleotides to clone the ABD of Enaptin into the yeast two hybrid vector

624fullGFP5'end

GGAATTCATGGCAACCTCCAGAGCATCTTC

y2hABD3'

TGCGTCGACC TACTTGACTT CCATGAAGAG CTCCCTCC

2.1.8 Buffers and other solutions

Buffers and solutions not listed below are described in the methods section.

PBS (pH 7.2):
10 mM KCl
10 mM NaCl
16 mM Na_2HPO_4
32 mM KH_2PO_4

10x NCP-buffer (pH 8.0):
100 mM Tris/HCl
1.5 M NaCl
5 ml Tween 20
2.0 g sodium azide

10x MOPS (pH 7.0/ pH 8.0):
20 mM MOPS
50 mM sodium acetate
1 mM EDTA in 1x PBS

PBG (pH 7.4):
0.5% BSA
0.045% fish gelatine

20x SSC:
3 M NaCl

TE-Puffer (pH 8.0):
10 mM Tris/HCl (pH 8.0)

0.3 M sodium citrate	1 mM EDTA (pH 8.0, adjusted with NaOH) autoclaved

2.1.9 Materials

cryotubes, 1 ml	Nunc
Eppendorf tubes, 1.5 ml and 2 ml	Sarstedt
hybridization tubes	Hybaid
3MM filters	Whatmann
nitrocellulose, type BA85	Schleicher and Schüll
nylon membrane, Biodyne	PALL
filter, sterile 0.45 µm and 0.2 µm	Gelman Science
plastic cuvettes	Greiner
quartz cuvettes Infrasil	Hellma
Superdex75 PC3.2/30	Pharmacia Biotech
15 ml tubes, type 2095	Falcon
50 ml tubes, type 2070	Falcon
X-ray film X-omat AR-5	Kodak

2.1.10 Instruments

blotting chamber Trans-Blot SD	Bio-Rad
centrifuges: Beckman Avanti J25	Beckman
Sorvall RC 5C plus	Sorvall
Biotech fresco	Heraeus Instruments
crosslinker UVC 500	Hoefer
pH-meter 766	Knick
heating blocks: type DIGI-Block JR	neoLab
type thermomixer	Eppendorf
hybridization oven	Hybaid
incubator Lab-Therm	Kühner
microscope: light microscope, Type DMI	Leica
laser scan microscope	Leica
Multiphor II/Immobiline focussing system	Pharmacia Biotech

PCR-thermocycler	MWG-Biotech
pump system Biologic Workstation	Bio-Rad
rotors: type JA-10	Beckman
typeJA-25.50	Beckman
SLA-1500	Sorvall
SLA-3000	Sorvall
SS-34	Sorvall
TLA 45	Beckmann
shaker 3015	GFL
lab-shaker	Kühner
SMART-system	Pharmacia Biotech
spectral photometer type Ultraspec 2000	Pharmacia Biotech
Ultra-Turrax	IKA Labortechnique
ultracentrifuge Optima TLX	Beckmann
UV-Monitor TFS-35 M	Faust
UV-transilluminator	MWG-Biotech
Vortex REAX top	Heidolph
water bath	GFL

2.1.11 Computer programs

For alignment analysis of cDNA sequences the GCG software package (University of Cologne) and the BLAST (NCBI) program were used. Protein sequences were aligned using the programs ClustalW and TreeView. For prediction of motif and pattern searches the ExPaSY (SIB) software package was used. Annealing temperatures of primers were calculated with the program "Primer Calculator" available in the Internet (http://www.williamstone.com).

2.2 Molecular biological methods

2.2.1 Plasmid-DNA isolation from *E. coli* by alkaline lysis miniprep

With this DNA isolation method plasmid DNA was prepared from small amounts of bacterial cultures. Bacteria were lysed by treatment with a solution containing sodium dodecylsulfate (1% SDS) and 0.5 M NaOH (SDS denatures bacterial proteins and NaOH

denatures chromosomal and plasmid DNA). The mixture was neutralized with potassium acetate, causing the plasmid DNA to reanneal rapidly. Most of the chromosomal DNA and bacterial proteins precipitate, as does SDS forming a complex with the potassium, and are removed by centrifugation. The reannealed plasmid DNA from the supernatant was concentrated by ethanol precipitation.

2.2.2 Plasmid-DNA isolation with a kit from Macherey-Nagel

NucleoSpin Plasmid is designed for the rapid, small-scale preparation of highly pure plasmid DNA (minipreps) and allows a purification of up to 40 µg per preparation of plasmid DNA.The principle of this plasmid-DNA purification kit is based on the alkaline lysis miniprep. Plasmid DNA was eluted under low ionic strength conditions with a slightly alkalibuffer. For higher amounts of plasmid DNA, the Nucleobond AX kit from Machery-Nagel was used. The plasmid DNA was used for sequencing and transfection of eukaryotic cells. The protocols were followed as described in the manufacturer's manual.

2.2.3 DNA agarose gel electrophoresis

10x DNA-loading buffer:
40% sucrose, 0.5% SDS
8.0) 57.5 mL acetic acid

50X Tris acetate buffer (1000 ml) (pH:8.5)
242.2 g Tris0.25% bromophenol blue, in TE (pH

100 ml of 0.5 M EDTA (pH:8.0, adjusted with NaOH)

Agarose gel electrophoresis was performed to analyse the length of DNA fragments after restriction enzyme digests and polymerase chain reactions (PCR), as well as for the purification of PCR products and DNA fragments. DNA fragments of different molecular weight show different electrophoretic mobility in an agarose gel matrix. Optimal separation results were obtained using 0.5-2% gels in TAE buffer at 10 V/cm. Horizontal gel electrophoresis apparatus of different sizes were used. Before loading the gel, the DNA sample was mixed with 1/10 volume of the 10x DNA-loading buffer. For visualization of the DNA fragments under UV-light, agarose gels were stained with 0.1µg/ml ethidium bromide. In order to define the size of the DNA fragments, DNA molecular standard markers were also loaded onto the gel.

2.2.4 Isolation of total RNA from mouse tissue with RNeasy Mini/Midi kit

Working with RNA always requires special precautions in order to prevent degradation by ubiquitous RNases, e.g. wearing gloves and using RNase-free water and material. The RNeasy technology combines the selective binding properties of a silica-gel-based membrane with centrifugation. A specialized high-salt buffer system allows up to 100 µg (mini) or 1 mg (midi) of RNA longer than 200 bases to absorb to the RNeasy silica-gel membrane. An appropriate amount of different mouse tissues was transferred into a lysis buffer containing guanidine isothiocyanate and β-mercaptoethanol followed by disruption and homogenization using a rotor homogenizer. After centrifugation the supernatant was transferred to a new tube and mixed with one volume of 70% ethanol. This mixture was loaded on the RNeasy spin column placed in a collection tube. After another centrifugation and discarding the flow through, the RNeasy column was treated with DNase I and washed with a washing buffer. To elute the RNA from the column an appropriate volume of RNase-free water was pipetted directly onto the spin-column membrane. The obtained RNA was used for cDNA synthesis by RT-PCR and for northern blot analysis. Exact compositions of the buffers used for RNA isolation are listed in the Qiagen RNeasy Handbook.

2.2.5 RNA agarose gel electrophoresis and northern blotting

RNA-buffer:	RNA loading dye:
50% formamide	50% sucrose
6% formaldehyde	0.25% bromophenol blue
in MOPS buffer (pH 8.0; see 2.1.8)	in RNase free water

The agarose gels were made under RNase free conditions and separation of RNA was performed overnight with 2 V/cm voltage. After washing the gels with water and equilibrating in a high salt solution (20x SSC), the RNA was transferred onto a nylon membrane overnight using the setup similar to the one for Southern blotting. Next day the membrane was washed in 2x SSC, briefly air-dried and the RNA was UV-crosslinked to the membrane.

2.2.6 Labeling of DNA probes

DNA probes used for radioactive labeling were obtained by PCR. About 25 ng DNA was denatured by heating for 5 minutes at 92°C and cooled immediately on ice. After adding random hexanucleotide primer, α-^{32}P-dATP (50 µCi) and/or α-^{32}P-dCTP, the reaction mix

was incubated for 30 min at 37°C with 2 U Klenow-Enzyme for DNA synthesis. Unincorporated nucleotides were separated from the probe by centrifugation through a Sephadex G-50-column. Before using, labeled probes were denatured at 100°C for 10 minutes.

2.2.7 Hybridization of labeled probes

Church buffer:	Wash buffers:
0.5 M Na_3PO_4 (pH 7.15)	1) 2x SSC, 1% SDS
7% SDS	2) 0.4x SSC, 1% SDS
1 mM EDTA	3) 0.2x SSC, 1%SDS
1% BSA	
50 µg/ml salmon sperm	

After 1 hour of prehybridizing the blots at 65˚C in Church buffer, radioactively labeled probes were added to a portion of fresh Church buffer and hybridization took place for 18 hours at the same temperature. Several washing steps were performed at 65˚C, as needed. Afterwards blots were exposed to an X-ray film at –70 °C.

2.2.8 Elution of DNA fragments from agarose gels

Elution of DNA fragments from agarose gels was performed using the „NucleoSpin Extract 2 in 1“ kit from Macherey-Nagel. Bands of interest were cut out of the gel and the agarose melted at 50°C in a binding buffer. After several centrifugation steps with wash buffer, the DNA bound selectively to a silica membrane column and was eluted with a low salt solution.

2.2.9 Measurement of DNA and RNA concentrations

Concentrations of DNA and RNA were estimated by determining the absorbance at a wavelength of 260 nm. A ratio of OD_{260}/OD_{280} >2 indicates negligible protein contaminations. Protein contaminations were estimated from absorance at 280 nm.

2.2.10 Restriction digestion of DNA

Digestion of DNA with restriction endonucleases was performed in buffer systems provided by the manufacturers at the recommended temperatures.

2.2.11 Dephosphorylation of 5´-ends of linearized vectors

10x CIAP-Puffer (pH 9.0):

0.5 M Tris/HCl (pH 9.0)

10 mM $MgCl_2$

1 mM $ZnCl_2$

10 mM spermidin

In order to prevent linearized vectors from religation, the 5'end phosphate groups were hydrolyzed with calf intestinal alkaline phosphatase (CIAP) for 30 minutes at 37°C followed by heat inactivation at 70°C for 10 min.

2.2.12 Creation of blund ends

Due to the 3' exonuclease activity of Klenow enzyme it is possible to transform overhanging 3' ends of DNA (sticky ends) into blunt ends. After the reaction for 30 minutes at 37°C, heat inactivation for 10 minutes at 70°C was necessary.

2.2.13 Ligation of vector- and DNA-fragments

T4-DNA-ligase catalyzes the ligation of DNA fragments and vector DNA. 1 U T4-ligase was incubated with about 25 ng of DNA fragment overnight at 10°C.

2.2.14 Polymerase chain reaction (PCR)

PCR can be used for *in vitro* amplification of DNA fragments (Saiki *et al*., 1985). A doublestranded DNA (dsDNA) serving as a template, two oligonucleotides (primers) complementary to the template DNA, desoxyribonucleotides and heat resistant *Taq*-DNA-polymerase are required for this reaction. Primers may be designed having non-complementary ends with sites for restriction enzymes. First step in PCR reactions is the denaturing of dsDNA at 94°C. Second, the reaction mix was incubated at different annealing temperatures, depending on the G/C content of the primers. Different programs provide an accurate calculation of the annealing temperature based on the nearest neighbours method and are free available in the Internet. The third step with a temperature of 72°C allows the elongation of the new strand of DNA by the *Taq*-DNA-polymerase. A PCR machine (thermocycler) can be programmed to regulate these different cycles automatically. A "standard program" is presented below:

I. Initial denaturing: 94°C, 5 min

II. Cycles (25-35):

Denaturing (94°C, 15 sec.)

Annealing (60-68°C, 30 min)

Elongation (72°C, 1-10min)

III. Final elongation: 72°C, 10 min

IV. Cooling to 4°C

2.2.15 Transformation of *E. coli* cells with plasmid DNA

LB-Medium:	SOC-Medium:
10 g Bacto-Trypton	20 g Bacto-Trypton
5 g yeast extract	5 g yeast extract
5 g NaCl	0.5 g NaCl
	20 mM Glucose

For transformation of *E. coli* cells the heat shock method was used. DNA and competent cells were incubated for 15 minutes on ice and then for 40 seconds at 42°C. After cooling on ice for 2 minutes, the bacteria were incubated for 1 hour at 37°C in SOC-medium without any antibiotics. Finally, the bacteria were plated on agar plates containing selective antibiotics, and incubated overnight at 37°C. For further analysis single colonies were picked, inoculated and incubated for 12 hours in LB-medium on a shaker. From clones of interest glycerol stocks were made. For this, samples of *E. coli* cultures were mixed with an equal volume of 50% glycerol and frozen at -80°C.

2.2.16 Correction of a deletion in Enaptin-165 by site directed mutagenesis and cloning in GFP and yeast two hybrid vectors

Full length Enaptin-165 was amplified from brain cDNA using 624fullGFP5'end and 624fullGFPC2-3'end primers and cloned in pGEMTeasy vector by Braune. The deletion in the full length sequence was corrected using site directed mutagenesis. Site directed mutagenesis is a technique by which nucleotides can be altered specifically in a plasmid DNA. It involves a first step of PCR with two primers (one forward and one reverse) designed to the area around the base or bases which are to be mutated, with nucleotides modified in such a way that the PCR product gives the desired mutation. After 25 rounds of PCR, the PCR product is checked on the gel. The template DNA is digested by an enzyme called Dpn1,

which digests methylated DNA, thus leaving the amplified PCR product undigested. The amplified PCR product is then transformed in *E. coli* cells. Plasmid is isolated randomly from the transformants and the site directed mutation is confirmed by sequencing. The deletion of a base A at position 939 of Enaptin-165 in pGEMTeasy was corrected by site directed mutagenesis using the primers del.for and del.rev for PCR amplification. The corrected Enaptin-165 was digested by EcoRI and SalI and cloned in both EGFPC2 and pGBKT7 vectors.

2.3 Protein methods and immunofluorescence

2.3.1 Cloning of GFP fusion protein and yeast two hybrid cloning

For expression of Enaptin GFP fusion proteins a cDNA encoding the Enaptin-165 was digested with restriction enzymes EcoRI at the 5'-end and SalI at the 3'-end from pGEMTeasy vector and introduced into pEGFP-C2 with the GFP fused N-terminal to Enaptin-165 or into pGBKT7, yeast two hybrid bait vector, encoding a fusion protein with the N-terminal BD of Gal4. ABD of Enaptin was amplified from pGEMTeasy with primers having restriction sites EcoRI at the 5'-end and Bam HI at the 3'-end and cloned into pGEMTeasy. This was further digested with the same enzymes, EcoRI and BamHI and cloned into pGBKT7 vector. The constructs were checked by sequencing.

2.3.2 Expression and purification of recombinant 6xHis-tag protein

For expression of recombinant 6xHis-ABD-Enaptin the QIAexpress system by Qiagen was used. 6xHis-tag enables the purification of the fusion protein by metal-affinity chromatography on a Ni-matrix. The host strain *E. coli* M15 was transformed with the pQE-30 vector encoding the His-tag fusion protein and expression was induced by the addition of IPTG, which leads to inactivation of the lac repressor protein.

2.3.2.1 Expression

A single colony was inoculated in 3 ml LB-medium containing both ampicillin (100 μg/ml) and kanamycin (25 μg/ml) and was grown overnight at 37°C. The overnight culture was inoculated into 500 ml LB-medium with ampicillin and kanamycin and incubated at room temperature in a shaker (250 Upm) until the cell density reached an OD_{600} of 0.8. Afterwards the recombinant protein expression was induced with 0.1 mM IPTG. Bacteria were incubated at room temperature for another 4 hours. Subsequently cells were collected by centrifugation at 4,000 g for 20 minutes and the pellet was frozen at –20°C.

2.3.2.2 Purification by affinity chromatography

Buffers: (pH 8.0)

Lysis buffer:	Wash buffer:	Elution buffer:
50 mM NaH_2PO_4	50 mM NaH_2PO_4	50 mM NaH_2PO_4
300 mM NaCl	300 mM NaCl	300 mM NaCl
10 mM imidazole	20 mM imidazole	250 mM imidazole

The pellet was thawed on ice and resuspended in lysis buffer containing protease inhibitors (Complete Inhibitor Cocktail). After adding lysozyme (1 mg/ml), the lysate was incubated for 30 minutes on ice followed by sonication. The lysate was centrifuged at 10,000 g for 30 minutes at 4°C and the supernatant was used for subsequent steps.

The cleared cell lysate was incubated with 50% Ni-NTA slurry shaking overnight at 4°C. Then the mixture was loaded onto a column and the flow-through was collected for SDS-PAGE analysis. The column was washed with 10 ml wash-buffer and protein was finally eluted with an elution buffer containing 250 mM imidazole . Purified 6xHis-ABD-Enaptin was used for immunization of mice and for actin binding assay.

2.3.3 Affinity purification of polyclonal antibodies

TBS : 8 g NaCl, 0.2 g KCl and 3 g Tris/HCl in 1 litre, pH 7.2

Buffer I : 1% BSA, 0.05% Tween 20 in PBS

Buffer II : 0.1 M glycin, 0.5 M NaCl, =.05% Tween 20, pH 2.6

The recombinant protein, hich was used to produce the polyclonal antibody is run on a SDS gel and the protein is transferred to PVDF membrane. The membrane is stained with Ponceau S and the blot corresponding to the recombinant protein is cut out. The blot is then destained with TBS. The cut out blot is blocked by incubating for 2 hours in buffer I. 1 volume of serum is diluted with 4 volumes of TBS and incubated with the stripes at 4˚C for 2 hours and the unbound antibody is washed with TBS 4x 5minutes at 4˚C. After washing, antibodies bound to the recombinant protein in the stripes are eluted with buffer II, 1 mL, 2x, 1.5 minutes at 4˚C. The eluted antibody is neutralised with 100 µl of 1M Tris (pH 8.0) immediately after elution. The antibody can be stabilised with 0.5% BSA.

2.3.4 Extraction of protein homogenate from mouse tissues and cell cultures

For characterization of monoclonal antibodies and identification of endogenous Enaptin, homogenates from mouse tissues and cell cultures were extracted. For this, mice were sacrificed by cervical dislocation. Dissected organs were briefly rinsed in ice-cold PBS buffer and frozen in liquid nitrogen. Afterwards ice-cold PBS containing protease inhibitors was added. After homogenization, the cell lysate was mixed with SDS-loading buffer boiled at 95°C for 5 minutes and centrifuged for 10 minutes at 15,000 rpm. The following cell lines were used for extraction of protein homogenates from cell cultures: mouse embryonic fibroblasts (C3H/10T1/2), mouse myoblasts (C2/C3), monkey SV40 transformed kidney cells (COS7) And human keratinocytes (A431). When these cell cultures were used, about 2-5 x 10^7 cells were collected, centrifuged for 5 minutes at 1,000 rpm and resuspended in ice-cold PBS containing protease inhibitors. Afterwards samples were treated as described for the tissues.

2.3.5 SDS-polyacrylamide-gel electrophoresis (SDS-PAGE) (Laemmli, 1970)

5x SDS-loading buffer:
2.5 ml 1 M Tris/HCl, pH 6.8
4.0 ml 10% SDS
2.0 ml glycerol
1.0 ml 14.3 M β-mercaptoethanol
200 µl 10 % bromophenol blue

10x SDS-PAGE-running buffer:
0.25 M Tris
1.9 M glycine
1 % SDS

Molecular weight standard marker:
LMW-Marker (Pharmacia) (kDa): 94; 67; 43; 30; 24; 20.1; 14.4
HMW-Marker (Pharmacia) (kDa): 200; 116; 97.4; 66; 45; 29

For SDS-PAGE analysis 3% - 15% gradient gels were run at a voltage of 9-15 V/cm with SDS-PAGE running buffer. Protein samples mixed with SDS-loading buffer were heated for 5 minutes at 95°C and loaded on the gel. Afterwards the gels were either stained with Coomassie-blue or transferred onto a nitrocellulose membrane for western blot analysis.

Coomassie-blue-staining

Staining solution:
0.1% Coomassie-brilliant-blue R 250

Destaining solution:
10% ethanol

50% ethanol 7% acetic acid

10% acetic acid

Gels were stained for at least 15 minutes. Unbound Coomassie-blue was washed away with destaining solution.

2.3.6 Western blotting (Kyhse-Andersen, 1984)

Protein transfer

Buffer:

Anode buffer (AP1): 300 mM Tris (pH 10.4)

Anode buffer (AP2): 25 mM Tris (pH 10.4)

Cathode buffer (KP): 40 mM ε-aminocapron acid

25 mM Tris/HCl (pH 9.4); all three buffers contain 10% methanol and 0.05% SDS

Western blotting allows the transfer of proteins from a polyacrylamide gel onto a nitrocellulose membrane. In this work the semi-dry blotting method was used: One layer of Whatmann paper, soaked in AP1, was placed in the blotting chamber. Then two layers of Whatmann paper, nitrocellulose membrane and the gel, all soaked in AP2 were overlaid. Finally three layers of Whatmann paper, in KP-buffer, where placed on top. The transfer was performed at 12 V for two hours. Blotting efficiency was controlled with Ponceau S staining.

Ponceau S-staining

Staining solution:

2 g Ponceau S (Sigma) solubilized in 100 ml 3% Trichloroacetic acid

Nitrocellulose membrane was incubated for 1 minute in Ponceau S and briefly washed with water. Bands of interest were marked and afterwards the membrane was destained in NCP (see 2.1.8).

Immunolabeling and detection of proteins on nitrocellulose membrane

Luminol:

2 ml 1 M Tris/HCl (pH 8.5)

200 µl (0.25 M in DMSO) 3-aminonaphthylhydrazide

89 µl (0.1 M in DMSO) p-coumaric acid

18 ml water

6.1 µl 30% H_2O_2

After protein transfer, the nitrocellulose membranes (blots) were blocked with 5% milk powder in NCP overnight. Blots were incubated for one hour with primary purified antibodies or with hybridoma supernatant overnight at 4°C. Before incubation with the secondary peroxidase-conjugated antibody, the membrane was washed in NCP three times for 5 minutes. Unspecific bound antibodies were washed away with NCP for 20 minutes. Immunolabeling was visualized by adding the substrate (luminol) to the peroxidase-conjugated antibodies. This reaction was detected exposing the blots to an X-ray film for 5 sec to 30 min.

2.3.7 Cell fractionation

For nuclei preparation, COS7 cells were sonicated in hypotonic buffer (10 mM HEPES, pH 7.5, 1.5 mM $MgCl_2$, 1.5 mM KCl, 0.5 mM DTT, 0.2 mM PMSF) supplemented with Protease Inhibitor Cocktail CompleteTM, Mini (Boehringer Mannheim). Nuclei were sedimented at 1,000 g at 4°C for 15 minutes. For further fractionation the supernatant was centrifuged at 100,000 *g* for 30 minutes at 4°C. Both pellets were resuspended in hypotonic buffer and analyzed on immunoblots with polyclonal anti-Enaptin antibodies, anti-emerin, anti-tubulin and anti-annexin A7 mAbs.

2.3.8 Cell culture methods

Various adherent cell lines were used for immunofluorescence or western blotting analysis.

Trypsin was used to detach cells from the plates when passaging subconfluent cultures. Each cell line needed special growth medium as listed below.

C3H/10T1/2 mouse fibroblasts	: DMEM, 10% FCS, 1% penicillin-streptomycin (P/S), 1% glutamine.
COS7 monkey kidney cells	: DMEM, 10% FCS, 1% glutamine, 1% pyruvate and 1% P/S.
C2F3 mouse myoblasts	: DMEM, 10% FCS, 1% glutamine, 1% pyruvate and 1% P/S.

2.3.9 Immunofluorescence

Cells are grown on coverslips kept on six well plates. Nicely spread cells are used for fixing. Fixing can be done by three different ways. In the first way, the cells are incubated with 3% paraformaldehyde for 20 minutes at room temperature and permeabilised with 0.5% Triton X-100 for 5 minutes. In the second method, the permebilisation is done first followed

by fixing. The cells are incubated with 0.5% Triton X-100 and 3% paraformaldehyde for 5 minutes and followed by incubation with 3% formaldehyde for 20 minutes. In the third method, the cells are fixed and permeablised by incubating with ice cold methanol for 10 minutes followed by ice cold acetone. The fixed cells are then washed with PBS for three times for 5 minutes. After washing, the cells are incubated with the primary antibody for one hour or so, depending on the concentration of the antibody. After one hour, the cells are washed with PBS for 3 times for 5 minutes. Then, the cells are incubated with the secondary antibody, which has a fluorescent tag for one hour. The cells are then washed again and embedded in slides with Gelvatol.

2.3.10 Immunohistchemical staining of formalin-fixed paraffin-embedded sections

Solutions

Xylene

Ethanol

0.01 M Phosphate bufferes saline (pH 7.4)

Solution of gelatine in PBS (PBG)

Citric buffer, pH 6.0

9 ml of solution A (0.1 M Citric acid)

41 ml of solution B (0.1 M sodium citrate) and made upto 500 ml with water.

The paraffin in the sections are removed by incubating them in xylene for 3 times for 5 minutes and the sections are rehydrated with a series of incubations in different percentages of ethanol - 96% (2 times, 5 minutes), 80% (3 times, 5 minutes), 70% (3 times, 5 minutes) and finally rinsed with water. The slides are washed with freshly prepared citrate buffer and boiled in a microwave in the same buffer for 15 to 20 minutes. The sections are cooled to room temperature for about 20 minutes, rinsed in distilled water and then in PBS (3times, 5 minutes). The sections are incubated with the primary antibody for 24 hours at 4˚C. the slides are washed for 3times for 4 minutes. The sections are now incubated with secondary antibody with fluorescent tags for 0ne hour in room temperature. The sections are washed again as before and mounted in Gelvatol.

2.4 Yeast two hybrid and GST pull down

2.4.1 Construction of yeast two hybrid and GST fusion proteins of Sun1

All yeast two hybrid constructs and GST fusion proteins were first cloned in pGEMTeasy vector before cloning into the target vectors. The perinuclear region of Enaptin

(LE or PNE) was amplified from the genomic DNA isolated from ES cells using lumenaptin.5prime and lumenaptin.3prime and cloned in pGEMTeasy vector. The 90 bp insert was later digested by EcoRI and SalI and cloned into pGBKT7 vector. The same insert was also cloned into pGEX4TI vector for expressing the protein as a GST fusion protein. The C-terminus of Sun1 (CT+AD) was amplified by Ctermouseunc84.5prime and Ctermouseunc84.3prime primers and digested with EcoRI and BamHI and cloned in pGADT7 and pGBKT7 vectors. The ΔSUN domain of Sun1 (ΔSUN) was amplified using Ctermouseunc84.5prime and bSUNy2h.3prime and digested by EcoRI and BamHI and cloned into pGADT7 and pGBKT7 vectors. SUN domain was amplified using SUNy2h.5prime and Ctermouseunc84.3prime and digested by EcoRI and BamHI and cloned into pGADT7 and pGBKT7 vectors. The N-terminal part of Sun1 with two transmembrane domains (NT+2TM) was amplified using Ntermouseunc84.5prime and Ntermouseunc84.3prime primers and digested by EcoRI and BamHI and cloned in pGADT7 vector. The N-terminus of Sun1 (NT) was amplified using Ntermouseunc84.5prime and Y2HNT-3TMUNC84.3prime primers and digested with EcoRI and BamHI and cloned in pGADT7 vector. The N-terminus of Sun1 was also amplified using Ntermouseunc84.5prime and gstmunc84.3prime primers and digested by EcoRI and SalI and cloned in pGEX4TI vector. SUN domain was amplified using SUNy2h.5prime and Munc84dsred.3prime primers and digested by EcoRI and SalI and cloned in pGEX4T1 vector.

Primer sequences

Ntermouseunc84.5prime

CGAATTCATG GACTTTTCTC GGCTGCACAC GTAC

Ntermouseunc84.3prime

CGGATCCCTT GCAAATATTT CGAAGGCACC TGGTAAG

Ctermouseunc84.5prime

CGAATTCGTC TCCCTGTGGG GCCAGGGAAA CTTC

Ctermouseunc84.3prime

CGGATCCCTA CTGGATGGGC TCTCCGTGGA CTC

bSUNy2h.3prime

CGGATCCTTG GGAGTACAGC TTCAGAGCAT TG

SUNy2h.5prime
CGAATTCGACAAGACGGGGATGGTGGACTTTGCTC

Y2HNT-3TMUNC84.3prime
CGGATCCGGC AGCTCTAGTC CTTCGCAGTG C
gstmunc84.3prime
CGTCGACGGA GGTGGTCCCG TGGATGGC

lumenaptin.5prime
CGAATTCTCA GAGAAAGACT ACAGCTGTGC CCTC

lumenaptin.3prime
CGTCGACTCA GAGTGGAGGA GGACCGTTGG TATATC

Munc84dsred.3prime
CGTCGACAAC TGGATGGGCT CTCCGTGGAC TC

2.4.2 Yeast transformation

Stock solutions
50%PEG 3350 prepared in water
100% DMSO : 0.1 M Tris-HCl (pH 7.5), 10 mM EDTA
10X LiAc : 1M LiAc, pH 7.5

50 ml of YPD or SD medium are innoculated overnight with several colonies of Y190 yeast strain and incubated overnight at 30˚C for 16 to 18 hours with shaking of 250 rpm to stationary phase. 30ml of overnight culture is transferred 300ml of YPD or SD and again incubated at 30˚C for 3 hours until the O.D becomes 0.4 to 0.6. The cells are centrifuged and the cells resuspended in TE buffer or water and centrifuged again. The pellet is resusupended again in 1XTE/1XliAc(the resuspended cells are called competent cells). 0.1 µg of plasmid DNA and 0.1 mg of herring testes carrier DNA are added to a 1.5ml tube and mixed. 0.1 ml of yeast competent cells is added. 0.6 ml of sterile PEG/LiAc solution is added and vortexed and incubated at 30˚C overnight. 70 µl of DMSO is added and mixed gently and heat shocked at 42˚C for 30 minutes. The cells are centifuged for 10 seconds, supernatant discarded. The pellet is resuspended in 100 µl of water and plated on SD-Trp-Leu plates and the plates incubated at 30˚C for 3 to 4 days. The transformed cells were further streaked onto

SD-Trp-Leu-His with 3-AT concentrations varying from 25 to 60 mM and the growth monitored over a period of one week.

2.4.3 Yeast plasmid rescue

STET: 8% sucrose, 50 mM Tris-HCl (pH 8.0), 50 mM EDTA, 5% Triton X-100

2.0 ml of yeast overnight culture is grown under selective conditions. The cells are harvested in micricentrifuge tube by spanning at 14,000 rpm for 1 minute. The cell pellet is resuspended in 100 µl of STET buffer and ¾ volume of 0.45 mm glass beads is added and another 100 µl of STET is added. The tube is vortexed briefly and placed in a heating block at 95˚C for 5 minutes. After 5 minutes, the tube is cooled briefly on ice and spun on microcentrifuge tube at 14,000 rpm, 4˚C for 10 minutes. 150 µl of supernatant is transferred to a fresh tube containing 75 µl of 7.5 M ammonium acetate and incubated at –20˚C for one hour and centrifuged in a microcentifuge at the same spped and temperature for 10 minutes. 200 µl of the supernatant is added to 400 µl of ice-cold ethanol. The DNA is recovered by centrifugation and washed with 70% ethanol and dried in Speedvac for 5 minutes. The DNA is resuspended in 20 µl of 10mM Tris-HCl (pH 8.0). 10 µl of this resusupended DNA is used to transform competent bacteria.

2.4.4 X-gal colony-lift filter assay

Z buffer: Na_2HPO_4 7 H_2O: 16.1 g/l, NaH_2PO_4 H_2O: 5.50 g/l, KCl: 0.75 g/l and $MgSO_4$ $7H_2O$: 0.246 g/l (pH 7.0)

X-gal stock solution: 20 mg/ml of DMF

β-mercaptoethanol

Yeast colonies grown on SD-Trp-Leu plates are carefully transferred onto a nitrocellulose membrane by placing it on the yeast plate. The membrane containing the yeast colonies is soaked in liquid nitrogen and then placed on a petri plate with a filter paper, which is already soaked in Z buffer/X-gal solution. The plate is then kept in 30°C in dark until there is a development of blue colour.

2.4.5 GST-pull down

50 mM Tris/HCl (pH 7.5), 150 mM NaCl, 1% Triton X-100 and protease inhibitors

GFP-CT, GFP-ΔSUN and GFP-SUN fusion constructs were separately transfected in COS7 cells and grown overnight. The transfected cells were trypsinised from the plates and

lysed by sonication in the above stated buffer. The cell lysate was centrifuged ate 13,000 rpm for 15 minutes and followed by 45,000 rpm for 30 minutes in an ultracentifuge. The supernatant was collected and mixed with GST and GST-PNE proteins, which were calibrated with the lysis buffer behorehand, in two different micro centrifuge tubes and incubated overnight at 4°C. The mixture was centrifuged shortly in the following day and the supernatant collected. The pellet was washed four to five times in PBS and centrifuged. The supernatant and final washed pellet were mixed with protein loading dye and loaded on a 12% polyacrylamide gel. The gel was transferred onto PVDF membrane overnight in a wet-blot chamber at 4°C. The membrane was probed with antibodies specific to GFP and the result analysed.

2.5 Construction of GFP fusion proteins and transfection

All the GFP fusion constructs were amplified by PCR using Sun1 IMAGE clone as a template and cloned in pGEMTeasy vector before cloning it in the final vector. The full-length GFP-Sun1 was amplified using Ntermouseunc84.5prime and Ctermouseunc84.3prime and digested by EcoRI and BamHI and cloned in EGFPC2 vector. GFP-NT+2TM was amplified using Ntermouseunc84.5prime and Ntermouseunc84.3prime primers and digested by EcoRI and BamHI and cloned in EGFPC2 vector. GFP-CT+2TM was amplified using GFPCT+3TM UNC84.5prime and Munc84dsred.3prime primers and digested by EcoRI and SalI and cloned in EGFPC2 vector. The C-terminus of Sun1 (GFP-CT) was amplified by Ctermouseunc84.5prime and Ctermouseunc84.3prime primers and digested with EcoRI and BamHI and cloned in EGFPC2 vector. The ΔSUN domain of Sun1 with three transmembrane domains (bSUN+3TM or ΔSUN+3TM) was amplified using GFPCT+3TMUNC84.5prime and bSUNy2h.3prime and digested by EcoRI and BamHI and cloned into EGFPC2 vector. The ΔSUN domain of Sun1 (bSUN or ΔSUN) was amplified using Ctermouseunc84.5prime and bSUNy2h.3prime and digested by EcoRI and BamHI and cloned into EGFPC2 vector. The SUN domain of Sun1 was amplified using SUNy2h.5prime and Ctermouseunc84.3prime and digested by EcoRI and BamHI and cloned into EGFPC2 vector. All the GFP-fusion constructs were transfected in COS7 cells by electroporation and the transfected cells fixed in the following day.

Primer sequence

Munc84dsred.3prime

CGTCGACAAC TGGATGGGCT CTCCGTGGAC TC

GFPCT+3TMUNC84.5prime
CGAATTCGGGTGGTCTGTGGCCGAGGCCGTG

2.6 Generation of knock in mouse

2.6.1 Target vector construction

pBS SK^+ vector was used for the target vector construction. GFP was amplified from pEGFP-N1 vector using GFPN1 and GFPC1 primers and cloned in pGEMTeasy vector. The insert was later digested by HindIII and EcoRV and cloned in the target vector. The NEO cassette was retrieved from NEO-pGK with EcoRV and XmaI and cloned in the target vector. Genomic DNA isolated from IB10 ES cells was used as a template. The 5'arm was amplified from genomic DNA using 5arm5prime and 5arm3prime and cloned in pCR-Blunt II-TOPO vector. The insert was later digested with SalI and HindIII and cloned in the target vector. The 3' arm was amplified using 3arm5prime and 3arm3prime and cloned in pCR-Blunt II-TOPO vector. The insert was later digested by SacII and cloned in the target vector. Two probes outside the 5' arm and 3' arm were also cloned in the pGEMTeasy vector. The 5' probe was amplified using 5probe5prime and 5probe3prime and cloned. The 3' probe was amplified using 3probe5prime and 3probe3prime and cloned. The target vector was purified by EndoFree Plasmid Maxi kit (Qiagen) and linearised by SalI. The linearised vector was purified by phenol-chloroform extraction procedure.

Primer sequences
GFPN1
GCGAAGCTTATGGTGAGCAAGGGCGAGGAG

GFPC1
GCGGATATCCACAACTAGAATGCAGTG

5arm5prime
CGTCGACCTC TAAGGCAGAG TCACCCTGAT GGAG

5arm3prime

CAAGCTTGTC AGAACGGGAG GAATCGGAGC CATC

3arm5prime

CACACAAGTG CAGGCAGTAA GAGGAGAAGG

3arm3prime

CCACCATCAC CAAAGCATCC AAGTATATGC

5probe5prime

CAGTTGCTTT CATGTGCCTA ACAGGTC

5probe3prime

CATATCTCTT AATGGAAGAA AGCATCATG

3probe5prime

CAGCTTACAA GCTACCTCCT AGTTGAAG

2.6.2 Transfection and colony picking

MEF media	DMEM (4500 mg/l glucose) (Sigma):		500 ml
FCS	:		50 ml
L-glutamine	:		5 ml
Non-essential amino acids	:		5 ml
Pen/Strep	:		5 ml

ES cells media	DMEM knockout (GIBCO)	:	500 ml
	FCS	:	90 ml
	L-glutamine	:	7 ml
	Non-essential amino-acids	:	7 ml
	Pen/Strep	:	10 ml
	Pyruvate	:	5 ml
	ESGRO (Murine LEF)	:	70 µl
	β-mercaptoethanol	:	7 µl

Selection media : ES cell media and 400 µg/ml of G418

Freezing media : ES media, 30% FCS and 20% DMSO

Gelatin (2%)

Mitomycin C (400 µg/mL)

Mouse embryonic fibroblasts were grown on MEF media on 0.1% gelatinised plates and mitomycin C (150 μL stock solution in 10 ml medium) treated when they reached approximately 70% confluence. RI ES cells were grown on mitomycin C (0.6 μg/mL) treated MEF cells. The ES cells were transfected by electroporation using linearised target vector at 500 μF and 230 volts. The transfected cells were plated on four MEF cells plates already treated with mitomycin C and the cells grown on selection media. Colonies starting to appear after four days were picked and grown on 24 well plates. The ES cells were trypsinied after the cells achieved approximately 70 to 80% confluence and half of the trypsinised ES cells were frozen using the freezing media and the other half grown further for genomic DNA isolation.

2.6.3 Genomic DNA isolation

TNES 50 mM Tris (pH: 7.4)
100 mM EDTA (pH:8.0)
400 mM NaCl
0.5% SDS

6M NaCl

Proteinase K : 20 mg/ml

Trypsinised ES cells were mixed with 500 μL of TNES buffer and 10 μL of proteinase K solution and incubated at 55°C overnight in a shaking incubator. 150 μL of saturated NaCl was added to this the following day to salt out the proteins. The sample was centrifuged at high speed for 5 minutes and the pellet thrown out. The genomic DNA in the supernatant was precipitated by 100% ethanol and washed with 70% ethanol. The pellet was dried and the genomic DNA was resuspended in 50 μL of water.

2.6.4 Southern blotting (Southern, 1975)

Southern blotting is the transfer of DNA fragments from an electrophoresis gel to a membrane. After immobilization, the DNA was subjected to hybridization analysis to identify the bands containing DNA complementary to the radioactively labeled probe. In this work the alkaline transfer on a nylon membrane was performed. First the gel was washed in 0.25 M HCl for 10 minutes, incubated in 0.4 M NaOH for 10 minutes and placed on top of two layers of Whatmann 3MM paper having contact to a reservoir of 0.4 M NaOH. After overlaying the gel with Zeta-probe GT Genomic Tested Blotting membrane (Bio-Rad), that had been wetted

with the transfer buffer, three wet Whatmann 3MM paper and a thick stack of paper towels, the transfer was performed for about 18 hours. After washing the membrane in 2% SSC, it was air-dried.

2.6.5 Labeling of DNA probes and hybridization

Prehybridisation solution and hybridization solution

: 0.25 M sodium phosphate (pH:7.2) and 7% SDS

Wash buffer : 20 mM sodium phosphate (pH:7.2) and 5% or 1% SDS

0.5% sodium phosphate,pH:7.2

Stock A : 0.5 M $NaH_2PO_4.H_2O$

Stock B : 0.5 M $Na_2HPO_4.7H_2O$

316 mL of Stock A and 684 mL of Stock B are combined to make 0.5% sodium phosphate,pH:7.2

DNA probes used for radioactive labeling were obtained by digesting the 5' probe and 3' probe in pGEMTeasy vector with EcoRI enzyme and gel extracted. About 25 ng DNA was denatured by heating for 5 minutes at 92°C and cooled immediately on ice. After adding random hexanucleotide primer, α-^{32}P-dATP (50 μCi), the reaction mix was incubated for 30 min at 37°C with 2 U Klenow-Enzyme for DNA synthesis. Unincorporated nucleotides were separated from the probe by centrifugation through a Sephadex G-50-column. Before using, labeled probes were denatured at 100°C for 10 minutes. The membrane was prehybridised with prehybridisation buffer for 30 minutes at 65°C. The labeled probes were added to the membrane in 10 mL of hybridisation buffer and kept for shaking overnight at 65°C.

Results

RESULTS

3 Characterisation, tissue distribution and subcellular localisation of Enaptin

3.1 Analysis of the *Enaptin* gene sequence

The full-length human Enaptin cDNA sequence consists of 27,669 bases with an open reading frame encompassing 26,247 bases (accession number: AF535142). It codes for a protein of 8,749 amino acids with a predicted mass of about 1,005,000 dalton. The putative start codon at position 438 of the cDNA together with the surrounding sequence ACCATGG matched the Kozak consensus sequence. This sequence was identified as the optimal sequence for initiation of translation by eukaryotic ribosomes when analysing the effects of single base substitutions around the ATG initiator codon in a cloned preproinsulin gene. Mutations within that sequence modulated the yield of this gene over a 20-fold range (Kozak, 1986). An inframe stop codon was observed 40 bases upstream, making this ATG the translational start site.

The human *Enaptin* gene maps to the long arm of the chromosomal region 6q24-25. It spreads over a region of about 550 kb between positions 152,000 kb and 152,550 kb of chromosome 6 and has 147 exons. The location of the *Esr1* gene encoding the estrogen receptor closely apposed to the C-terminus of *Enaptin* and *Esr2* gene close to *NUANCE* indicates the probable duplication of these genes.

3.2 Isoform diversity and domain analysis of Enaptin

The longest isoform of *Enaptin* consists of 8,749 amino acids and gives rise to a protein of approximately 1,005,000 D. Figure 3.1 represents the structural domains predicted by the SMART computer programme. The N-terminus of this protein is predicted to contain a CH1 and CH2 domain, which make up the actin binding domain (ABD) which has been found to be functional by in vitro actin binding assays (Braune, 2000). The C-terminus of the protein includes a type II transmembrane domain (TM) closely related to the one in the *Drosophila* Klarsicht protein which is required for temporally regulated lipid droplet transport in developing embryos and for the stereotypical nuclear migrations in differentiating cells of the developing eye (Mosley-Bishop et al., 1999; Jäckle and Jahn, 1998). The N-terminal actin binding domain is separated from the C-terminal transmembrane domain by a long rod portion harboring 50 spectrin repeats. The programme also predicts two leucine zippers (LZ).

Leucine zippers are usually found in DNA binding proteins and allow dimer formation. Leucine zippers fold into α-helices, which in the dimer are held together by hydrophobic interactions between leucine residues, which are located on one side of each helix. Six nuclear localisaton signals (NLS) were predicted by the SMART computer analysis. NLSs are stretches of 4 to 20 basic amino acids, mostly lysine and arginine, which serve to localise the protein to the nucleus.

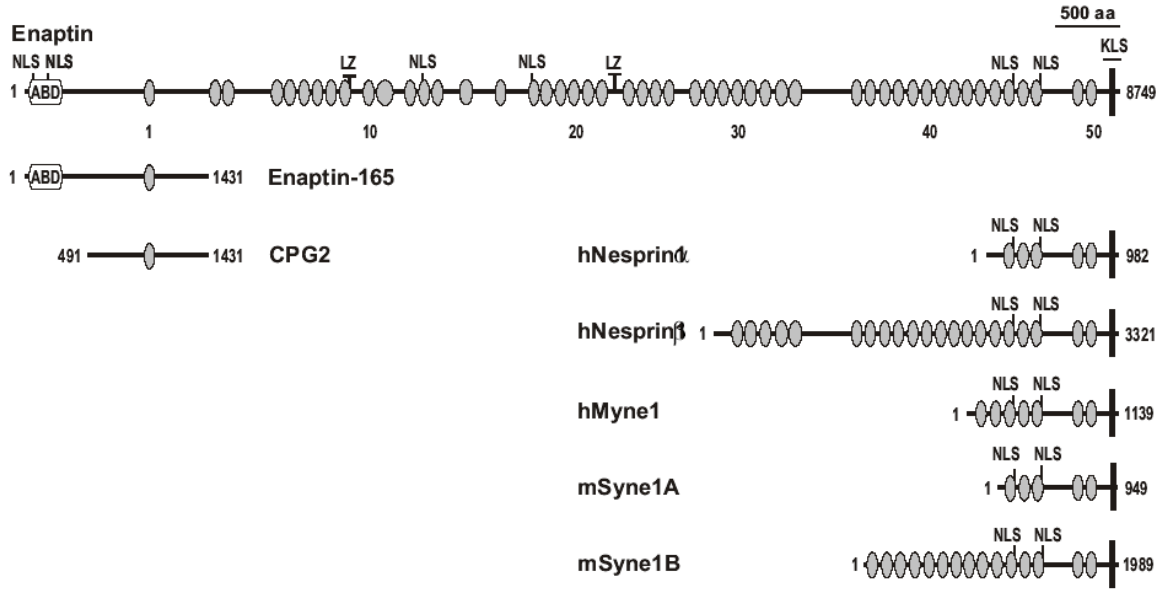

Figure 3.1: Domain architecture of Enaptin predicted by the computer programme SMART (Simple Modular ARchitecture Research Tool). The programme predicts an ABD domain at the N-terminus and a transmembrane domain at the C-terminus (TM). The ABD and TM domains are separated by 50 spectrin repeats. Two Leucine zippers (LZ) and five nuclear localisation signals (NLS) were also predicted. Various N- and C-terminal Enaptin isoforms characterised are depicted in this figure.

We have identified an N-terminal truncated version of the full-length Enaptin namely, Enaptin-165. Enaptin-165 is a rather small protein of 1,431 amino acids with a predicted molecular mass of 165,000 dalton. The cDNA was cloned from mouse brain cDNA. Domain prediction by the SMART software predicts an actin binding domain followed by a coiled coil region which contains a spectrin repeat. The C-terminus of this protein is highly homologous to a protein called CPG2 (candidate plasticity gene 2), one of the genes found to be expressed in response to light in the adult cerebral cortex and being regulated during development (Nedivi et al., 1996).

Five C-terminal isoforms of Enaptin have been reported, human Nesprin-1α, human Nesprin-1β, mouse Syne-1A, Syne-1B and human Myne-1 (Apel et al., 2000; Mislow et al., 2000; Zhang et al., 2000). All these isoforms lack the N-terminal ABD domain but harbor the C-terminal transmembrane domain with different numbers of spectrin repeats.

3.3 Multiple alignment of the actin binding domain of Enaptin with other related ABDs

The 100 amino acids calponin homology (CH) domain is one of about a dozen protein domains, which are shared by signaling and cytoskeletal proteins. Type 1 and type 2 CH domains together form the actin binding region of a large number of F-actin interacting proteins involved in a variety of cytoskeleton and cytoskeleton-membrane linkages. While the

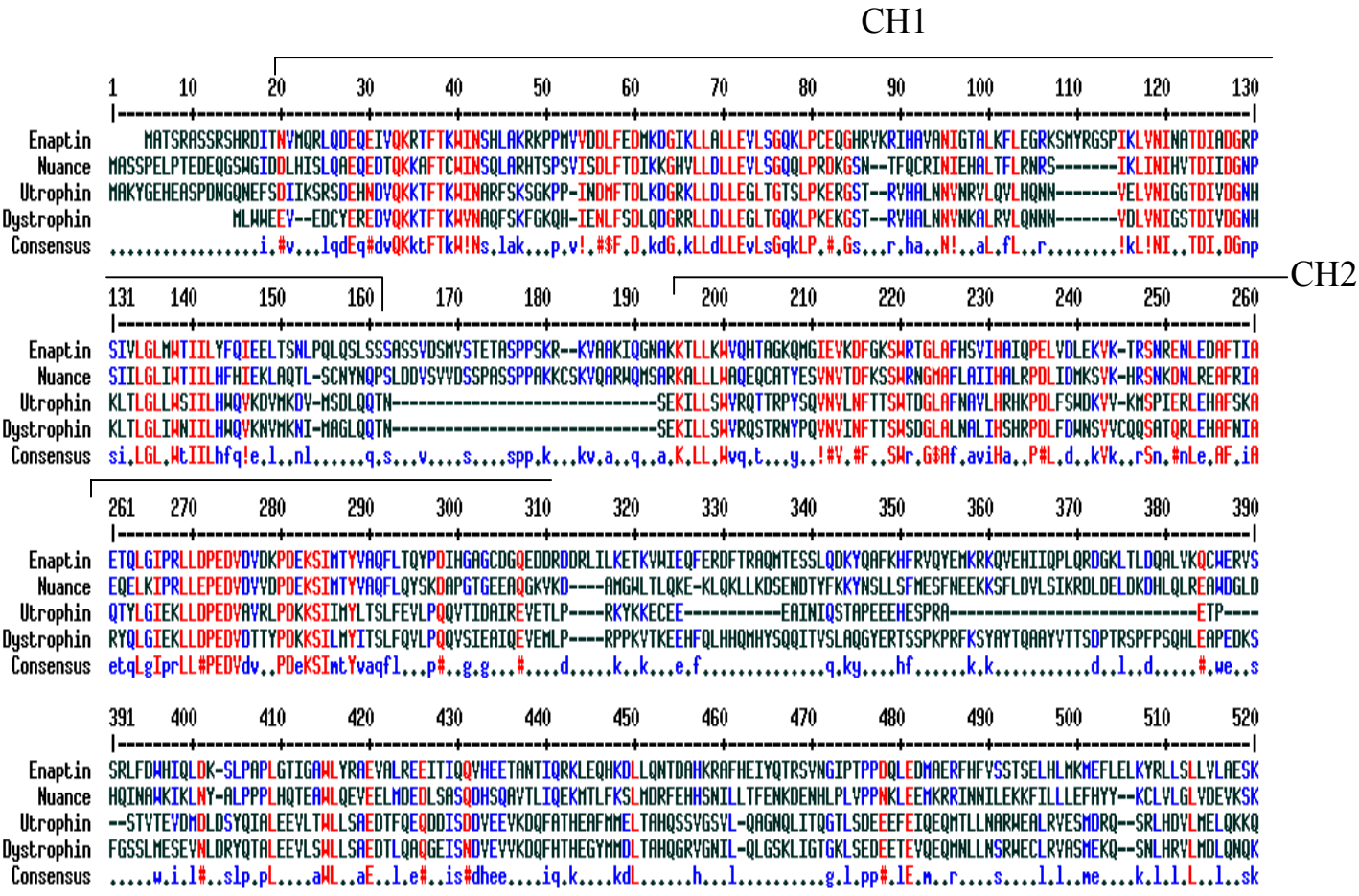

Figure 3.2: Multiple alignment of the actin binding domains. Human Enaptin (residues 1-512, accession number AAN03486), human NUANCE (residues 1-501, accession number AAL33548), human dystrophin (residues 1-456, accession number P11532), and human utrophin (residues 1-426, accession number P46939) were used for the alignment (Corpet et al., 1988). Red colour denotes high consensus, blue colour low consensus and black is the background colour.

ABDs as a whole are functionally equivalent; the CH domains they comprise are functionally distinct (Gimona et al., 1998). Type 1 CH domains have the intrinsic ability to interact with F-actin on their own while the type 2 CH domains do not (Way et al., 1992). Clearly, however, despite the type 2 domain having no intrinsic actin binding activity, it contributes

substantially to the interaction of the complete actin binding domain, perhaps by functioning as a locator or providing low affinity docking site on the actin filament.

The actin binding domain of Enaptin is comprised of a calponin homology domain type 1 and 2 (CH1 and CH2). It shares about 40% identity with the ABDs of NUANCE, dystrophin and utrophin (Figure 3.3). But, unlike utrophin and dystrophin the CH1 and CH2 domains of Enaptin and NUANCE are separated by a serine rich 29 amino acid stretch. NUANCE is another actin binding protein, which displays strong homology to Enaptin and is located in the nuclear membrane. The actin binding affinity of the ABD of Enaptin has been studied previously by an *in vitro* actin binding assay (Braune, 2000). The binding affinity of recombinant 6xHis-ABD-Enaptin (residues 2-294) to actin (Kd: 5.7±1.2 μM) was found to be higher than the affinity of the corresponding ABDs of dystrophin (Kd: 44 μM) and utrophin (Kd: 19 μM) (Way et al., 1992; Winder et al., 1995).

To show the relationship amongst the ABDs of actin binding proteins, we constructed a phylogenetic tree (Figure 3.3). The phlyogenetic tree suggests that the actin binding domain of Enaptin is more closely related to the ABDs of NUANCE, dystrophin and utrophin than to the ones of other actin binding proteins.

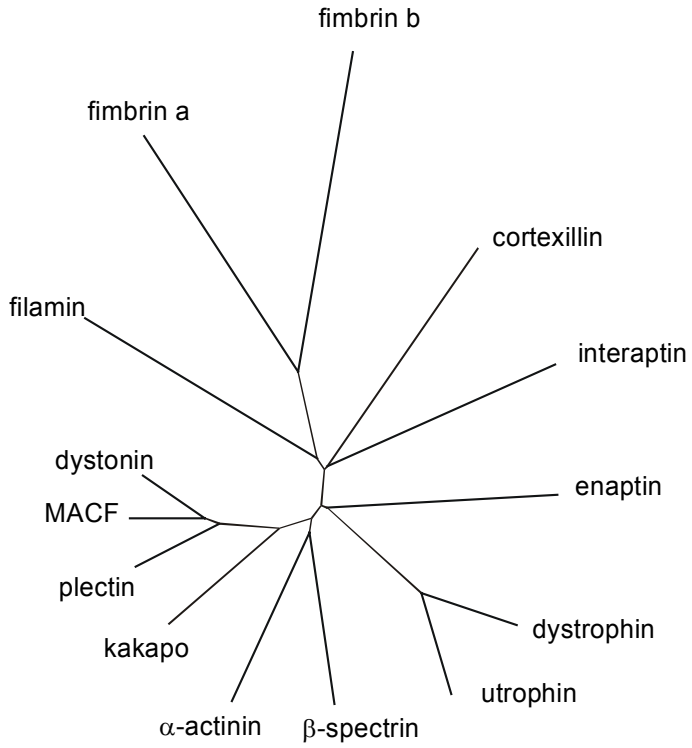

Figure 3.3: Phylogenetic tree of the actin binding domains of Enaptin and the ABDs of other proteins of the α-actinin superfamily based on the calculation from ClustalW alignment of these domains.

3.4 Analysis of the C-terminal transmembrane domain of Enaptin

During a homology search we found that the C-terminal domain of Enaptin is closely related to the C-terminal sequences of NUANCE and the *Drosophila* Klarsicht protein (Figure 3.4). The *Drosophila* gene *klarsicht* is required for temporally regulated lipid droplet transport in developing embryos and for the stereotypical nuclear migrations in differentiating cells of the developing eye. Klarsicht is thought to coordinate the function of several molecular motors that are bound to a single lipid droplet or to facilitate the attachment of dynein to the cargo (Moshley-Bishop et al., 1999). Recently Klarsicht was shown to be required for connecting the microtubule organizing center (MTOC) to the nucleus (Patterson et al., 2004).

The last 62 amino acids of Enaptin's C-terminus are similar to NUANCE and Klarsicht sequences with 33% identity (Figure 3.4). The highly conserved hydrophobic stretch of 22 amino acids (residues 8697-8718) in the Klarsicht domain was identified as a transmembrane domain, which is flanked by an N-terminally positioned neck domain and the C-terminal tail.

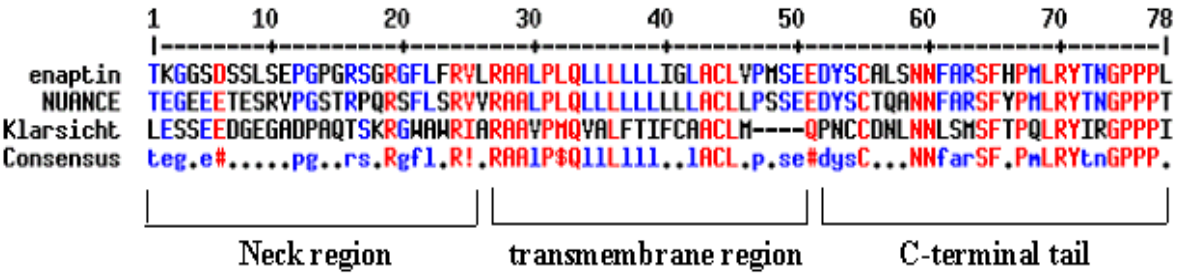

Figure 3.4: Multiple alignment of the transmembrane domain

Enaptin (residues 8672-8749, accession number AAN03486), with human NUANCE (residues 6807-6885, accession number AAL33548), and Klarsicht (residues 2189-2262, accession number AAD43129) were used for the analysis (Corpet et al., 1988). Red colour denotes high consensus, blue colour low consensus and black is the background colour.

3.5 Analysis of the spectrin repeats of Enaptin

Spectrin repeats are domains composed of three α-helices (Figure 3.5). A number of aromatic residues in the hydrophobic domain are typically conserved. Spectrin repeats are best known from the spectrin super family of proteins (spectrin, α-actinin, dystrophin and utrophin), in which they are typically found together with actin binding domains of the CH type, EF-hand motifs, which are Ca^{2+}-binding sites and various signaling domains. Spectrins

normally occur as tetramers in which functional parts like ABDs and EF hands are separated by the spectrin repeats. In addition to their spacer function, spectrin repeats have also been reported to function as a docking surface for cytoskeletal and signal transduction proteins. Certain spectrin repeats seem to have specialised as dimerisation domains determining in this way the functional molecular architecture of the overall multimeric protein.

The full-length Enaptin molecule is predicted to have 50 spectrin repeats. Sequence analysis of the different spectrin repeats shows that the amino acid sequence of different repeats are not closely related to each other with respect to sequence homology.

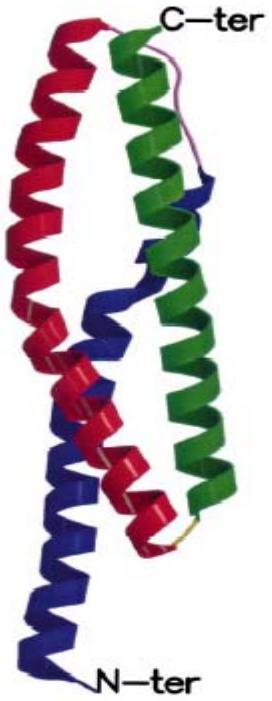

Figure 3.5: Ribbon presentation of the second spectrin repeat of α-actinin. Helices 1, 2, and 3 are depicted in blue, red and green, respectively (Djinovic-Carugo et al., 2001).

3.6 Generation of polyclonal antibodies

To study Enaptin at the biochemical and cellular level we have generated polyclonal antibodies against the recombinant His-tagged ABD of Enaptin. Amino acids 2 to 294 of the small mouse Enaptin-165 N-terminal isoform were cloned in the expression vector pQE-30, which led to the expression of these amino acids fused with the His-tag at its N-terminus. The recombinant protein was purified from *E. coli* strain M15 by affinity purification using a Ni-NTA column. The purified protein was resolved in SDS-PAGE. The predicted molecular weight of the 6xHis-ABD Enaptin is 34 kDa. In addition to the protein with the expected size, a 24 kDa protein eluted from the affinity column which was identified in work done by S.

Braune to be a degradation product of the 6xhis-ABD Enaptin encompassing residues 2-210. The purified fusion protein was used for immunisation of two rabbits and the serum was collected after 60, 90, 130 and 160 days, respectively. The serum was checked by western blot analysis against the recombinant ABD protein. The polyclonal antibodies both from animal 1 (pab1) and animal 2 (pab2) detected the recombinant protein using dilutions as low as 1:10,000. The sera were also checked against protein homogenates prepared from COS7 cells that had been transfected with an Enaptin-165 GFP fusion protein. Cell homogenates from cells expressing a GFP fusion protein of the ABD of NUANCE were used for control in order to demonstrate the specificity of the Enaptin antibodies (Figure 3.6).

The monoclonal anti-GFP antibody recognises both the GFP fusion proteins, GFP-ABD-NUANCE and GFP-Enaptin-165. Pab1 recognises GFP-Enaptin-165 and GFP-ABD-NUANCE. This could be due to the high homology of the ABDs of Enaptin and NUANCE. In contrast, pab2 recognises GFP-Enaptin165 and does not cross-react with the GFP-ABD-NUANCE fusion protein. Thus, pab2 appears to be specific for Enaptin and was used for all further studies including western blotting, immunofluorescence and immunohistochemistry.

The polyclonal serum collected after 160 days from animal 2 was also affinity purified using the recombinant His-ABD Enaptin immobilised on a PVDF membrane and used for immunofluorescence and immunohistochemistry.

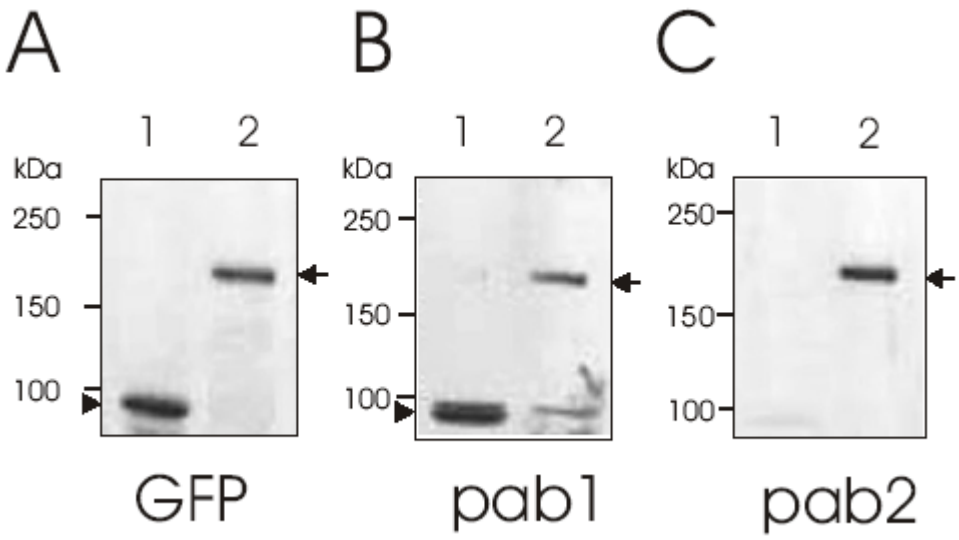

Figure 3.6: Western blot analysis of cell homogenates from COS7 cells transfected with GFP-ABD-NUANCE (1) and GFP-Enaptin-165 (2) using the polyclonal antibodies raised against the ABD of Enaptin (pab1 and pab2). The proteins were separated on 3-15 % SDS-PAGE gradient gels and transferred to a PVDF membrane. Panel A represents the blot probed with a GFP-specific monoclonal antibody, where the GFP antibody recognises both GFP fusion proteins as marked by the arrow. In B, the blot was probed with pab1. These antibodies recognise both proteins as indicated by the arrows. In C, the blot was probed with pab 2. These

antibodies recognise only the Enaptin GFP fusion protein (arrows) but not the ABD-NUANCE GFP fusion protein (arrowheads). The expected molecular weight of GFP-ABD-NUANCE is 90 kDA and of GFP-Enaptin-165 is 190 kDa. In all the blots, the secondary antibody used was coupled to peroxidase. Detection was performed with enhanced chemiluminescence (ECL).

3.7 Expression of Enaptin in various cell lines and in brain

Pab2 was used in western blots to analyse the expression of Enaptin in various cell lines and brain. Protein homogenates prepared from different cell lines such as COS7 (monkey kidney cells), C2F3 (mouse myoblasts), C3H/10T1/2 (mouse fibroblasts) and A431 (human keratinocytes) and brain lysate from mouse were used (Figure 3.7).

In the brain lysate, a protein of 170 kDa was detected (Figure 3.7A). This could represent the small N-terminal isoform of Enaptin, which we have previously cloned from brain cDNA (Enaptin-165). In the cell lysates derived from COS7, A431, C2F3 and C3H/10T1/2 a protein of 400 kDa was observed, which could represent a large isoform of Enaptin, containing the actin binding domain. No signal was detected at the size expected for the full-length of Enaptin, which exceeds 1,000 kDa.

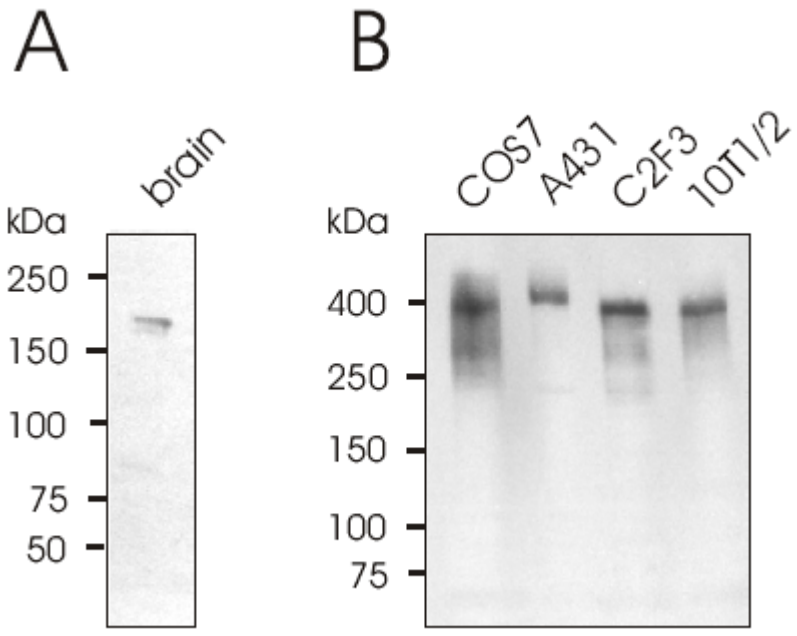

Figure 3.7: Presence of Enaptin in mouse brain and cell lines. Pab2 was used as primary antibody with a dilution of 1:1000. The secondary antibody used was anti-rabbit IgG conjugated with peroxidase. In mouse brain homogenate (A), pab2 recognises a band of about 170 kDa, which could represent the small N-terminal isoform of Enaptin, Enaptin-165. B, Cell homogenates from COS7, A431, C2F3, C3H/10T1/2 were separated on a 3-15% gradient gels as described for Figure 3.10, transferred to a PDVF membrane and probed with pab2. Pab2-

binding was detected using a peroxidase-coupled goat anti rabbit antibody. Detection was performed with ECL. In these cell lines, the Enaptin polyclonal antibodies detect a band of about 400 kDa.

3.8 Immunofluorescence studies of Enaptin in various cell lines

In order to study the subcellular localisation of Enaptin, affinity purified pab2 was used for immunofluorescence studies in different cell lines, COS7, C3H/10T1/2 and C2F3. The cells were usually fixed with 3% paraformaldehyde or methanol-acetone. In Figure 3.8, the cell lines which all express a protein with a molecular mass of 400,000 dalton were fixed with methanol- acetone.

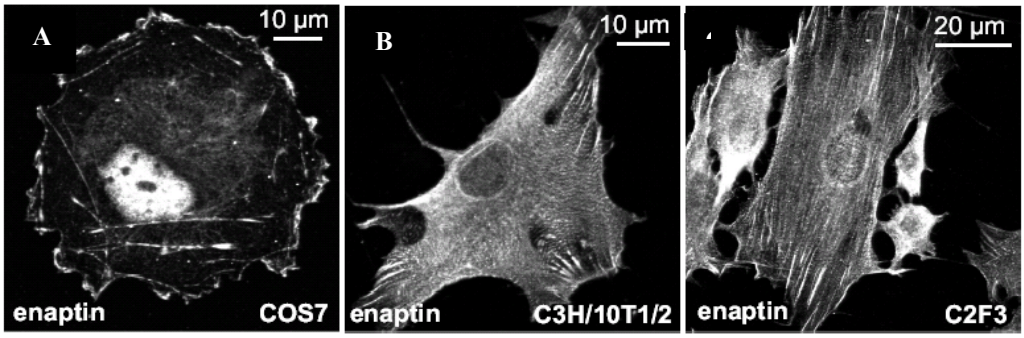

Figure 3.8: Subcellular localisation of Enaptin in various cell lines. COS7, C3H/10T1/2 and C2F3 cells fixed with methanol-acetone were stained with pab2. The antibody was detected with an anti-rabbit IgG secondary antibody, conjugated with Alexa 568. The pictures were taken using a confocal microscope.

In COS7 cells, Enaptin was predominantly localised in the nucleus and in the cortical area presumed to be the cortical actin cytoskeleton (Figure 3.9A). Furthermore, a few fiber-like structures were stained. In C3H/10T/2 and C2F3 cells, Enaptin stained the nuclear membrane and also structures resembling focal contacts (Figure 3.9, B and C). There was also a staining of fiber like structures and a weak diffused staining throughout the cytoplasm.

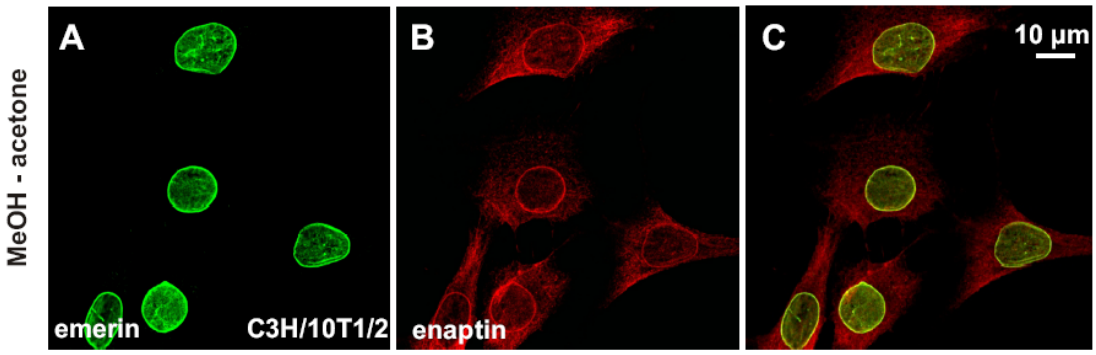

Figure 3.9: Nuclear envelope localisation of Enaptin. Confocal images of the nuclear envelope localisation of Enaptin in fibroblasts (panel B) were confirmed by costaining with an emerin specific monoclonal antibody (panel A). Panel C is the merged image. Secondary antibodies tagged with Alexa-488 and Alexa-568 were used for emerin and Enaptin visualisation.

The nuclear envelope staining of Enaptin was confirmed by colocalisation studies with an emerin antibody (Figure 3.9). Emerin is a 34 kDa nuclear envelope protein and mutation or absence of this protein has been implicated in the generation of Emery-Dreifuss muscular dystrophy (EMDM) (Manilal et al., 1996).

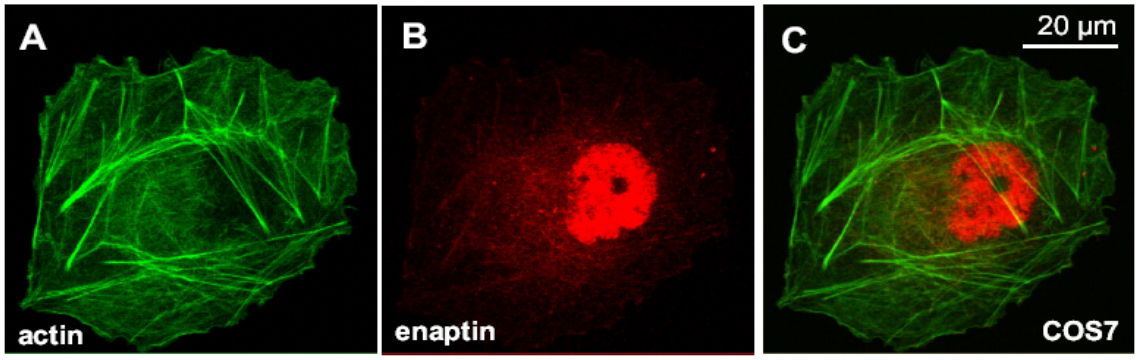

Figure 3.10: Subcellular localisation of Enaptin in COS7 cells. COS7 cells fixed with 3% paraformaldehyde and permeabilised with 0.5% Triton X-100 were stained with FITC-phalloidin for detection of actin-fibers (A) and pab2 for Enaptin. The pictures were taken by confocal microscopy. The secondary antibody conjugated with Alexa 568 detected Pab2 binding (B). The overlay picture is shown in C.

In order to study the association of Enaptin with the actin cytoskeleton in COS7 cells, we fixed cells with 3% paraformaldehyde and costained them with FITC-phalloidin (Figure 3.10). Phalloidin is a toxin from a fungus called *Amanita phalloides,* which specifically interacts with F-actin. COS7 cells fixed with 3% paraformaldehyde and stained with pab2 gave a very bright staining of the nucleus and filamentous cytoplasmic structures that colocalized with the cortical actin cytoskeleton or at stress fibres.

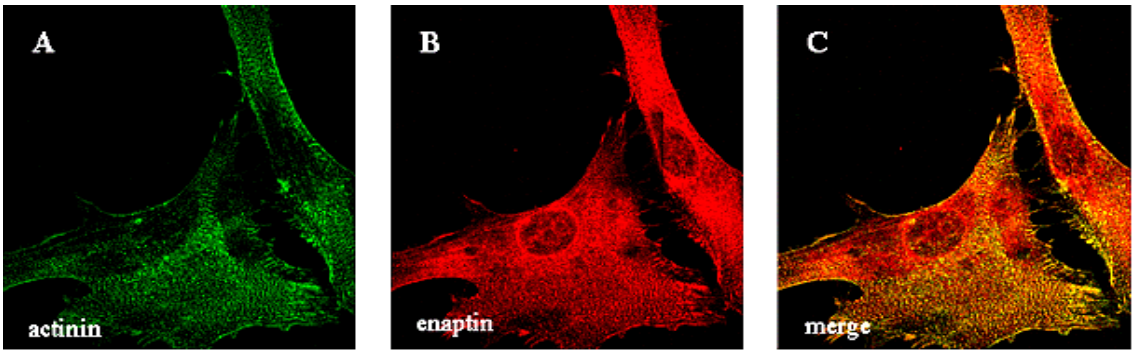

Figure 3.11: Coimmunofluorescence studies of C3H10T1/2 cells with pab2 and anti-α-actinin antibody. Confocal images of cells fixed with methanol-acetone. Panel A shows the α-actinin staining, B shows the Enaptin staining, C, merged picture. Enaptin and α-actinin staining were visualised by secondary antibodies conjugated with Alexa-488 and Alexa-568.

To investigate the actin associated structures of Enaptin in more detail, C3H/10T1/2 cells fixed with methanol-acetone were stained with pab2 and an α-actinin specific monoclonal antibody (Figure 3.11). We observed that Enaptin was colocalising with α-actinin

at the periphery of the cells and in structures that might correspond to focal adhesions and the striations in the stress fibres. In general, the Enaptin staining was prominent at the nuclear membrane, but was also present throughout the cytoplasm.

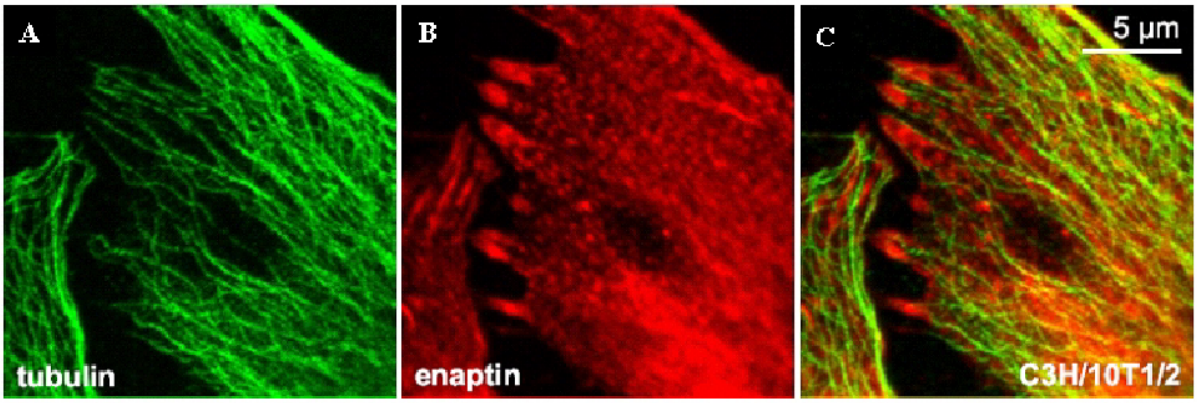

Figure 3.12: Enaptin does not associate with the microtubule network in C3H/10T172 cells. Confocal images of C3H/10T1/2 cells fixed with methanol-acetone and double stained with pab2 and a monoclonal anti-α-tubulin antibody. Panel A represents C3H/10T/2 cells stained with an ∝-tubulin specific antibody and panel B represents the Enaptin staining. Panel C represents the merged image. A secondary anti-rabbit IgG antibody conjugated with Alexa 568 detected Pab2 and the anti-tubulin antibody was detected with a secondary anti-mouse IgG antibody conjugated with Alexa 488.

As other large cytoskeletal proteins have been shown to bind to several filaments we investigated whether Enaptin localises to the microtubule network. For this C3H/10T1/2 cells were double stained with Enaptin and tubulin specific antibodies (Figure 3.12). We did however not detect a colocalisation of Enaptin with the microtubule network.

3.9 Cell fractionation studies of fibroblast cell lysates

The inability to detect the 1,000 kDa Enaptin in western blots, and the observed nuclear membrane staining in a variety of cells encouraged us to investigate the subcellular localization of the 400 kDa protein detected in C3H/10T1/2 cells. The cells were fractionated into cytosol, nucleus and membrane structures, and the samples were subjected to immunoblot detection. Enaptin staining was observed in both the cytosolic and nuclear fractions. Control experiments were done with annexin A7 antibodies, which detects a band slightly below 50 kDa in all the fractions, tubulin is detected in the cytosolic fraction and emerin was detected in both the nuclear and membrane fractions as expected (Figure 3.13). It might well be that the 400 kDa protein has an actin binding domain but lacks the transmembrane domain supported by the EST clone CA425673.

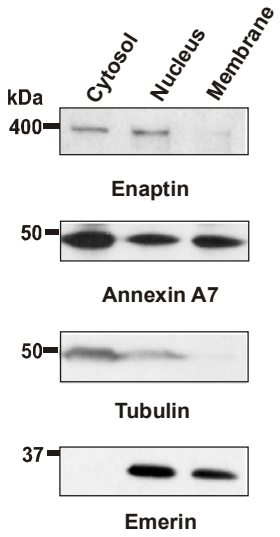

Figure 3.13: Cell fractionation study of fibroblast cells. Immunoblot investigation of fibroblast cells, which were fractionated into cytosol, nuclei and cytoplasmic membranes. The samples were resolved on a 12% SDS gel, blotted onto PVDF membrane and the blots were analysed with Enaptin pab2, annexin A7, ∝-tubulin and emerin specific monoclonal antibodies. Detection was performed with ECL.

3.10 Generation of various Enaptin GFP fusion proteins

To study the contribution of various domains of Enaptin to its cellular localization, we generated GFP fusion constructs of the ABD and the Enaptin-165 isoform. The plasmids that allowed expression of green fluorescent protein (GFP) tagged Enaptin fusion proteins were transfected into COS7 cells. The actin binding domain of Enaptin was fused to GFP at its C-terminus, the second construct consisted of the full-length Enaptin-165 which carried the GFP at its amino terminus (Figure 3.14).

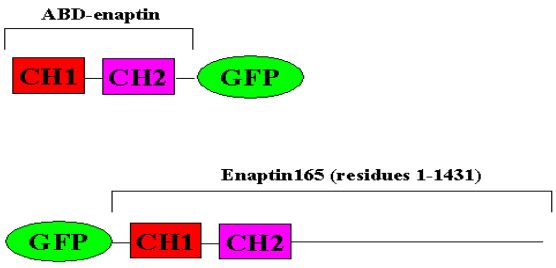

Figure 3.14: Schematic representation of the GFP constructs used for transfection studies. The ABD of Enaptin (residues 2-296) was cloned into the EGFPN3 vector and the full-length Enaptin-165 (residues 1-1431) was cloned into the EGFPC2 vector.

The plasmid allowing the expression of ABD-GFP was transfected into COS7 cells and the cells were costained with TRITC-phalloidin for analysis of cytoskeletal association of the protein (Figure 3.15).

In COS7 cells, the GFP tagged ABD-Enaptin colocalised with the actin stress fibres (Figure 3.15, big arrows), which are not so prominent in this cell line, the cortical actin cytoskeleton (Figure 3.15, arrowheads) and was also found very prominently in the nucleus. In C3H/10T1/2 cells, ABD-Enaptin was found to localise along the stress fibres and it colocalised with vinculin in the focal contacts (Braune, 2002). Vinculin is one of the many proteins specifically found in focal contacts. The GFP fusion protein was also present in the nucleus (Figure 3.15, small arrows). The localisation of ABD-Enaptin-GFP inside the nucleus in both COS7 cells and C3H/10T1/2 cells might be due to the presence of two nuclear localisation signals present in the ABD of Enaptin which may allow its entry into the nucleus.

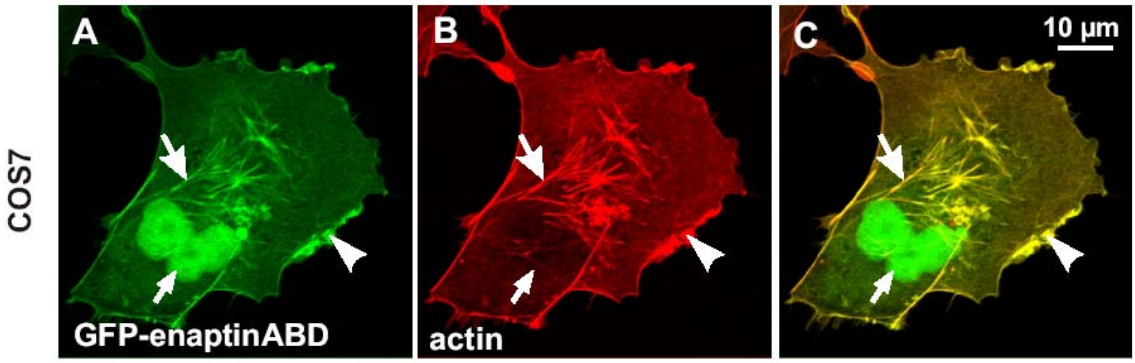

Figure 3.15: The ABD of Enaptin colocalises with the F-actin network in COS7 cells. COS7 cells transfected with the GFP-Enaptin ABD plasmid were stained with TRITC-phalloidin. The cells were fixed with 3% paraformaldehyde and permeabilised with 0.5% Triton X-100. Panel A represents the localisation of the GFP fusion protein, B shows phalloidin-TRITC staining and C shows the merged picture. The pictures were taken using the confocal microscope.

GFP-Enaptin-165 was also transiently transfected in COS7 cells and the cells were fixed with 3% paraformaldehyde and costained with TRITC-phalloidin. As an alternative fixation procedure we used methanol-acetone to allow a staining with an anti-α-tubulin monoclonal antibody (Figure 3.16). These stainings indicate that the GFP-Enaptin-165 fusion protein is present along the stress fibres (big arrows) and that it is also present in the cortical actin cytoskeleton (arrow heads). There is no colocalisation however with the microtubule network, which is in accordance with results obtained with the pab2 staining patterns obtained in COS7 cells (Figure 3.16, D-F). Interestingly, the fusion protein is again prominently located in the nucleus (small arrows). Enaptin-165 harbors three predicted nuclear localisation signals, which might be responsible for this localisation.

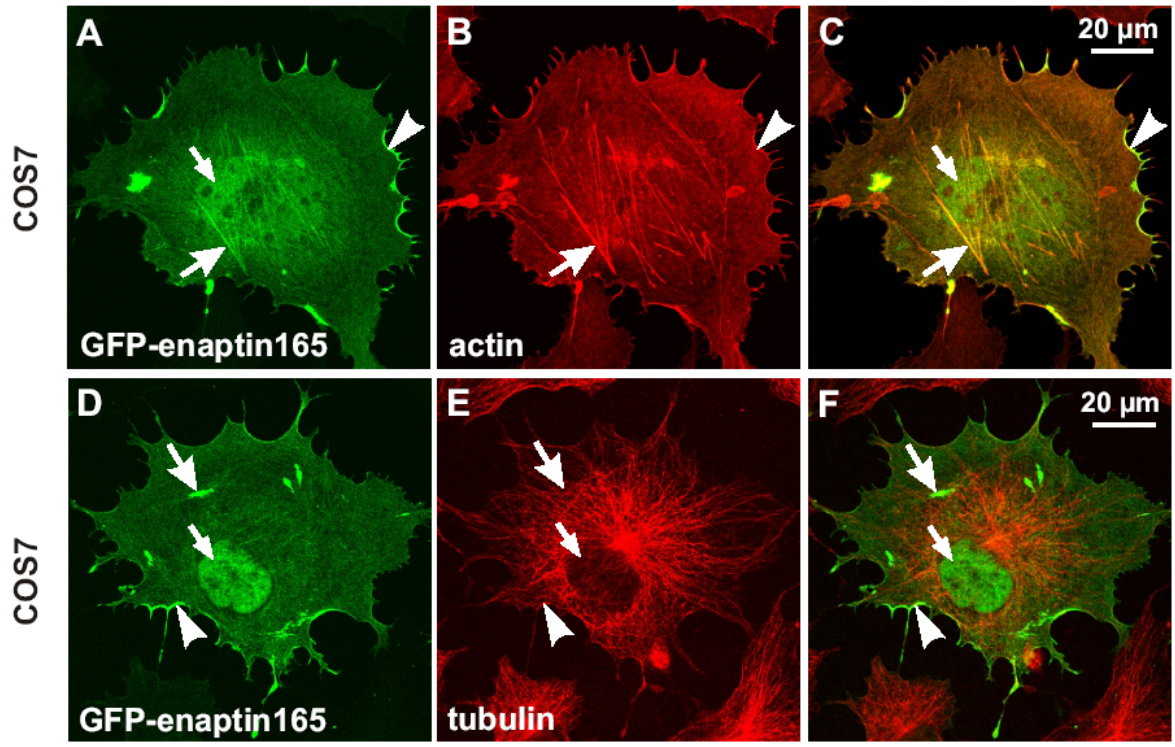

Figure 3.16: Expression of GFP-tagged Enaptin-165 in COS7 cells. COS7 cells transfected with GFP-Enaptin-165 were costained with both TRITC-phalloidin and anti-α-tubulin antibody. The top panels represent Enaptin-165 transfected cells co-stained with TRITC-phalloidin. The cells were fixed with 3% paraformaldehyde and permeabilised with 0.5% Triton X-100. Panel A represents the GFP-Enaptin-165 localisation, B, the TRITC-phalloidin staining; and C, merge. The bottom panels show GFP-Enaptin-165 transfected cells costained with anti-∝-tubulin antibody. D, GFP-Enaptin-165; E, tubulin staining as detected with a Cy3-conjugated anti mouse IgG antibody; F, overlay. Big arrows indicate the stress fibers, small arrows the nucleus, and the arrowheads cortical actin cytoskeleton structures.

3.11 Enaptin localisation in mouse skeletal muscle

A higher expression of Enaptin in muscle as found by multiple tissue expression array analysis (Abraham, 2004) and a possible involvement of Enaptin in muscular dystrophy as evidenced by the association of Enaptin with proteins like lamin A and emerin (Mislow et al., 2002) encouraged us to analyse the distribution of Enaptin in skeletal muscle. Paraffin embedded tissue sections of adult mouse were used for this purpose. The affinity purified pab2 was used at a dilution of 1:10. Muscle sections were costained with anti-skeletal myosin (Figure 3.17, A-C) and anti-desmin antibodies (Figure 3.17, D-F). Myosin is found in muscle sarcomeres which together with actin fibres coordinates the muscle contraction. Desmin is the main intermediate filament protein found in skeletal and heart muscle.

Our Enaptin antibody stains the muscle sarcomeres in adult muscle sections. Double labeling experiments with desmin indicated that Enaptin and desmin only partially colocalise.

Whereas desmin is clearly confined to the Z-disc (arrow heads), Enaptin shows a much wider distrubution around the Z-disc and appears to surround desmin and is located in the neighbouring I-bands (arrows). This finding is confirmed in coimmunofluorescence studies with myosin antibodies which show the myosin location at the A-bands (Figure 3.17, A-C).

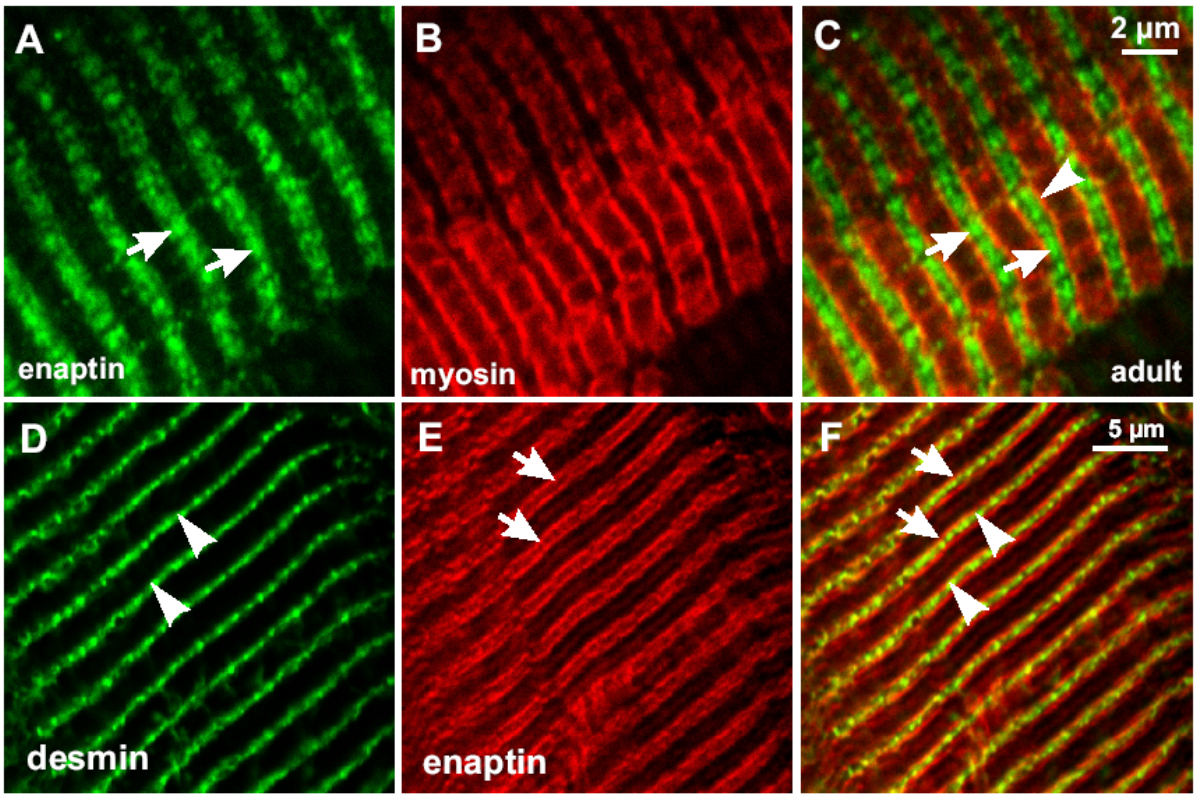

Figure 3.17: Localisation of Enaptin in skeletal muscle. Adult mouse muscle sections stained with Enaptin specific pab2 were costained with myosin and desmin specific monoclonal antibodies. A-C represent a comparison of Enaptin and myosin distribution in mouse skeletal muscle. A, Enaptin staining; B, myosin staining; C, merged picture. D, desmin staining; E, Enaptin staining; F, overlay. Enaptin was detected by anti-rabbit IgG secondary antibody tagged with Alexa 568 and myosin and desmin by a anti-mouse IgG secondary antibody tagged with Alexa 488. Arrows indicate Enaptin staining and arrowheads desmin or myosin staining.

To investigate the distribution of Enaptin in patients affected with a desmin-related myopathy, we stained muscle sections with pab2 and an anti-desmin antibody (Figure 3.18). In these specimens, an aggregation of desmin is observed in addition to the normal desmin location. The sections were prepared by Dr. R. Schröder from the University Hospital in Bonn. We observed a striated pattern (arrows) of desmin distribution as well as the presence of aggregates (Figure 3.18). The Enaptin pattern was not affected by the unusual aggregates of desmin in patient muscle although some Enaptin appeared to be associated with the aggregates.

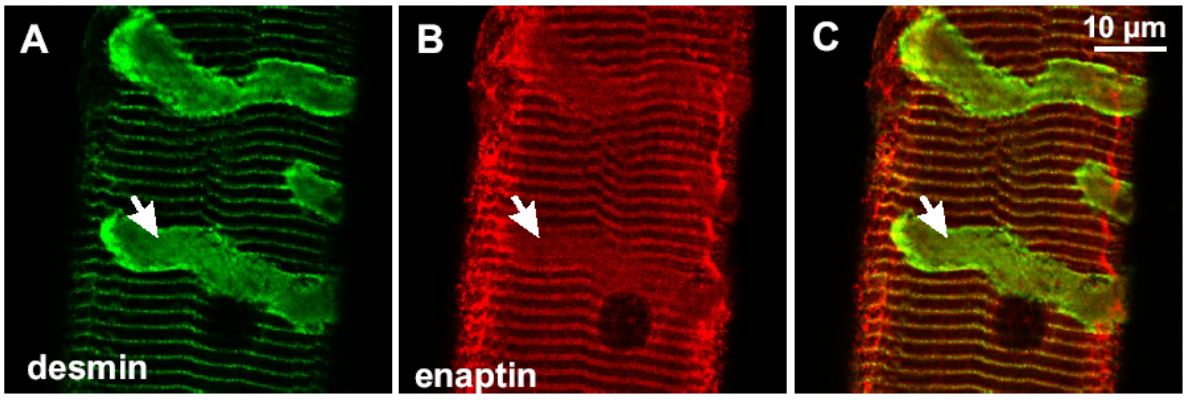

Figure 3.18: Distribution of Enaptin in skeletal muscle obtained from a patient suffering from a desmin-related myopathy. Muscle sections from patients with a desmin related myopathy were costained with pab2 and a monoclonal anti-desmin antibody. Secondary anti-rabbit IgG antibody tagged with Alexa 568 detected Pab2 and an anti-mouse IgG antibody tagged with Alexa 488 detected desmin. A, desmin staining; B, Enaptin staining; C, overlay. The arrows indicate the desmin aggregation.

3.12 Enaptin localisation in human skin

The skin is considered the largest organ of the body and has many different functions. The skin functions in thermoregulation, protection, metabolic functions and

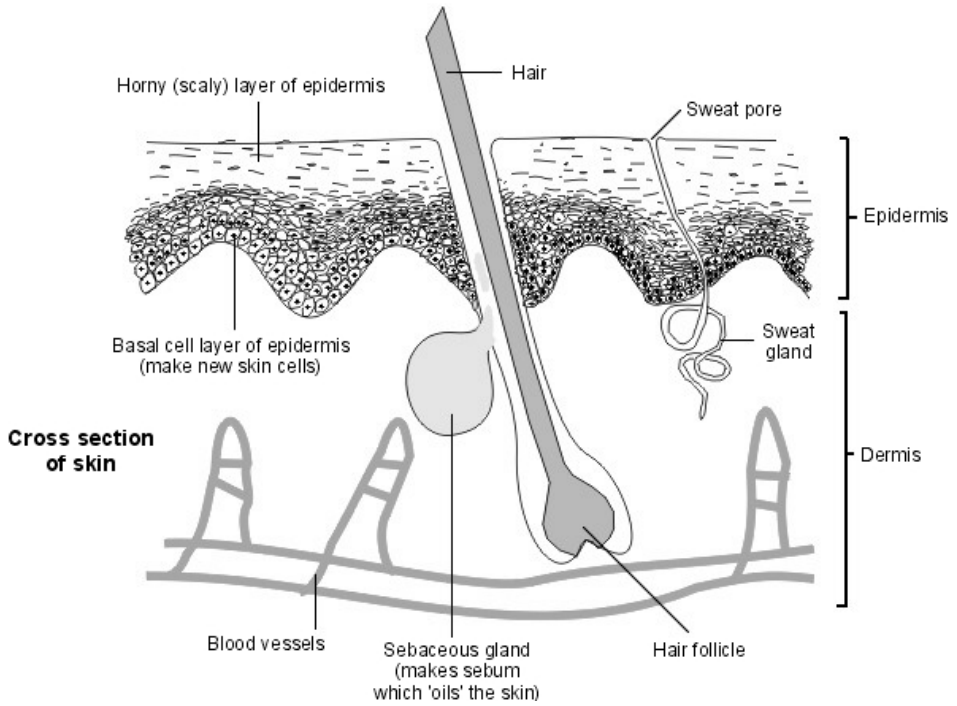

Figure 3.19: A diagram showing a cross section of skin, illustrating its overall histology.

sensation. The skin is divided into two main regions, the epidermis, and the dermis, each providing a distinct role in the overall function of the skin (Figure 3.19). The dermis is attached to an underlying hypodermis, also called subcutaneous connective tissue, which stores adipose tissue and is recognised as the superficial fascia of gross anatomy.

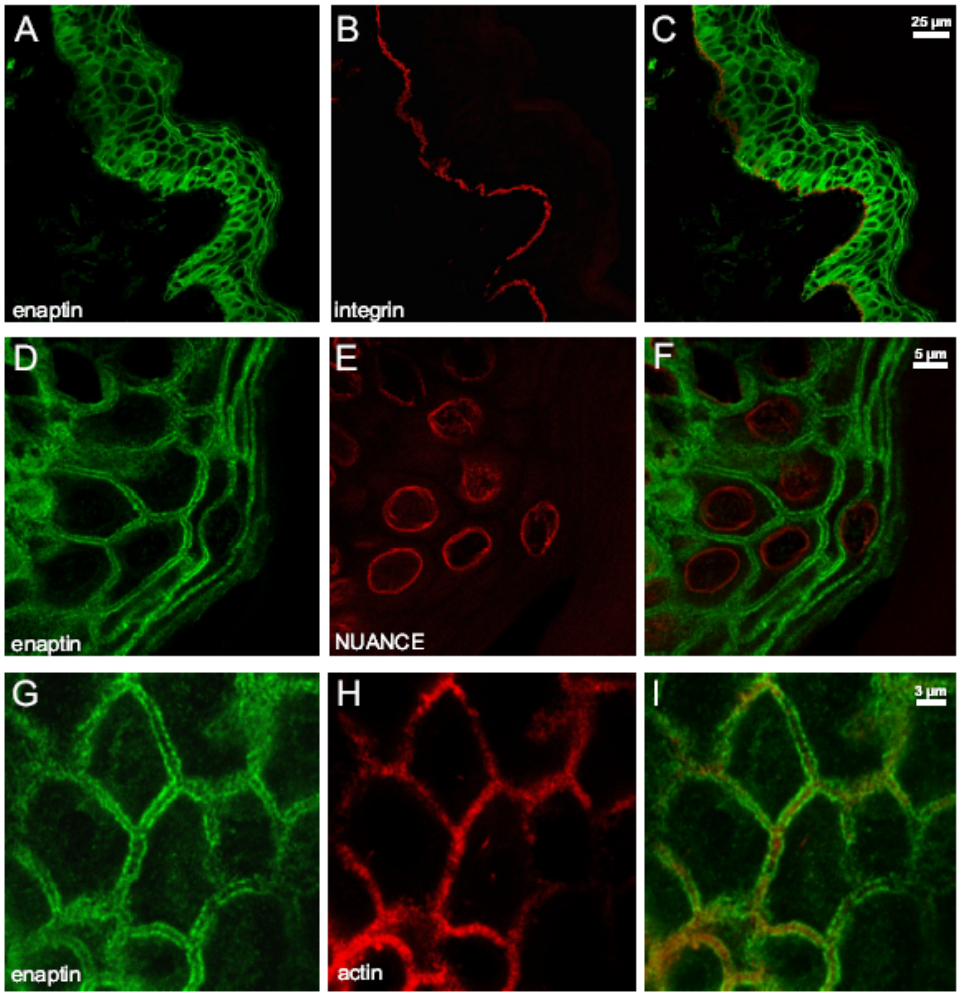

Figure 3.20: Immunofluorescence studies of Enaptin in skin. Confocal pictures of human skin sections stained with pab2 and double stained with rat monoclonal anti-$\alpha_6\beta_4$ antibody (A-C), monoclonal mouse anti-NUANCE antibody (D-F) and Phalloidin-TRITC (G-I). The $\alpha_6\beta_4$ was visualized by secondary antibody conjugated with Alexa 568 and NUANCE by secondary antibody conjugated with Cy3.

Human skin sections were used for the investigation of the localisation of Enaptin. Enaptin polyclonal antibodies stained epidermis of the skin which is shown by double staining with $\alpha_6\beta_4$ (Figure 3.20, A-C). $\alpha_6\beta_4$ is a hemidesmosome specific integrin present in the basal layer of the skin which binds to laminin in the extracellular matrix (van der Flier and Sonnenberg., 2001). $\alpha_6\beta_4$ staining in skin can be seen as a thin layer between the dermis and epidermis. The N-terminal specific pab2 antibodies stain the periphery of all the cells in the epidermis whereas the related protein NUANCE stains the nuclear membrane (Figure 3.20, D-F). This double layered staining around the periphery of the skin cells was further investigated by costaining with phalloidin (Figure 3.20, G-I). Enaptin was found to be present surrounding the actin cytoskeleton with partial colocalisation. The absence of nuclear membrane staining may be due to the presence of Enaptin isoforms in skin which lack the C-

terminal transmembrane domain. The significance of this interesting observation of the presence of Enaptin as a double layer around the cell periphery is yet to be understood.

3.13 Influence of cytoskeletal drugs on the subcellular distribution of Enaptin

The presence of an actin binding domain in the Enaptin protein and its ability to bind to actin both *in vitro* and *in vivo* prompted us to examine the effect of the actin depolymerising drug latrunculin B on the localisation of Enaptin. In latrunculin B untreated cells, the Enaptin antibody stained the nuclear envelope in addition to the actin associated structures (Figure 3.21, A-C). The nuclear envelope localisation of Enaptin remained unperturbed even after the disruption of the actin cytoskeleton. Interestingly the cytosolic localisation of the Enaptin pool was destroyed by this drug (Figure 3.21, D-F). Our results confirm that the cytoplasmic staining corresponds to actin based structures, which is lost with the depolymerisation of the actin cytoskeleton. The indifference in the nuclear envelope localisation of Enaptin maybe due to the fact that the actin cytoskeleton has no role in the NE localisation of Enaptin which is probably held to the nuclear envelope by some other proteins present in the nuclear envelope.

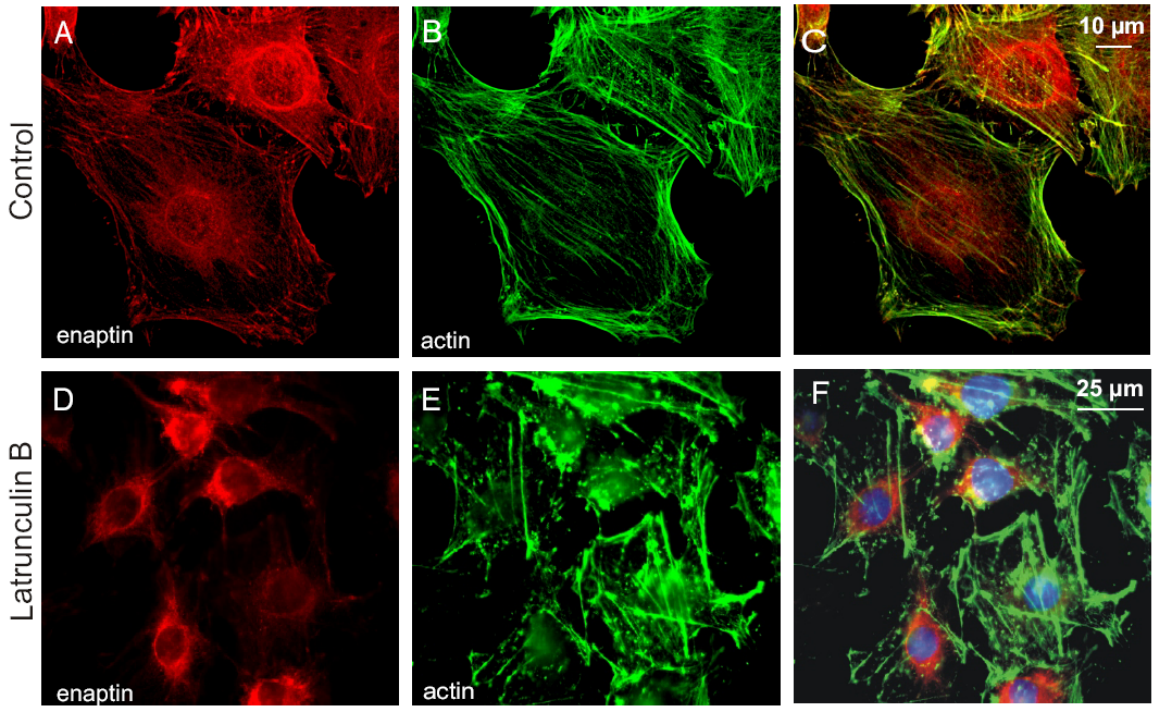

Figure 3.21: Effect of latrunculin B on Enaptin distribution. Mouse fibroblast cells were grown in the absence (A-C) and the presence (D-F) of latrunculin B. The cells were treated with latrunculin B (final concentration: 2.5 µM) for 10 min. The latrunculin B treated cells and untreated cells were fixed with methanol-acetone and stained with pab2 and anti-β-actin antibody and the images taken using a confocal microscope. The pab2 was probed with secondary antibody conjugated with Alexa 568 and the β-actin antibody was probed with secondary antibody conjugated with Alexa 488.

4 Characterisation, localisation and functional analysis of Sun1

4.1 The perinuclear region of Enaptin is highly conserved

The 30 amino acids after the transmembrane domain of Enaptin (PeriNuclear Enaptin; PNE) are highly conserved across different species of organisms. Sequences from mouse and human NUANCE, mouse and human Enaptin, *C. elegans* ANC-1, *Drosophila* Klarsicht, homologous EST clones of zebrafish and chicken were used for the alignment. Of the 30 amino acids used for alignment 12 amino acids are highly conserved in all the organisms (Figure 4.1). This observation suggested to us that this highly conserved region of the protein is involved in the association with a highly conserved protein.

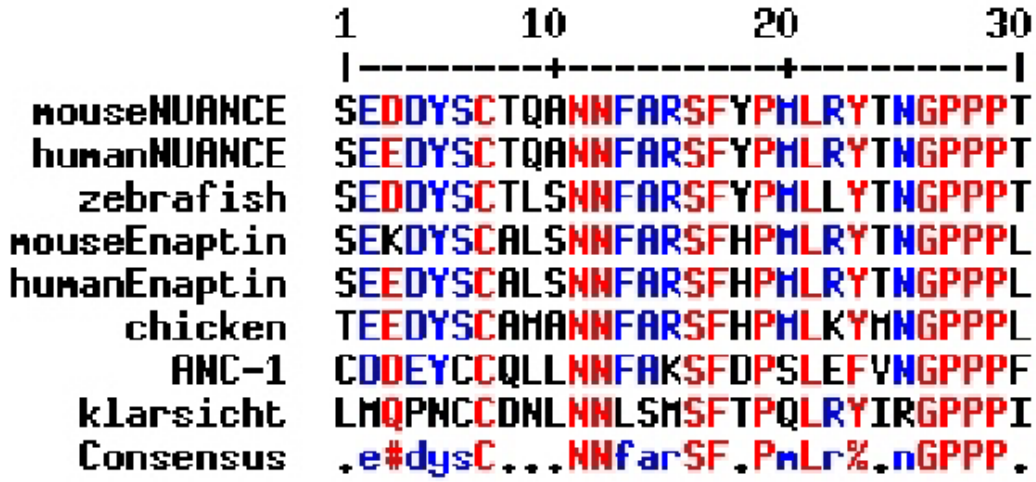

Figure 4.1: Multiple alignment of the perinuclear region of Enaptin with sequences found in homologous proteins. Multiple alignment of mouse NUANCE (CF739892, residues 134-163), human NUANCE (AF435011, residues 6854-6885), zebrafish (BI846027, residues 50-79), mouse Enaptin (BE917568, residues 109-138), human Enaptin (AF535142, residues 8720-8749), chicken (CD732830 residues 101-130), ANC-1 (BK000642, residues 8516-8545), klarsicht (AF157066, residues 2233-2262) using MultiAlin (Corpet et al., 1988).

4.2 SUN domain containing proteins

ANC-1 (*C. elegans* orthologue of Enaptin) failed to localize to the nuclear periphery in the *unc-84* null mutant and in strains carrying alleles that have missense mutations in or near the conserved SUN domain of UNC-84 (*C. elegans* orthologue of the mammalian Sun1 protein). Both proteins are involved in nuclear migration and anchorage in *C. elegans* (Starr and Han, 2002). The SUN domain derives its name from its homology between Sad1 which was found to be present in the spindle pole body of *S. pombe* (Iain and Mitsuhiro, 1995) and UNC-84 which has been shown to be involved in nuclear migration and anchorage in *C. elegans* (Malone et al., 1999). *C. elegans* has two SUN domain containing proteins, UNC-84

and SUN1. SUN1 in *C. elegans* has been shown to be involved in the attachment of centrosomes to the nucleus and also in nuclear migratory events (Malone et al., 2003).

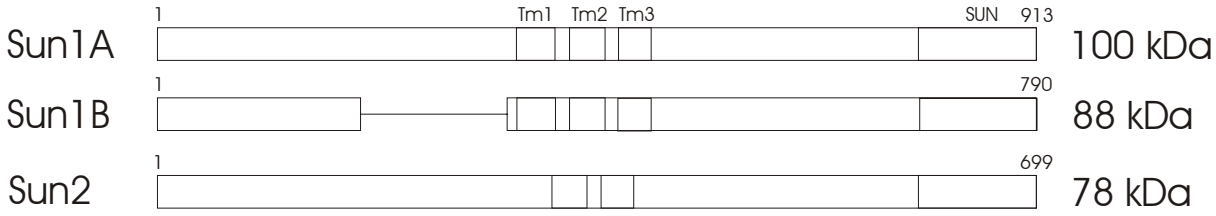

Figure 4.2: Schematic diagram of SUN domain containing proteins in mouse. The same gene *Sun1*, codes for the Sun1A and Sun1B transcripts, whereas a different gene codes for the Sun2 protein. Tm1, Tm2 and Tm3 are the three transmembrane domains and the highly conserved SUN domain is also depicted in the figure. Pictures are not drawn to the scale.

Humans and mice have two genes coding for SUN domain containing proteins, *Sun1* and *Sun2*. *Sun1* is located in the mouse chromosomal locus 5G.2 and codes for two isoforms, Sun1A and Sun1B and *Sun2* in the chromosomal locus 15E.2 coding for the Sun2 protein. Sun1B is an alternatively spliced isoform lacking amino acids 222-234 of Sun1A (Figure 4.2).

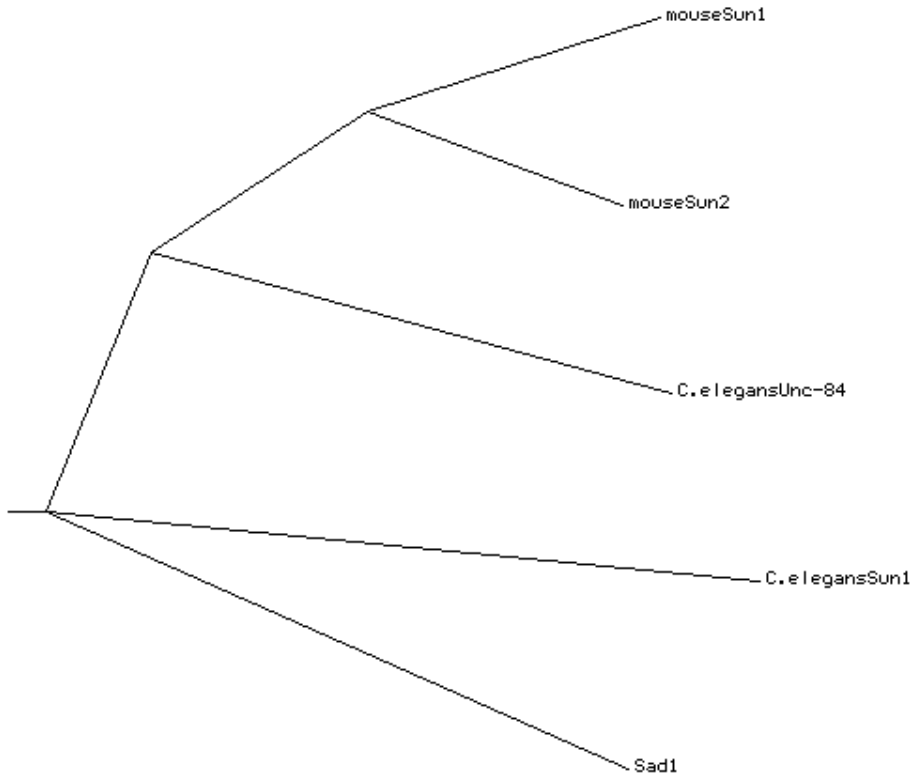

Figure 4.3: Phylogenetic tree of the SUN domain containing proteins. The SUN domains of mouse Sun1 and Sun2, *C. elegans* UNC-84 and Sun1 and yeast Sad1 were aligned on ClustalW alignment and the calculation used for the construction of this tree was done using Phylodendron Phylogenetic tree printer programme. .

The phylogenetic tree constructed by using the SUN domains of the known SUN domain containing proteins shows that the SUN domain of *C. elegans* UNC-84 is more closely related to the mouse Sun1 and Sun2 than that of *C. elegans* SUN1 (Figure 4.3). Interestingly, the SUN domain of mouse Sun1 is 47.8% identical to that of *C. elegans* UNC-84, whereas mouse Sun2 shares only 39.8% identity with the *C. elegans* UNC-84 (Figure 4.4).

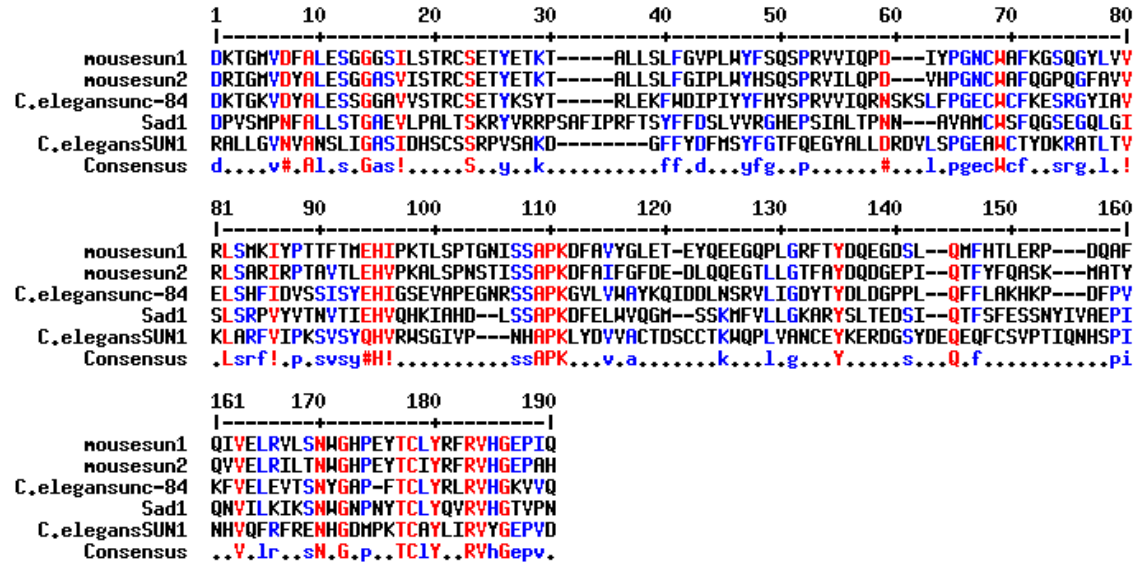

Figure 4.4: Multiple alignment of SUN domains. Mouse Sun1 (AAH48156, residues 738-913), mouse Sun2, *C. elegans* UNC-84 (CAA94142, residues 932-1110), *S. pombe* Sad1 (Q09825, residues 309-489) and *C. elegans* SUN1 (Q20924, residues 266-444) were used for the alignment (Corpet et al., 1988). The reported UNC-84 dependent localisation of ANC-1 and the close similarity between the SUN domains of Sun1 and UNC-84 led us believe that the localisation of Enaptin to the nuclear membrane may be facilitated by the binding of Enaptin with Sun1.

4.3 Sequence and domain analysis of Sun1

The cDNA of the mouse orthologue of UNC-84, Sun1 (accession number AAH48156) was obtained from the IMAGE consortium. Mouse Sun1 codes for a 100 kDa protein composed of 913 amino acids. The protein has three putative transmembrane domains located approximately in the middle of the protein. The N-terminus of the protein has a predicted ZnF-C2H2 domain, which is a DNA binding domain normally found in transcription factors. The C-terminus of the protein has two predicted coiled coil domains (cc1 and cc2) predicted by MULTICOIL programme (Ethan et al., 1997). The final 150 amino acids are highly homologous to *C. elegans* UNC-84 and *S. pombe* Sad1 and is called SUN domain (Figure 4.5 and 4.6).

```
  1 MDFSRLHTYT PPQCVPENTG YTYALSSSYS SDALDFETEH KLEPVFDSPR MSRRSLRLVT
 61 TASYSSGDSQ AIDSHISTSR ATPAKGRETR TVKQRRSASK PAFSINHLSG KGLSSSTSHD
121 SSCSLRSATV LRHPVLDESL IREQTKVDHF WGLDDDGDLK GGNKAATQGN GELAAEVASS
181 NGYTCRDCRM LSARTDALTA HSAIHGTTSR VYSRDRTLKP RGVSFYLDRT LWLAKSTSSS
241 FASFIVQLFQ VVLMKLNFET YKLKGYESRA YESQSYETKS HESEAHLGHC GRMTAGELSR
301 VDGESLCDDC KGKKHLEIHT ATHSQLPQPH RVAGAMGRLC IYTGDLLVQA LRRTRAAGWS
361 VAEAVWSVLW LAVSAPGKAA SGTFWWLGSG WYQFVTLISW LNVFLLTRCL RNICKVFVLL
421 LPLLLLLGAG VSLWGQGNFF SLLPVLNWTA MQPTQRVDDS KGMHRPGPLP PSPPPKVDHK
481 ASQWPQESDM GQKVASLSAQ CHNHDERLAE LTVLLQKLQI RVDQVDDGRE GLSLWVKNVV
541 GQHLQEMGTI EPPDAKTDFM TFHHDHEVRL SNLEDVLRKL TEKSEAIQKE LEETKLKAGS
601 RDEEQPLLDR VQHLELELNL LKSQLSDWQH LKTSCEQAGA RIQETVQLMF SEDQQGGSLE
661 WLLEKLSSRF VSKDELQVLL HDLELKLLQN ITHHITVTGQ APTSEAIVSA VNQAGISGIT
721 EAQAHIIVNN ALKLYSQDKT GMVDFALESG GGSILSTRCS ETYETKTALL SLFGVPLWYF
781 SQSPRVVIQP DIYPGNCWAF KGSQGYLVVR LSMKIYPTTF TMEHIPKTLS PTGNISSAPK
841 DFAVYGLETE YQEEGQPLGR FTYDQEGDSL QMFHTLERPD QAFQIVELRV LSNWGHPEYT
901 CLYRFRVHGE PIQ
```

Figure 4.5: Protein sequence of Sun1. Sun1 is a 913 amino acids containing protein. The amino acids shown in red are present only in Sun1A and not Sun1B. The transmembrane domains are highlighted in blue. The coiled coil domains are highlighted with pink and the SUN domain with green.

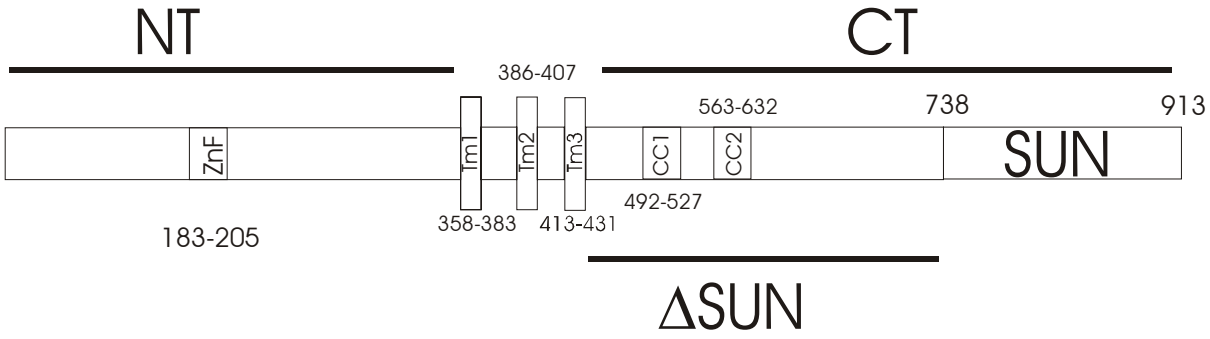

Figure 4.6: Domain architecture of Sun1 predicted by the computer program SMART (Simple Modular ARchitecture Research Tool) and TMpred (a transmembrane domain prediction software) and MULTICOILS program. Sun1 has three transmembrane domains in the middle of the protein. The N-terminus of the protein has a ZNF-C2H2 domain and the C-terminus has two coiled coil domains. The C-terminal end of the protein is highly homologous to the SUN domain.

4.4 The perinuclear segment of Enaptin binds to the C-terminus of Sun1 *in vivo* and the SUN domain is not required for this association

We used a yeast two hybrid assay to investigate the possible interaction between the perinuclear Enaptin sequence (PNE) and Sun1. PNE (the last 30 amino acids of mouse Enaptin) was fused to the binding domain (BD) of Gal4 (BD-PNE). Three different fusion constructs of Sun1 protein containing amino acids after the three transmembrane domains with the activating domain (AD) of Gal4 were made, namely AD-CT (residues 432-913), AD-ΔSUN (residues 432-737) and AD-SUN (residues 738-913). All the three AD fusion constructs were cotransformed into yeast strain Y190 with BD-PNE separately and grown on SD-Trp-Leu medium plates. Negative controls were performed with cotransforming BD fusion construct with AD alone and AD fusion constructs with BD alone. The growth of the transformed yeast cells streaked on SD-Trp-Leu-His (60 mM 3-AT) were monitored over a period of 5 to 7 days. The transformed cells were also streaked on SD-Trp-Leu plates and X-gal assays were performed on these cells.

Yeast two hybrid plasmid constructs		-Trp-Leu-His+ 3AT (60 mM)	X-gal
BD-LE	AD-CT	+++	++++
BD-LE	AD-ΔSUN	+++	++++
BD-LE	AD-SUN	+	++
BD-LE	AD	+	-
BD	AD-CT	+	-
BD	AD-ΔSUN	+	-
BD	AD-SUN	+	-

Figure 4.7: Yeast two hybrid experiments showing the interaction between perinuclear Enaptin and Sun1. The first column shows the different combinations of plasmids used for yeast transformation. The second column shows the result of growth of yeast cells on SD-Trp-Leu-His+3AT (60 mM) plates. The result is indicated by the symbol "+". The symbol "+++" was given when the growth was high and optimal. The symbol "+" was assigned when the growth was minimal. The third column shows the result from the X-gal assay. "++++" symbol was assigned when the intensity of the blue colour was high, "++" when it was half the intensity and "–" when there was no blue colour development.

Y190 cells cotransformed with the plasmids BD-PNE+AD-CT and BD-PNE+AD-ΔSUN grew very well on SD-Trp-Leu-His+3AT (60mM) plates but the cells cotransformed

with BD-LE+AD-SUN grew slowly and stopped growing after a minimal growth. This behaviour matched the growth of the yeast cells cotansformed with the negative control plasmids. The intensity of the blue colour after X-gal assay was found to be high and similar in BD-PNE + AD-CT, BD-PNE + AD-ΔSUN cotransformed cells, but well reduced in BD-PNE + AD-SUN cotransformed yeast. These two results indicate that the ΔSUN domain of Sun1 interacts with the perinuclear C-terminal Enaptin region. The SUN domain is obviously not required for this interaction. The observation of the reduced blue colour in the BD-PNE + AD-SUN could well be due to the fact that there might be some few amino acids in the SUN domain also involved in its binding. Further experiments with different fusion constructs have to be done to map the exact amino acids involved in the binding of the Sun1 protein to Enaptin.

4.5 The perinuclear Enaptin amino acids bind to the C-terminus of Sun1 also *in vitro*

A GST pull down experiment was performed to substantiate the fact that the interaction between the C-terminus of Sun1 and the PNE is indeed not a false positive artefact. The PNE construct was fused to GST using pGEX-4T1 vector and was expressed in *E. coli* and purified by affinity purification using GST beads. The CT, ΔSUN and SUN region of Sun1 were fused to GFP in the EGFP-C2 vector and transfected into COS7 cells. GST-PNE was used to pull down the overexpressed GFP-Sun1 fusion proteins. A negative control was performed where only the GST was used for the pull down experiment.

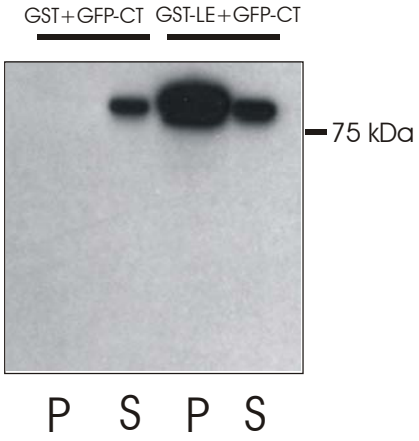

Figure 4.8: PNE binds to the C-terminus of Sun1 in a GST-pull down experiment. The first two lanes indicate the pellet (P) and supernatant (S) fractions after incubating cell lysates overexpressing the GFP-CT fusion protein with GST alone overnight. The final two lanes indicate the pellet and supernatant fractions obtained after the overnight incubation of GST-PNE and GFP-CT. The blot was probed with anti-GFP monoclonal antibody (K3-184-2). The expected molecular weight of GFP-CT is 82 kDa. The amount of protein homogenates loaded was not equal.

The GST-PNE fusion protein was able to pull down the GFP-CT fusion protein as opposed to the GST alone (Figure 4.8) which is consistent with the yeast two hybrid data where BD-PNE showed binding with AD-CT and AD-ΔSUN. However, we were unable to pull down the GFP-ΔSUN or GFP-SUN with the GST-PNE fusion protein.

4.6 A full-length GFP fusion protein of Sun1 localises to the nuclear membrane

Having observed that Enaptin binds to the C-terminus of Sun1 both *in vivo* and *in vitro*, we were interested to study the subcellular localisation of Sun1. The full-length cDNA of Sun1 was fused to the C-terminus of GFP. The fusion protein was overexpressed in COS7 cells and the cells were fixed with paraformaldehyde and observed using the confocal microscope. The full-length Sun1 localised strongly to the nuclear envelope (Figure 4.9).

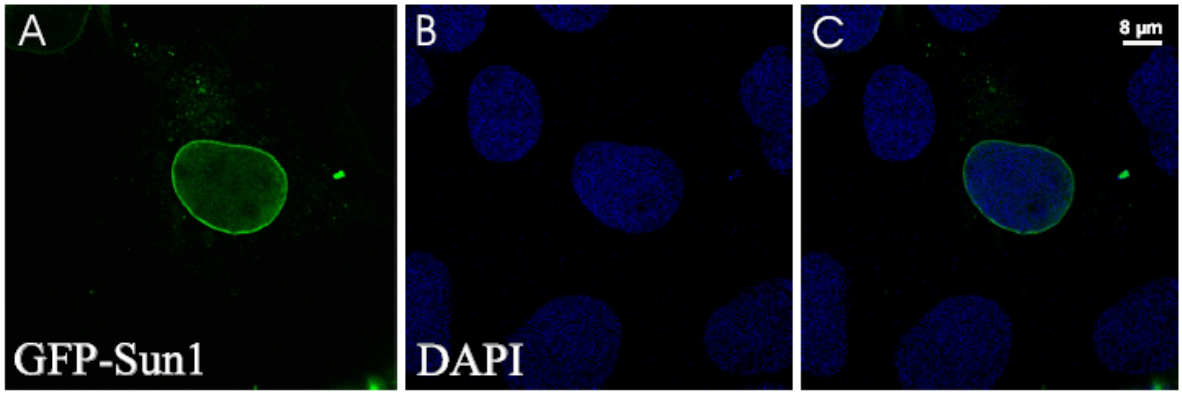

Figure 4.9: GFP-tagged full-length Sun1 localises to the NE when overexpresssed in COS7 cells. The plasmid coding for full-length GFP-Sun1 was transfected into COS7 cells by electroporation. The transfected cells were fixed with paraformaldehyde the next day. Panel A shows the GFP fusion protein expressing cells, panel B is a DAPI staining to reveal the nucleus and panel C shows the merged image. The confocal microscope was used for taking the pictures.

4.7 Endogenous Sun1 is present in the nuclear membrane in HEK cells

The presence of endogenous Sun1 was analysed by direct immunofluorescence. Polyclonal antibodies produced against the N-terminal (281) and C-terminal region (282) of Sun1

Figure 4.10: Schematic representation of the position of the epitopes used for the generation of the polyclonal antibodies 281 and 282.

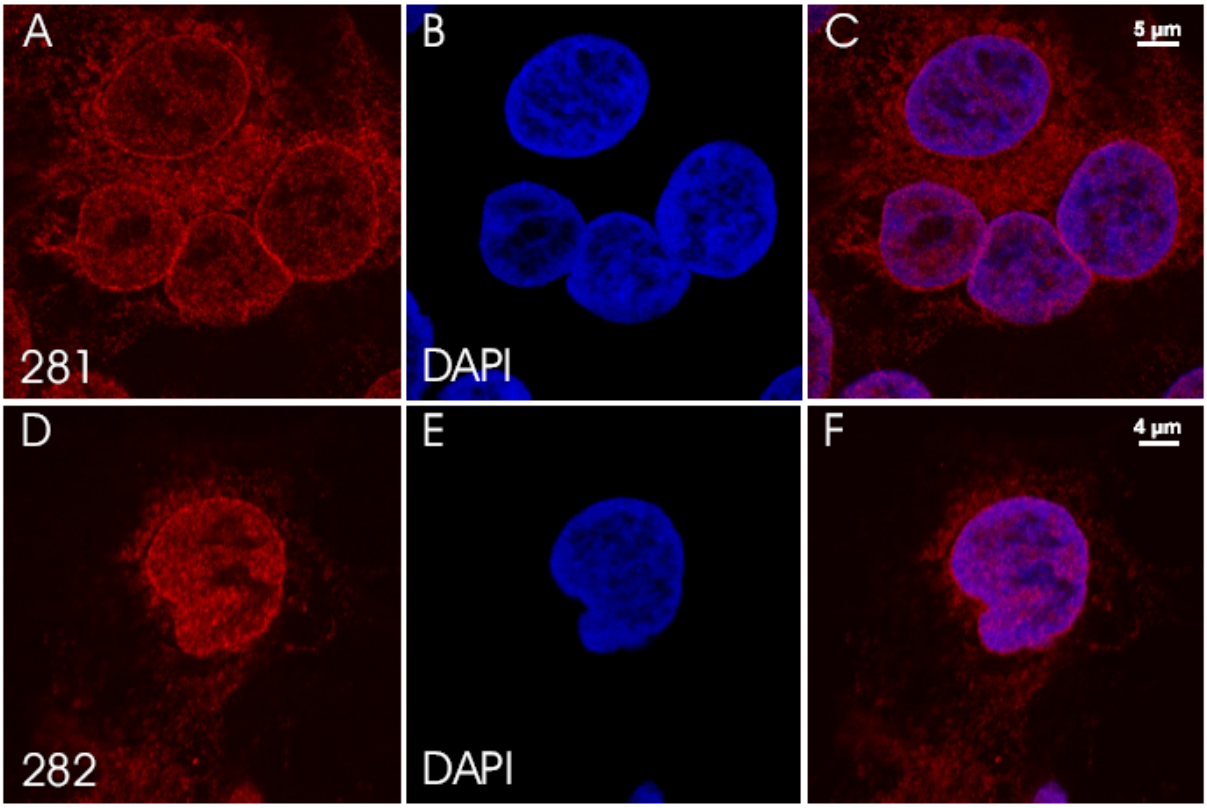

Figure 4.11: Endogenous Sun1 localises to the nuclear envelope in HEK cells. HEK cells were stained with polyclonal antibodies produced against peptides located at the N-terminus of Sun1 (281) and the C-terminus of Sun1 (282). The figures in the first (A-C) row show the cells stained with 281 and the second row (D-F) show the staining with 282 antibodies. The cells were fixed with paraformaldehyde and observed under the confocal microscope. The secondary antibody used was conjugated with Alexa 568. .

(Figure 4.10) were used to stain HEK cells. The antibodies are a kind gift from Dr. Josef Gotzmann (Biocenter, Vienna). Both the antibodies stained the nuclear envelope in addition to the diffused staining all across the nucleoplasm and cytoplasm (Figure 4.11).

4.8 Expression profile of Sun1 in COS7 and HEK cells

To learn more about Sun1, the expression levels of endogenous Sun1 in COS7 and HEK cells were investigated in western blotting using the 281 polyclonal antibodies. The 281 unpurified serum detected two different bands, one band between 75 and 100 kDa (Figure 4.12, arrow) and the other between 50 and 75 kDa (arrowhead, Figure 4.12). The band between 75 and 100 kDa in COS7 cells could correspond to the 88 kDa polypeptide predicted for the Sun1B isoform. However the Sun1A isoform (100 kDa) was not detected in either of the cell lines investigated. It might be expressed in other cell types not included in the present analysis. The inability to detect the 88 kDa protein in HEK cells maybe due to the degradation of endogenous Sun1 during lysate preparation with the observed ~60 kDa band being the

degradation product or may be the result of alternative expression pattern of the Sun1 gene in HEK cells.

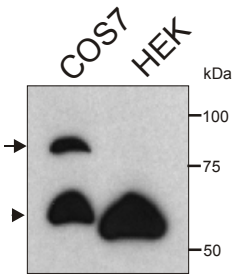

Figure 4.12: Expression profile of Sun1 in COS7 and HEK cells. Cell lysates prepared from COS7 and HEK cells were resolved on a 12 % SDS-PAGE and blotted onto a PVDF membrane. The blots were probed with the 281 polyclonal serum and the detection was performed with ECL. The arrow indicates the Sun1B isoform, and the arrowhead indicates an additional ~60 kDa immunoreactive product.

4.9 N- and C-terminal segments of Sun1 localise independently to the nuclear membrane

To further investigate the localisation of different domains of Sun1, various deletion constructs were made. The N-terminus of Sun1 with the first two transmembrane domains was fused to GFP (GFP-NT+2TM, residues 1-412) and the C-terminus of Sun1 with all three transmembrane domains was fused to GFP (GFP-CT+3TM, residues 368-913) (Figure 4.13). The plasmids were transfected in COS7 cells by electroporation.

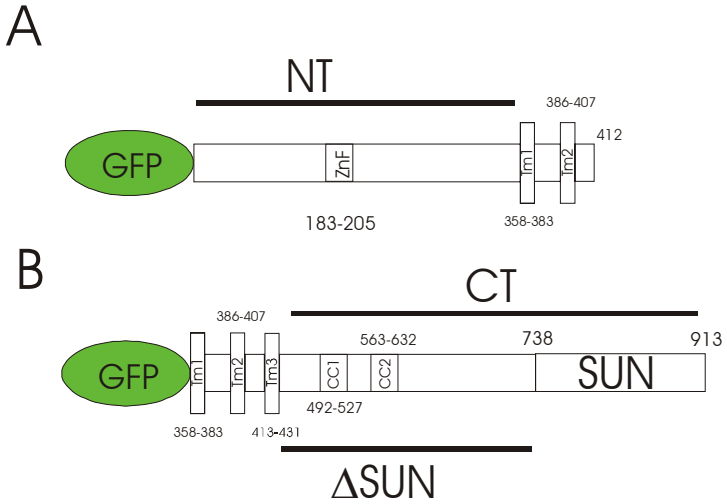

Figure 4.13: Schematic representation of two GFP fusion constructs of Sun1 GFP-NT+2TM (A) and GFP-CT+3TM (B).

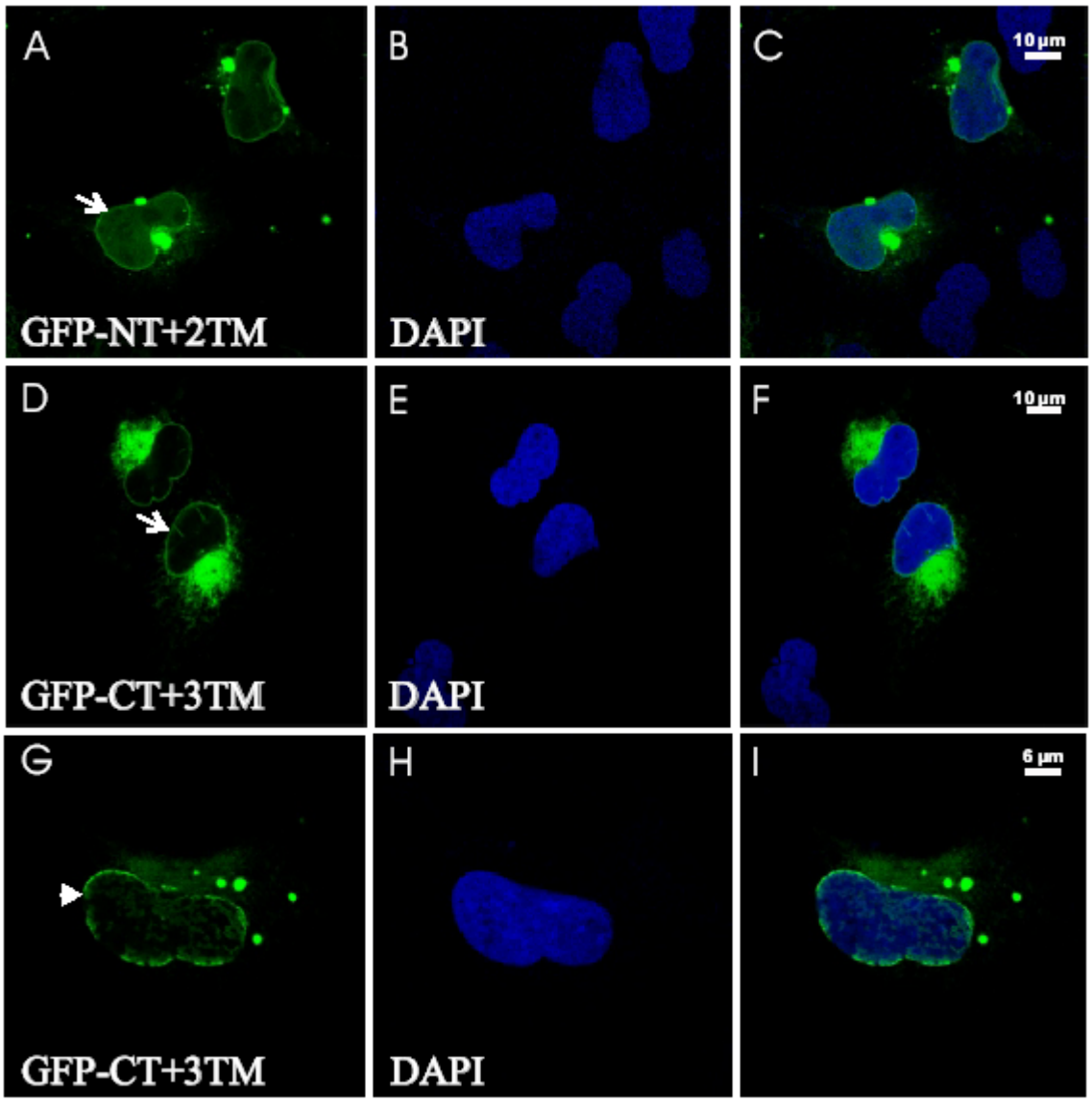

Figure 4.14: Overexpression of GFP-NT+2TM and GFP-CT+3TM in COS7 cells. Panels A-C represent cells transfected with GFP-NT+2TM. Panels D-F indicate the GFP-CT+3TM overexpression. The cells were fixed with paraformaldehyde and stained with DAPI and observed under confocal microscope. The arrows indicate the nuclear envelope staining and the arrowheads indicate the discontinuous nuclear membrane staining.

Both the N- and C-terminal GFP fusions of Sun1 were found to localise to the nuclear membrane (Figure 4.14, A-F). Interestingly, most of the cells transfected with GFP-CT+3TM gave a discontinuous nuclear membrane staining. (Figure 4.14, G-I, arrowheads). The overexpressed GFP-NT+2TM protein formed aggregates apart from the nuclear envelope staining. But on the other hand, GFP-CT+3TM seemed to be present also in structures similar to the endoplasmic reticulum in addition to the nuclear envelope localisation. This observation was confirmed by staining the transfected cells with antibodies against the specific endoplasmic reticulum marker PDI (protein disulfide isomerase) (Figure 4.15). PDI family

proteins are involved in the processing and maturation of secretory proteins in the ER by catalysing the rearrangement of disulfide bonds.

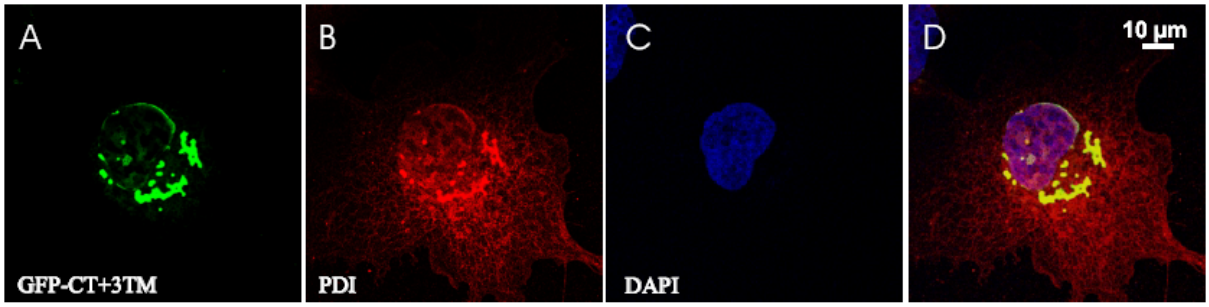

Figure 4.15: The GFP-CT+3TM fusion protein localizes to the ER and the nuclear envelope. Confocal images of COS7 cells transfected with GFP-CT+3TM. Cells were fixed with paraformaldehyde and permeabilised with Triton X-100 before staining. Rabbit anti-PDI polyclonal antibodies were used as an ER marker. PDI was visualised by probing with a secondary antibody conjugated with Alexa 568.

The C-terminus of Sun1 lacking the first transmembrane domain when fused to GFP (GFP-CT residues 432-913), failed to localise to the nuclear envelope. A diffused cytosolic staining was observed underlining the importance of the transmembrane domains for the NE localisation (Figure 4.16).

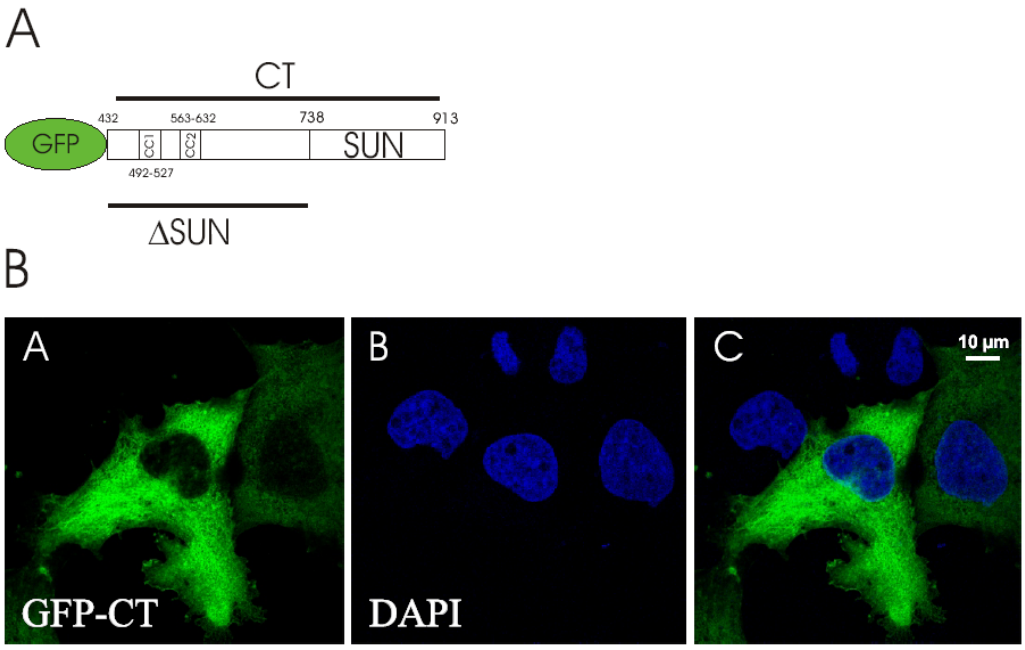

Figure 4.16: Overexpression of GFP-CT in COS7 cells gives a diffused cytosolic distribution. Figure A is the schematic diagram of the fusion construct used. Figure B shows the confocal images taken after transfecting this construct into COS7 cells. Panel A shows a diffused cytosolic distribution of this overexpressed fusion protein. Nuclear staining with DAPI is shown in panel B and panel C is the merged image.

4.10 Sun1 dimerises *in vivo*

α-Helical coiled-coils represent what is probably the most widespread assembly motif found in proteins. A coiled-coil model was first proposed by Crick in 1953 and is comprised of two, three, or four right-handed amphipathic α-helices, which wrap around each other in a left-handed supercoil with a crossing angle of approximately 20° between helices such that their hydrophobic surfaces are in continuous contact to form dimeric, trimeric, or tetrameric coiled-coils respectively. Two-stranded coiled-coils have traditionally been recognized as a dimerisation unit in fibrous proteins such as tropomyosin (Greenfield et al., 2003) and myosin (Malnasi-Csizmadia et al., 1998) as well as the longest coiled-coil found so far, NuMA (1485 residues) (Harborth et al., 1995). The MULTICOILS program predicts two coiled coil domains in Sun1 after the transmembrane domains (residues 492-527 and residues 563-632) (Figure 4.17).

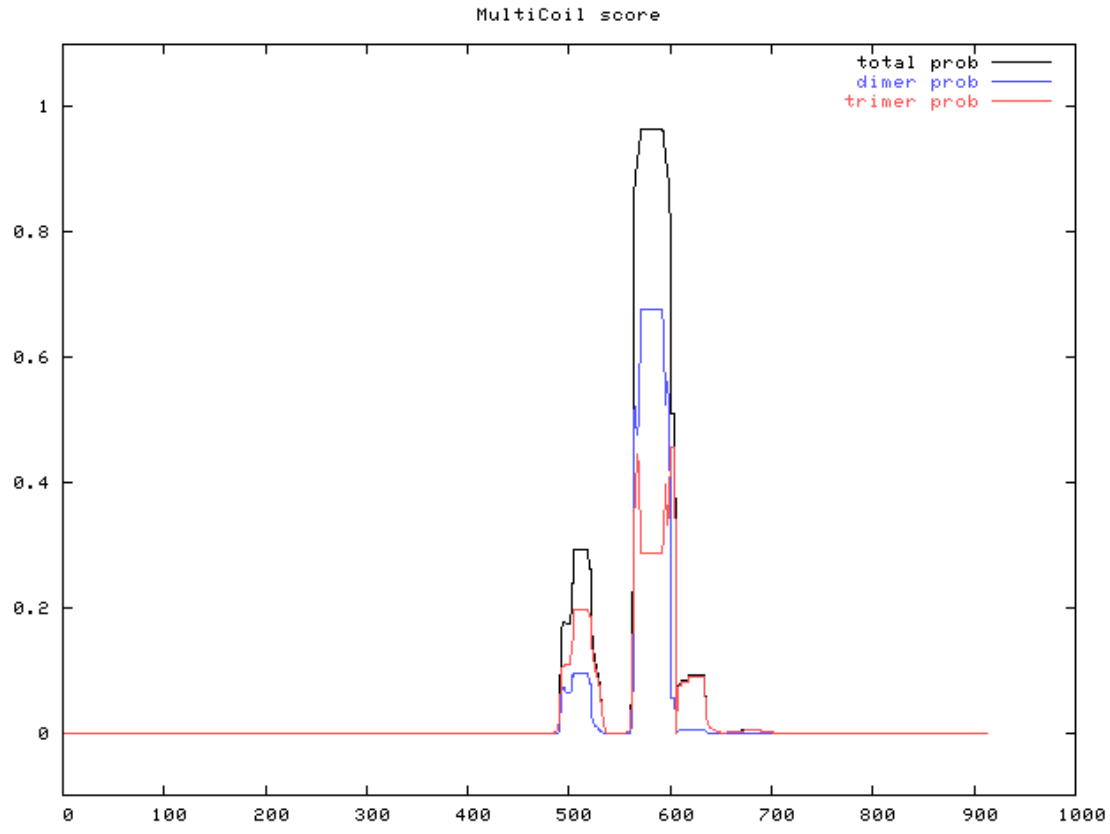

Figure 4.17: MULTICOILS program predicts two coiled coil domains in Sun1 (Ethan et al., 1997). This prediction matches with the coiled coil domains predicted by the SMART software.

It was earlier observed that ΔSUN interacts with Enaptin *in vivo* and in *vitro* (Figure 4.7 and 4.8). It is very unlikely that this GFP deletion construct is retained in the nuclear envelope by its association with Enaptin owing to the fact that the localisation of ANC-1 (*C. elegans* orthologue of Enaptin) to the nuclear envelope was Unc-84 dependent (*C. elegans*

orthologue of Sun1) and not *vice versa* (Starr and Han, 2002). This strengthened the notion that the ΔSUN domain has some association other than Enaptin or NUANCE for its retention to the NE and this is most likely due to dimerisation with endogenous Sun1.

In order to analyse the oligomerisation properties of the Sun1 molecule, the ΔSUN domain was fused to both the binding domain (BD) and the activating domain (AD) of Gal4 and these constructs were cotransformed on Y190 yeast cells. The transformed cells were selected on SD-Trp-Leu-His +3AT (60 mM) plates and also an X-gal assay was performed. Two negative controls were performed to prove that the interaction was not false positive. In contrast to the negative controls, the yeast cells transformed with the fusion constructs grew efficiently on SD-Trp-Leu-His +3AT(60 mM) plates and also turned blue in the X-gal assay (Figure 4.18). All these experiments prove that the ΔSUN domain interacts with itself *in vivo* in yeast two hybrid assays.

Yeast two hybrid constructs		-Trp-Leu-His+ 3AT (60 mM)	X-gal
BD-ΔSUN	AD-ΔSUN	+++	+++
BD-ΔSUN	AD	+	-
BD	AD-ΔSUN	+	-

Figure 4.18: Yeast two hybrid experiments show that Sun1 forms homodimers through the ΔSUN domain. Three sets of cotransformation were done, ΔSUN + ΔSUN and two negative controls, ΔSUN+AD and ΔSUN+BD. Dimerisation was marked by optimal growth of yeast cells on -Trp-Leu-His+3AT (60 mM) plates which is indicated by "+++" whereas the growth was inhibited in negative controls which is indicated by "+". Blue colour development in X-gal assay is indicated by "+++" and no development of blue colour in negative controls is symbolised with "-".

4.11 The SUN domain is not required for the NE localisation of Sun1

Having known that the N- and C-terminal fragments of Sun1 are able to localise to the NE independently, our focus turned into knowing the significance of the SUN domain in the NE localisation of the C-terminus of Sun1. A GFP construct composed of the C-terminus of Sun1 without the SUN domain but with all the transmembrane domains (GFP-SUN+3TM, residues 368-737) was constructed to address this issue (Figure 4.19). Interestingly enough, this construct was still able to localise to the nuclear membrane underlining that the SUN domain is not important for the NE localisation of Sun1 (Figure 4.20). The discontinuous NE

localisation as seen with the GFP-CT+3TM was not seen with this construct. The NE localisation of GFP-ΔSUN+3TM is probably because that ΔSUN domain can dimerise with the endogenous Sun1 protein present in the COS7 cells.

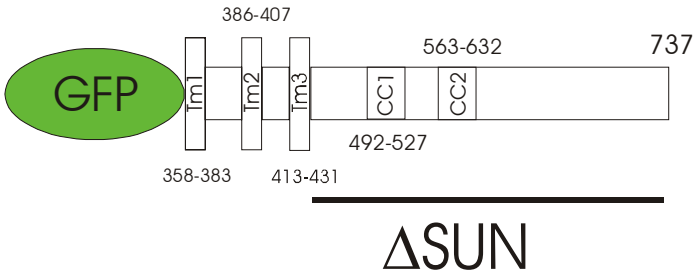

Figure 4.19: Schematic representation of the ΔSUN domain fused to GFP (GFP-ΔSUN+3TM).

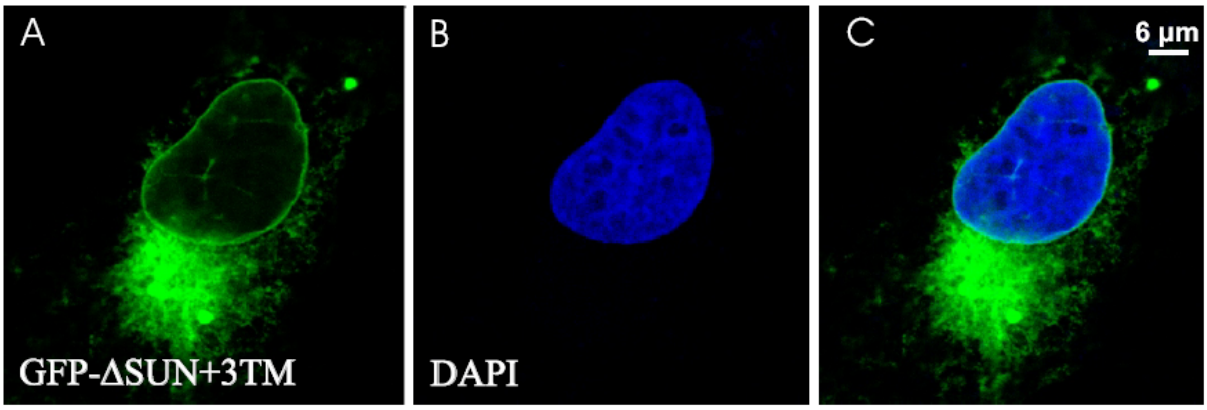

Figure 4.20: The NE localisation of overexpressed GFP-ΔSUN+3TM fusions in COS7 cells. The GFP-Sun1 fusion protein localises to the nuclear envelope along with a diffused presence in ER (panel A). The DAPI staining of nucleus (panel B) and the merged image (panel C) are also shown. The pictures were taken using the confocal microscope.

The beautiful rim-like staining around the periphery of the nucleus and the absence of discontinuous staining unlike that of GFP-CT+3TM is most likely due to the absence of the SUN domain. However, it is unclear how the SUN domain is able to bring about the unusual discontinuous staining and the largely ER aggregation of the GFP-CT+3TM consruct. This led to the hypothesis that Sun1 probably dimerises with the binding of SUN domain of one molecule to the ΔSUN of a neighboring Sun1 and the second to the third and thus could form a continuous polymer in the lumen of the ER. This pattern of polymerisation could finally segregate the fusion construct in the ER causing mislocalisation. On the other hand, SUN domain also could dimerise with itself bringing about the same effect. However, we were

unable to detect a direct binding between the SUN- ΔSUN domains and SUN-SUN domains in yeast two hybrid experiments (Figure 4.21).

Yeast two hybrid constructs		-Trp-Leu-His+ 3AT (60 mM)	X-gal
BD-SUN	AD-ΔSUN	+	-
BD-SUN	AD-SUN	+	-
BD	AD-ΔSUN	+	-
BD	AD-SUN	+	-
BD-SUN	AD	+	-

Figure 4.21: Yeast two hybrid experiments prove that SUN domain does not interact with ΔSUN domain and also does not dimerise with itself. The first two columns shows the different combinations of constructs used for yeast transformation. The second column shows the result of growth of yeast cells on SD-Trp-Leu-His+3AT (60 mM) plates. The result is indicated by the symbol "+". The symbol "+" was assigned when the growth was minimal. The third column shows the result from X-gal assay. The symbol "–" was assigned when there was no development of the blue colour.

The GFP-ΔSUN fusion construct (residues 432-737) without the transmembrane domains (Figure 4.22, A) was not able to localise to the nuclear membrane as expected (Figure 4.22, B).

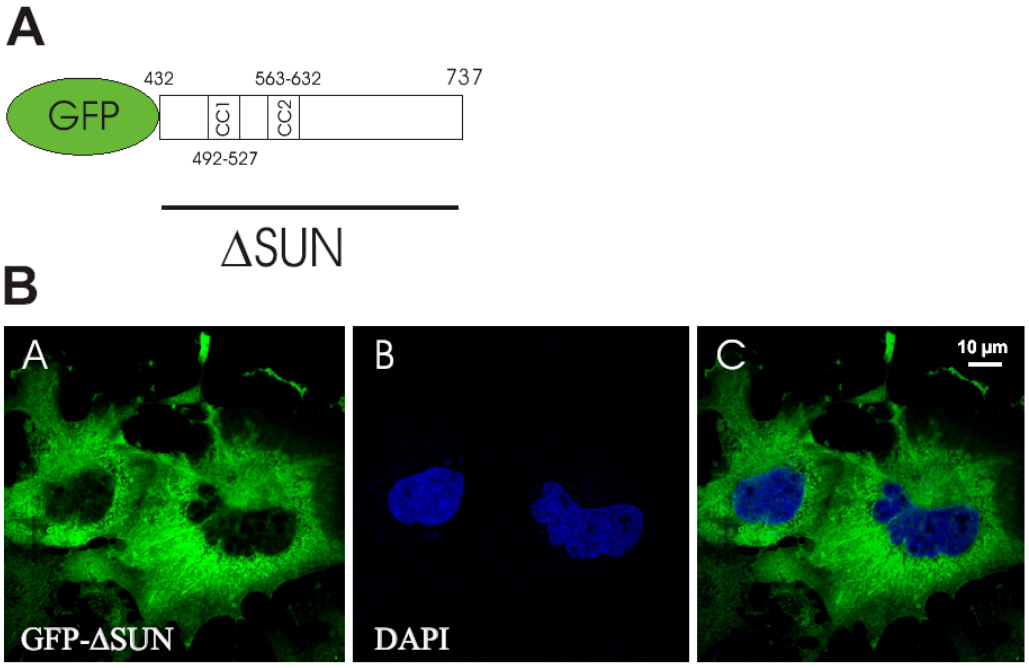

Figure 4.22: Overexpression of GFP-ΔSUN in COS7 cells. The figure A is a schematic representation of the fusion construct used for the transfection. Figure B are confocal images taken of COS7 cells transfected with this construct. The fusion protein is diffused throughout the cytoplasm (panel A). The cells were stained with DAPI for DNA (panel B). Panel C depicts the merged image.

When the SUN domain was fused to GFP (residues 738-913) it localised to the nucleus in COS7 transfected cells (Figure 4.23), though there is no predicted nuclear localisation signal present. This nuclear localisation is mostly due to the passive diffusion of this protein with GFP into the nucleus. The diameter of the channels of the nuclear pore complexes is 10 nm (Hinshaw et al., 1992) large enough to allow the diffusion of globular proteins with masses under approximately 60 kDa. The molecular weight of GFP-SUN fusion protein is 46 kDa, which is well below the cut-off molecular weight of the nuclear pores.

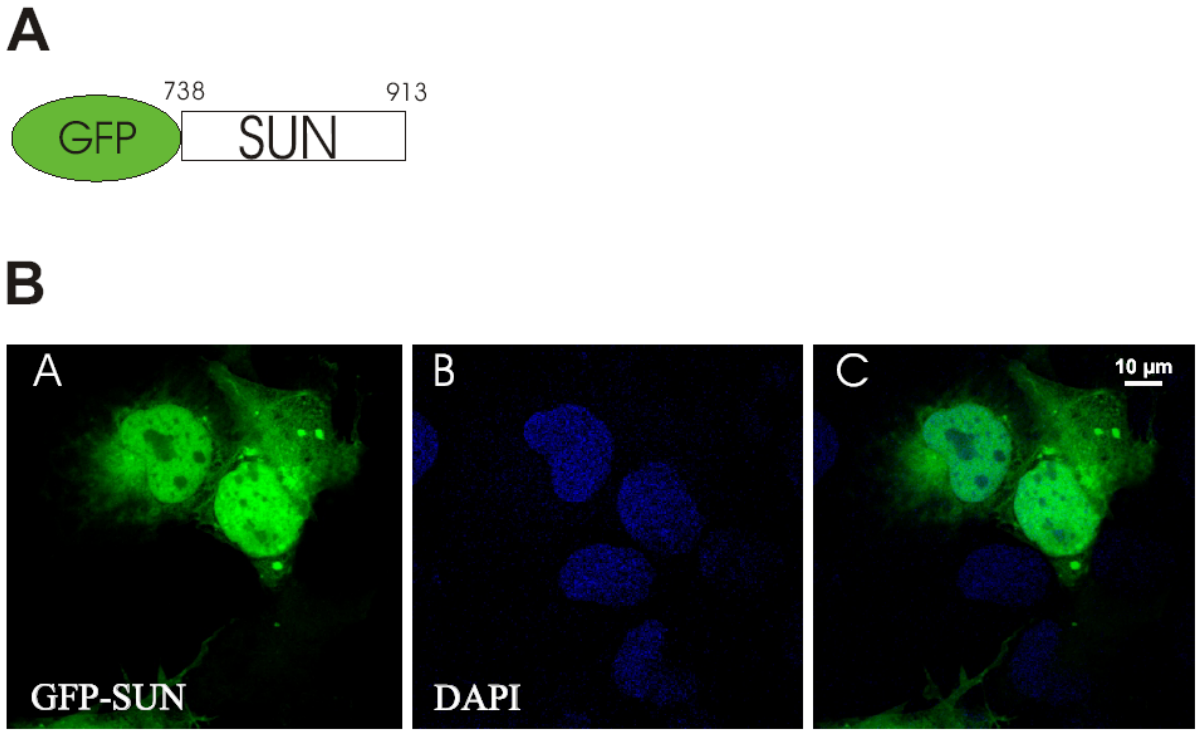

Figure 4.23: GFP-SUN fusion protein largely localises to the nucleus. Figure A is the schematic representation of the fusion construct used. Figure B shows confocal images taken after transfecting this construct in COS7 cells. GFP-Sun localises largely to the nucleus with some diffused staining in the cytosol (panel A). Panel B shows DAPI staining and panel C is the merged image.

4.12 Western blotting confirms the expression of all the GFP fusion proteins

The expression of all the GFP fusion constructs used in our studies was confirmed by western blotting with an anti-GFP monoclonal antibody (K3-184-2). COS7 cell lysates transfected with these constructs were resolved on a 12 % polyacrylamide gel and transferred onto a PVDF membrane. The schematic diagram representing the amino acids of all the fusion proteins used is depicted in Figure 4.24, A. All the fusion proteins detected had the expected molecular weights (Figure 4.24, B).

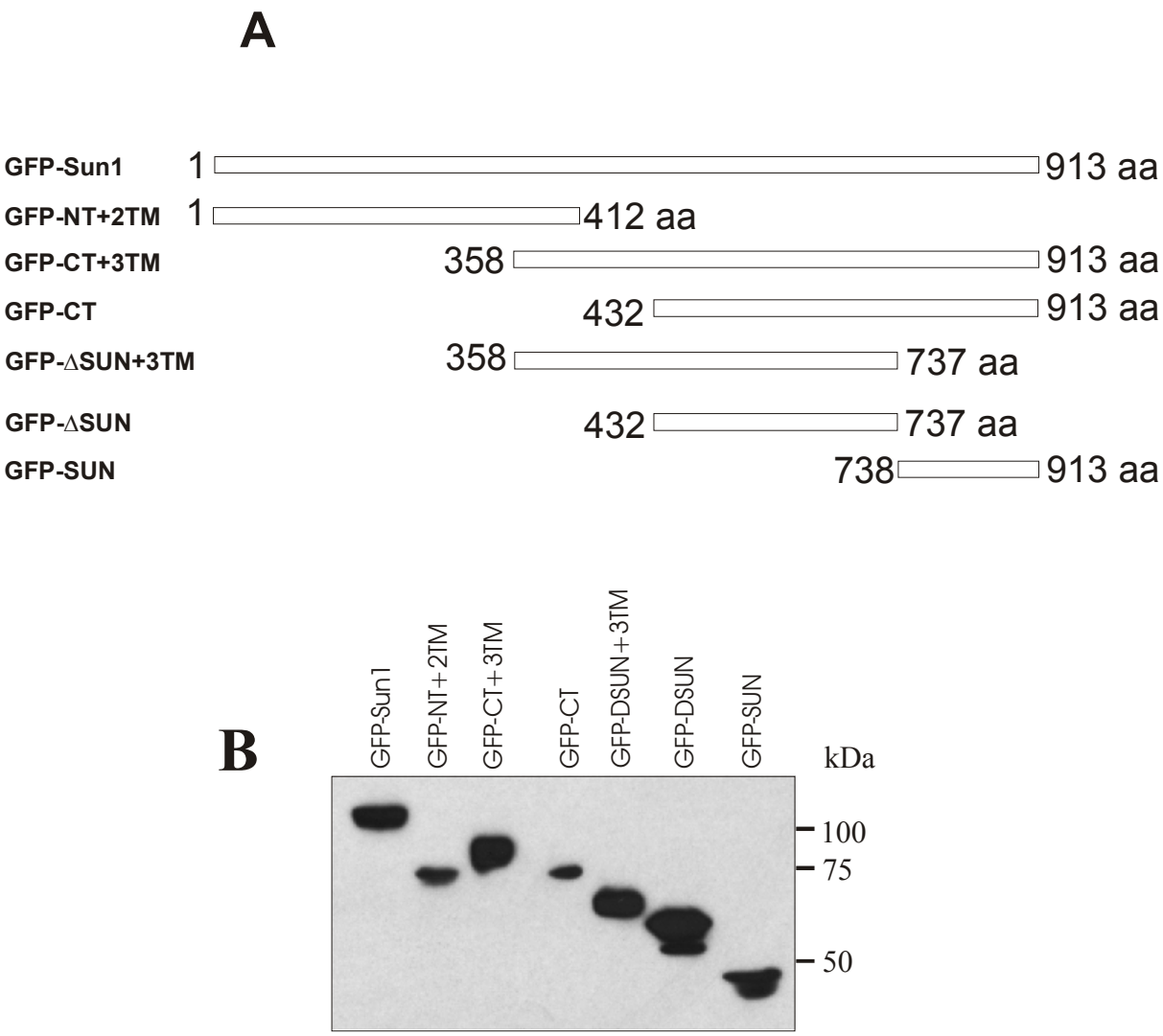

Figure 4:24: Western blotting of all the GFP fusion proteins used for our transfection experiments proves the expression and proper sizes of all the proteins. Figure A shows a schematic diagram of all the fusion proteins used for the COS7 transfection experiments. Figure B is the western blotting analysis of the various COS7 GFP-Sun1 laysates to prove the expression of all the GFP fusion proteins. All the fusion proteins were detected at the expected molecular weight, GFP-Sun1 (128 kDa), GFP-NT+2TM (73 kDa), GFP-CT+3TM (89 kDa), GFP-CT (82 kDa), GFP-ΔSUN+3TM (70 kDa), GFP-ΔSUN (62 kDa) and GFP-SUN (46 kDa). The blot was probed with anti-GFP monoclonal antibody. The detection was performed with ECL.

4.13 GFP-CT+3TM behaves like a dominant negative of Sun1 and displaces endogenous Sun1, NUANCE and emerin from the nuclear membrane

The discovery that Sun1 binds to Enaptin and NUANCE (Libotte, 2004) and the presence of Sun1 at the nuclear membrane encouraged us to do more experiments to find out the physiological relevance of these interactions of these proteins. We accidentally found that GFP-CT+3TM displaces NUANCE when we were looking for ways to knock Sun1 out of the nuclear membrane. Owing to the fact that COS7 cells are easily transfectable cell lines by

electroporation and the presence of NUANCE but not Enaptin in the NE of COS7 cell line, the analysis of NUANCE distribution but not of Enaptin was pursued in the following transfection experiments. It was observed that most of the COS7 cells transfected by this dominant negative (DN) construct stained negative for NUANCE in the nuclear membrane (Figure 4.25, E-H, arrowheads).

This interesting observation is probably the manifestation of the displacement of the endogenous Sun1 protein by this dominant negative construct, which was later substantiated by staining the transfected cells with antibodies specific to the N-terminus of Sun1 (281). Most of the transfected cells stained negative for Sun1 (Figure 4.25, A-D, arrowheads). However, the mechanism by which this DN construct displaces endogenous Sun1 is not understood.

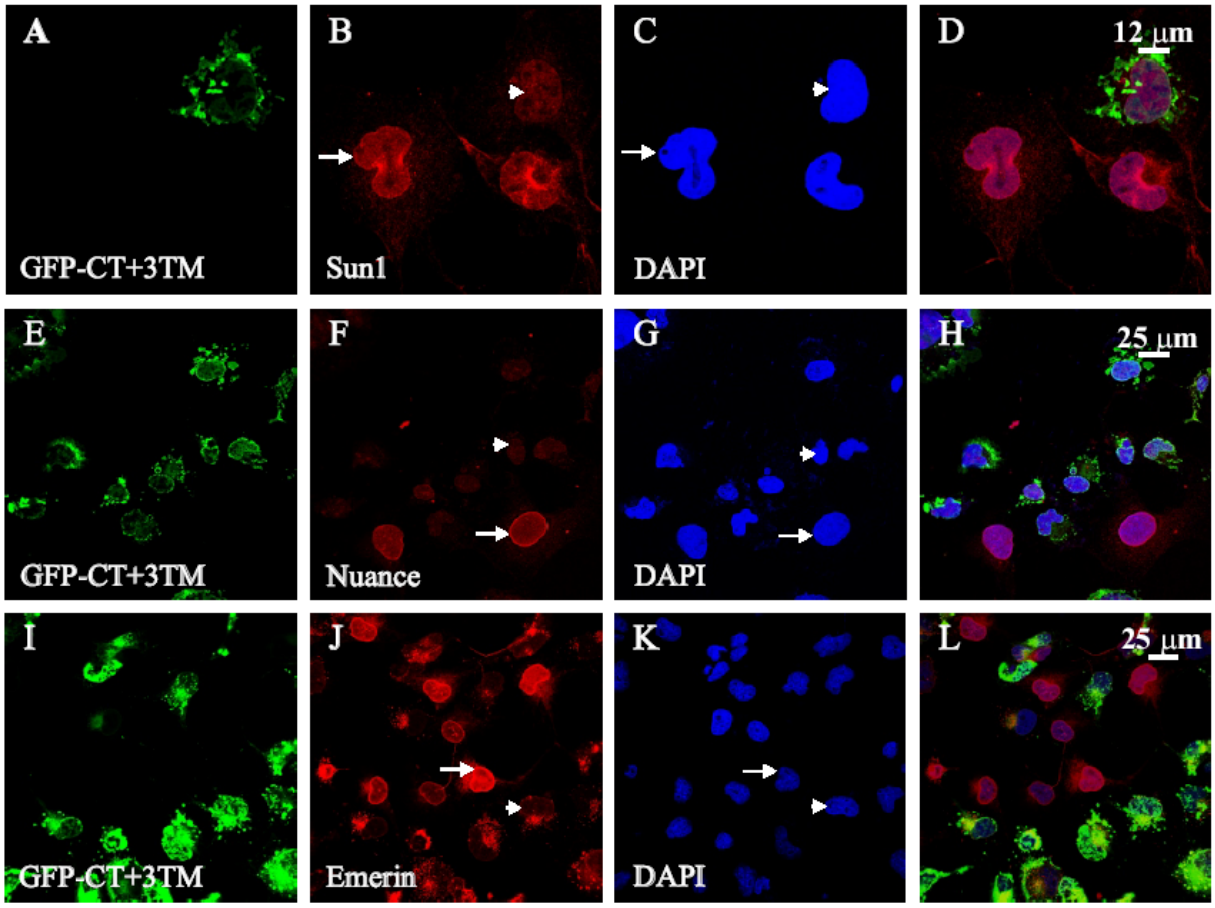

Figure 4.25: Dominant negative displacement of Sun1, NUANCE and emerin from the nuclear membrane. Panels A-D depict dominant negative displacement of endogenous Sun1. Panel A, E and I in green show COS7 cells transfected with the dominant negative construct. Panel B, F and J shows cells costained with Sun1 polyclonal antibodies (281), the NUANCE N-terminal monoclonal antibody (K20-478-4) and the emerin monoclonal antibody respectively. Panel C, G and K shows staining with DAPI and Panels D, H and L shows the merged Images. Arrows indicate transfected cells and arrowhead indicates untransfected cells. Sun1 was visualised by secondary antibody tagged with Alexa 568 and NUANCE and emerin by secondary antibody conjugated with Cy3.

The observation that emerin localisation to the nuclear envelope is partially dependent of NUANCE by RNAi knock down experiments by Thorsten Libotte compounded the belief that this DN construct could also have a similar effect on the NE localisation of emerin. This was confirmed by staining the transfected cells with antibodies specific to emerin (Figure 4.25, I-L). Emerin is another protein found in the inner nuclear membrane and mutations in emerin has been attributed to Emery Dreifuss Muscular dystrophy (Bione et al., 1994).

The overexpressed DN protein mostly formed some discontinuous structure around the nucleus and some aggregates, which were already proven to be positive for the ER marker PDI. Though it was interesting to find that the DN displaces all these three proteins, it is difficult to explain the mechanism by which this effect is carried out or what happens to the displaced proteins. However, displaced NUANCE was found to be present in the ER aggregates in some of the transfected cells (Figure 26, arrow).

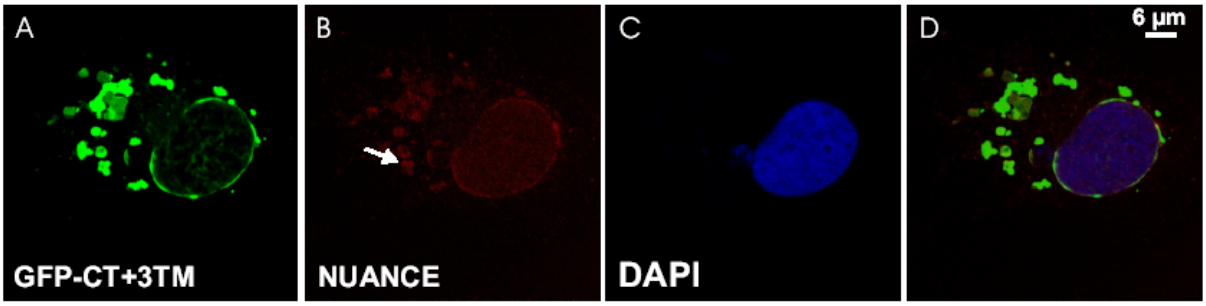

Figure 4.26: The ER aggregates of DN protein colocalises with NUANCE. Panel A shows a single COS7 cell transfected with the GFP-CT+3TM construct. Panel B shows NUANCE staining colocalising with the overexpressed protein marked by the arrow. Panel C shows DAPI staining and Panel D is the merged image. NUANCE was visualised by secondary antibodies tagged with Cy3. Pictures were taken using the confocal microscope.

4.14 Overexpression of GFP-CT+3TM has no effect on lamin A/C or Lap2 localisation

Lamins are nuclear intermediate filaments found in the nuclei of multicellular eukaryotes. They form stable filaments at the inner nuclear membrane and stable structures at the nucleoplam. The main components of nuclear lamina are the A-type and B-type lamins (Stuurman et al., 1998 and Gerrace et al., 1978). Both major (A and C) and minor (AΔ10 and C2) A-type lamin species are encoded by a single developmentally regulated gene *LMNA* and arise through alternative splicing (Fisher et al., 1986). By contrast, the main B-type lamins (B1 and B2) are encoded by two separate genes (*LMNB1* and *LMNB2*, respectively) (Hoeger et al., 1988, Hoeger et al., 1990, Peter et al., 1989 and Vorburger et al., 1989). A single minor

B-type lamin (B3) is a splice variant of laminB2 (Furukawa et al., 1993). Lap2 is also an inner nuclear membrane protein, which has been shown to bind to A-type lamins (Dechat et al., 2000) and BAF DNA complexes (Shumaker et al., 2001).

The ability of the dominant negative construct of Sun1 to displace Sun1, NUANCE and emerin from the nuclear envelope encouraged us to study the distribution of other known NE proteins like lamin A/C and Lap2. Staining with lamin A/C and Lap2 antibodies on GFP-CT+3TM transfected cells showed that the overexpressed DN protein has no effect on the normal subcellular localisation of these proteins. Both proteins remained on the nuclear membrane (Figure 4.27).

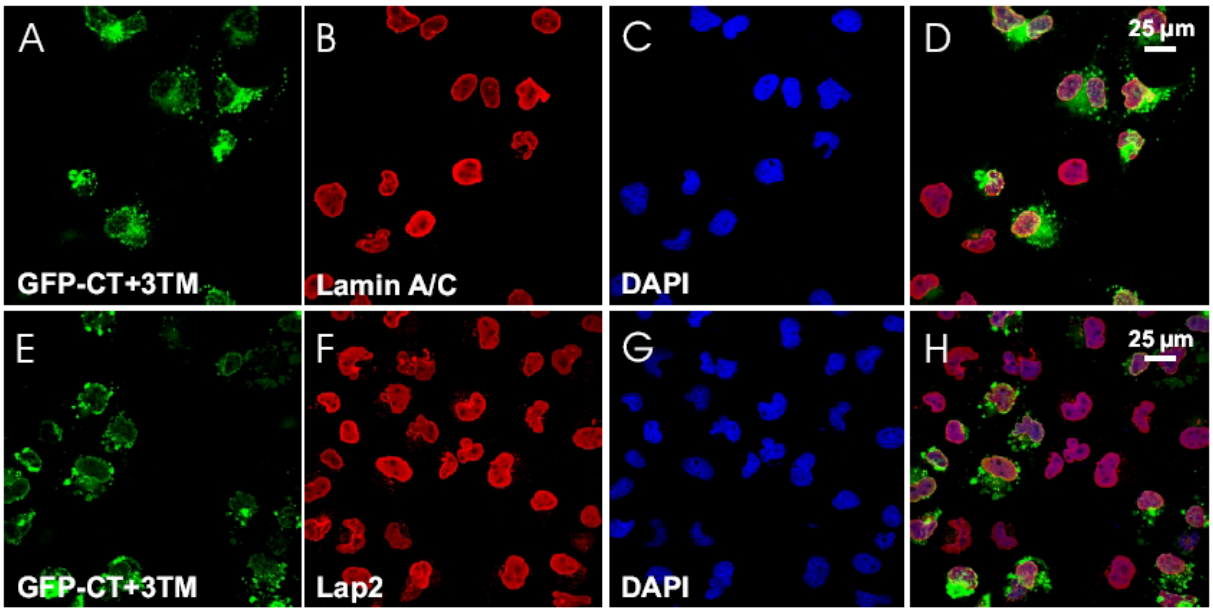

Figure 4.27: The GFP-CT+3TM overexpression has no effect on the NE localisation of lamin A/C and Lap2. Panels A and E depict the overexpressed DN Sun1 protein in green colour. Panels B and F show lamin A/C and Lap2 staining respectively. Panels C and G are nuclear staining by DAPI and panels D and H are the merged pictures. Secondary antibodies conjugated with Cy3 visualized both lamin A/C and lap2. Pictures were taken with confocal microscope.

4.15 Sun1 is an inner nuclear membrane protein

The nuclear membrane is composed of two layers of membranes, inner and outer membranes, which are connected at the nuclear pore sites. The outer nuclear membrane is continuous with the rough endoplasmic reticulum. The space between the inner and outer nuclear membrane is also continuous with the lumen of the endoplasmic reticulum.

Both Enaptin (Abraham, 2004) and NUANCE (Zhen et al., 2002) have been found to be present in the outer nuclear membrane, but the inner nuclear membrane localisation of these two proteins has not been studied in much detail. Lamin A/C, emerin and many other nuclear membrane proteins are found to be located only in the inner nuclear membrane. Integral proteins of the inner nuclear membrane are synthesised on the rough endoplasmic reticulum and reach the inner nuclear membrane by lateral diffusion in the connected ER and nuclear envelope membranes. Associations with nuclear ligands retain them in the inner nuclear membrane and this type of protein targeting is called 'diffusion-retention' model (Holmer and Worman, 2001).

Digitonin selectively permeabilises only the plasma membrane but not the nuclear membrane when the permeabilisation is done in a controlled manner. Digitonin permeabilisation studies were done to ascertain the exact localisation of Sun1 protein in the nuclear envelope. COS7 cells were fixed with paraformaldehyde and permeabilised with Triton X-100 and digitonin. Lamin A/C staining was used as a control for the inner nuclear membrane staining. Sun1 and lamin A/C

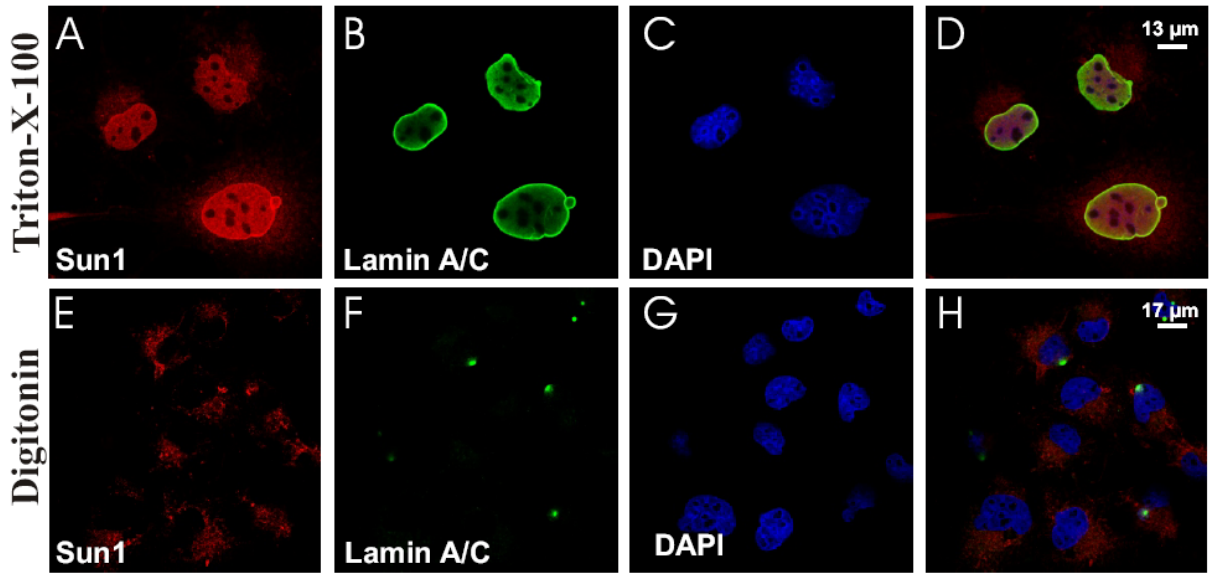

Figure 4.28: Digitonin extraction experiment establishes the location of Sun1 in the nuclear membrane. Panels A-D show cells fixed with paraformaldehyde and permeabilised with Triton X-100 and panels E-H, the cells permeabilised with digitonin. Panels A and E show Sun1 staining, B and F lamin A/C staining, C and D DAPI staining and D and H, the merged pictures. Lamin A/C was visualised by secondary antibody conjugated with Alexa 488. The pictures were taken using confocal microscope.

stain the nuclear envelope of COS 7 cells when permeabilised by Triton X-100 (Figure 4.28, A-D), whereas, the Sun1 and lamin A/C antibodies couldn't stain the nuclear envelope in digitonin permeabilised cells (Figure 4.28, E-H). However, the non-specific cytosolic staining

by Sun1 polyclonal antibodies, which is normally seen was still visible in the digitonin permeabilised cells (Figure 4.28, E) and lamin A/C staining was absent in these cells (Figure 4.28, E) indicating that the antibodies managed to reach the cytosol but not the nucleus because of the selective permeabilisation of the plasma membrane. These observations led to the conclusion that Sun1 is an element of the inner nuclear membrane, which is retained there by some association with some INM specific proteins, for example lamin A/C.

4.16 Sun1 localises to the nuclear envelope in a lamin A/C dependent manner

Most of the known inner nuclear membrane proteins bind to lamins for their retention in the NE. The *C. elegans* of Sun1, Unc-84 was already shown to be dependent on lamins for the NE localisation (Lee et al., 2002). This prompted us to investigate the lamin dependent localisation of Sun1 in mouse fibroblasts. Wild type and lamin A/C knockout fibroblasts were used for this experiment (Sullivan et al., 1999). The cells were stained with lamin A/C and Sun1 antibodies. Anti-Sun1 polyclonal antibodies stained the whole nucleoplasm in addition to a slightly brighter staining around the nuclear membrane in wild type fibroblasts (Figure 4.29, A-D), whereas Sun1 staining was completely diffused and faint all through the cytoplasm and nucleoplasm in fibroblasts, which are lamin A/C deficient (Figure 4.29, E-H).

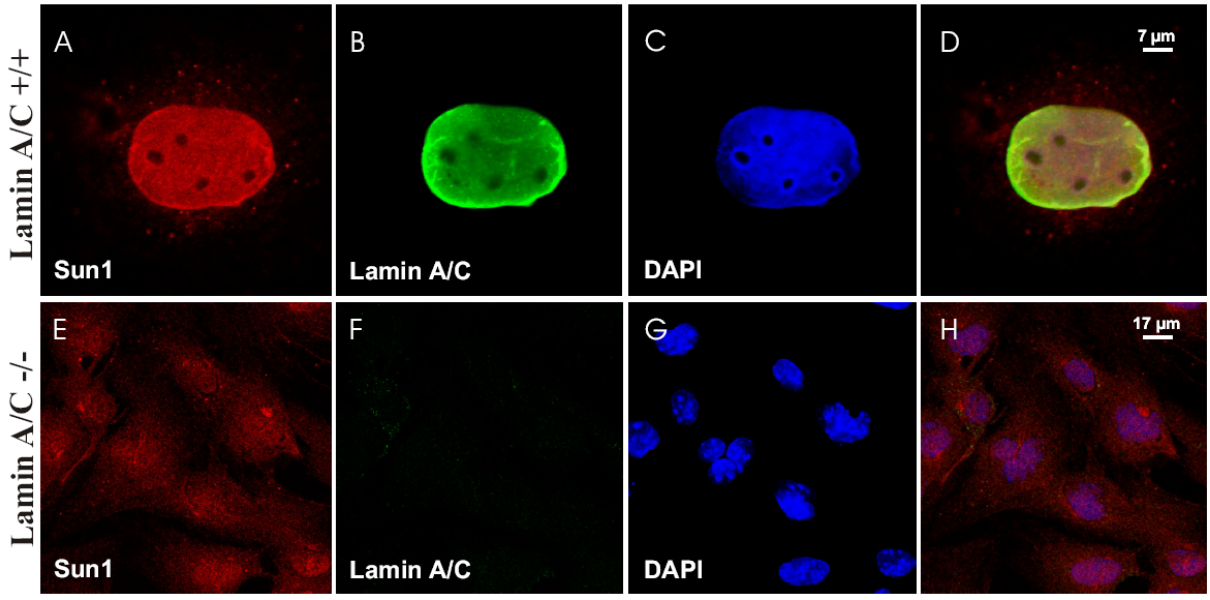

Figure 4.29: Lamin A/C dependent localisation of Sun1 in mouse fibroblasts. Panels A-D depict NE localisation of Sun1 staining in lamin A/C $^{+/+}$ fibroblasts and in the lamin A/C $^{-/-}$ cells (panels E-H). Panel A shows the NE presence of Sun1 staining and panel E shows the diffused staining of the same in contrast to wild type cells. Panel B shows lamin A/C staining and panel F shows the absence of lamin A/C in knockout fibroblasts. Panels C and G are nuclei stained with DAPI. Panels D and H are the merged pictures. The pictures were taken using the confocal microscope.

The disruption of the nuclear and NE localisation of Sun1 in the absence of lamin A/C signalled a possible direct interaction between these proteins in wild type cells. The N-terminus of Sun1 was fused to the AD of Gal4 to check if it interacts with lamin A or laminB, which are fused to the BD of Gal4. However, we were unable to detect any such interaction between these proteins in yeast two hybrid experiments (Figure 4.30).

Yeast two hybrid constructs		-Trp-Leu-His+ 3AT (60 mM)	X-gal
BD-LaminA	AD-NT	+	-
BD-LaminB	AD-NT	+	-

Figure 4.30: The N-terminal of Sun1 doesn't interact with lamins A and B in a yeast two hybrid assay. Lamin A and B fused to BD were cotransformed with the AD-NT of Sun1. The transformants stopped growing after a minimal growth on Trp-Leu-His+3AT (60 mM) which is indicated by "+" and also didn't turn blue in X-gal assay which is symbolised with "-".

5 Generation of a knock-in mouse expressing GFP-tagged full-length Enaptin without the transmembrane domain

5.1 Aim of the project

Gene targeting, introduction of site-specific modifications into the mouse genome by homologous recombination, is generally used for the production of mutant animals to study the gene function *in vivo*. In order to get further insight into the function of Enaptin, a mouse knock out mutant where the ABD is targeted is being generated in our lab. Enaptin is a huge 1,000 kDa protein with some alternatively spliced isoforms lacking the C-terminal transmembrane domain and some lacking the ABD (Figure 3.1). Though the previously mentioned approach to knock out *Enaptin* gene at the ABD would stop the transcription of the full-length protein and the isoforms which contain the ABD, it does not guarantee the knock down of other isoforms which lack ABD, for instance Nesprin1α, Nesprin1β, Myne1, Syne1A and Syne 1B. Having already known that Enaptin is a nuclear envelope protein and it localises to the NE using the single transmembrane domain and the final 30 amino acids, an approach to remove the transmembrane domain and the following 30 amino acids would ensure the absolute mislocalisation of all the Enaptin isoforms containing the transmembrane domain which would in affect enable us to study the functional significance of Enaptin and its isoforms in context with the nuclear envelope. We coupled this approach to fuse the rest of the protein with GFP, which can alternatively be utilised to study the tissue distribution of Enaptin (Figure 5.1).

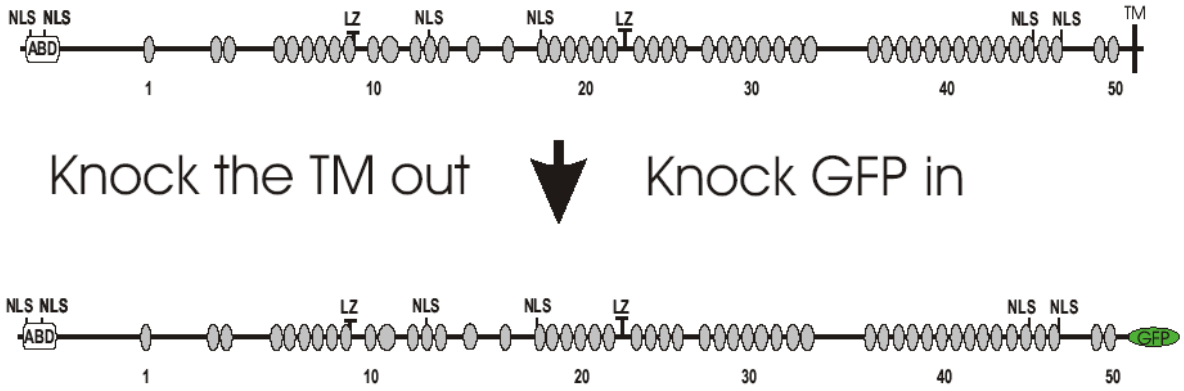

Figure 5.1: A schematic diagram showing the aim of the project, which is the ablation of the tranmembrane domain of Enaptin and its replacement by theGFP protein

5.2 The knock out strategy

The last exon (Exon 147) of the *Enaptin* gene codes for amino acids, which is comprised of the transmembrane domain and the perinuclear region. The 5' arm of the target

vector was designed to include 4 kb of genomic sequence comprising mostly of the intronic sequence with few amino acids of the last exon until few amino acids before the transmembrane domain (Figure 5.2).

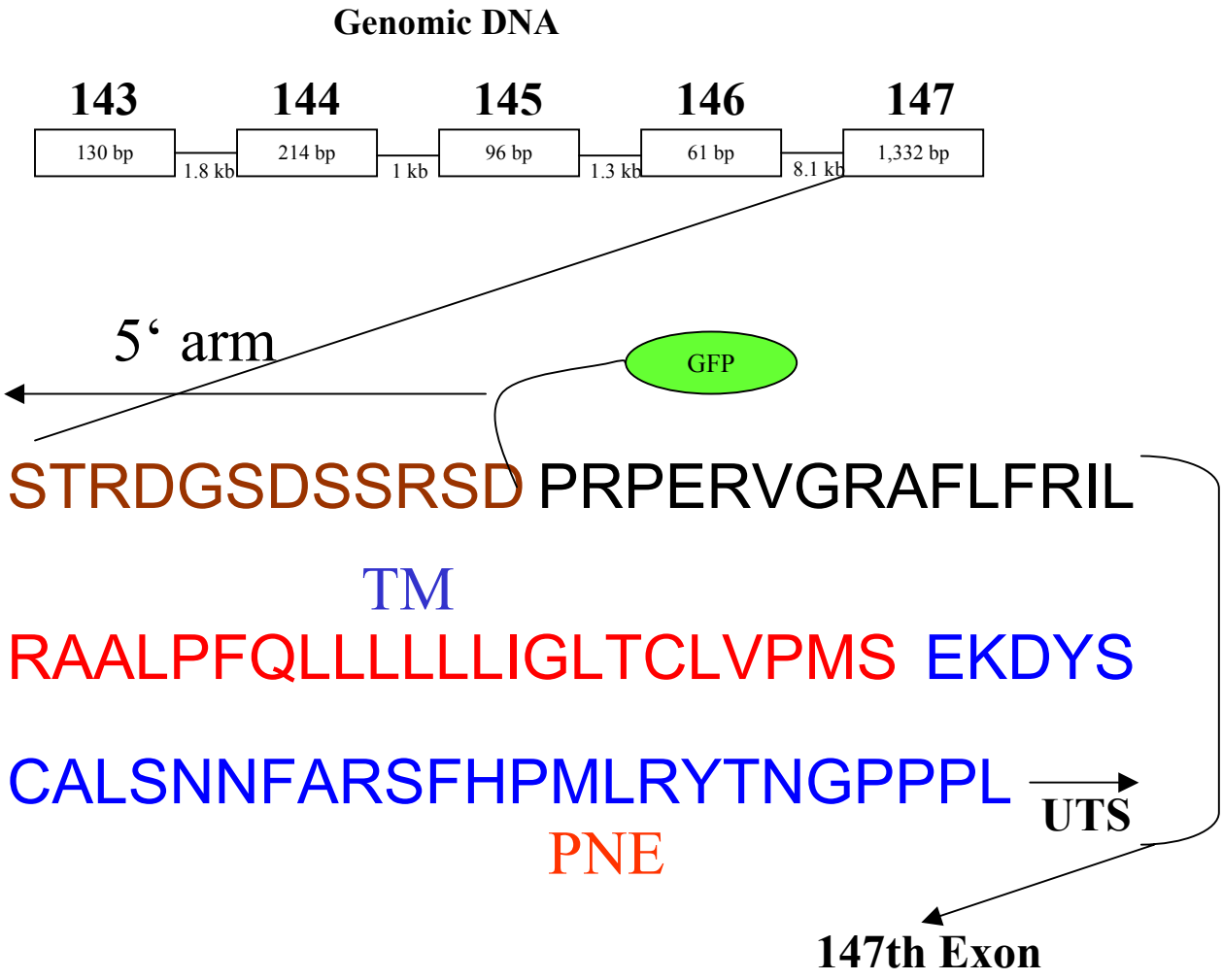

Figure 5.2: Schematic representation of the last five exons of *Enaptin* and the knock in strategy. The last five exons of *Enaptin* are depicted in the figure. The boxes represent the exons and the size of the exons and the lines, the introns and their size. The final exon of *Enaptin* codes 79 amino acids. The 4 kb 5'arm of the target vector includes sequence of the intron between the last exon and the one before with 12 amino acids (marked with brown colour) of the last exon. GFP was fused to the target vector immediately after the 5' arm. The amino acids indicated with red colour represent the transmembrane domain (TM) and the amino acids marked with blue colour indicate the perinuclear region of *Enaptin* (PNE). UTS indicates the untranslated sequence of the last exon including the stop codon.

The amplified 5' arm was cloned in pBLUESCRIPT vector followed by GFP, which was cloned in frame to the remaining amino acids of the last exon. Neomycin cassette was also cloned into the vector for the later selection of recombination event. 3'arm includes 1.9 kb of intronic sequence after the final exon of E*naptin* which was cloned after NEO cassette

in the target vector. Two probes were generated outside of 5' and 3' arms of the genomic sequence to select for clones site specifically recombined (Figure 5.3). *Hind*III enzyme was used for the screening of the clones, which was supposed to give rise to a 11.7 kb wild type signal and an additional knock-in 9.8 kb recombined fragment.

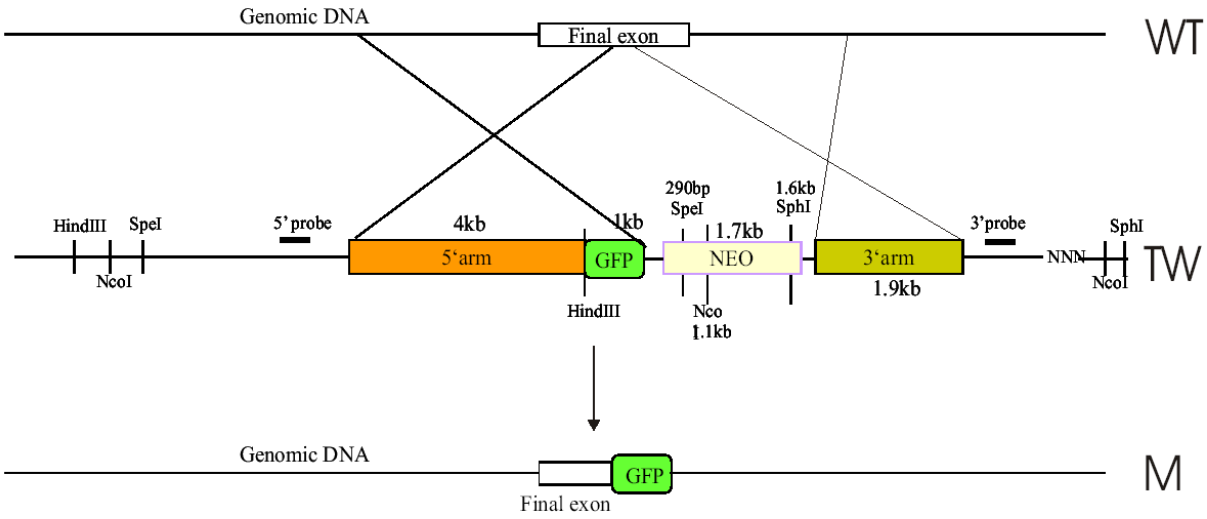

Figure 5.3: Schematic diagram of the knockout vector and the recombination with wild type genomic DNA. WT represents the wild type genomic DNA. TW (target vector) is the model of target vector constructed. M (mutant genomic DNA after recombination) shows the insertion of GFP in the final exon of *Enaptin* gene after recombination.

5.3 Transfection and screening

The 5' and 3' probes that were designed for identifying the recombined clones were first checked on wild type DNA (Figure 5.4). The target vector was linearised with *Sal*I and purified. The purified target vector was transfected into R1 ES cells by electroporation and selected on G418. Genomic DNAs isolated from 177 clones were digested by *Hind*III and probed with 5' probe.

Clones 43, 83 and 110 gave bands for the wild type and recombinant allele at the expected size when probed with both the probes. However, the clones when digested with *Hind*III and probed with 5' probe gave a band of the size of 7 kb instead of the expected the size of 9.8 kb (Figure 5.5).

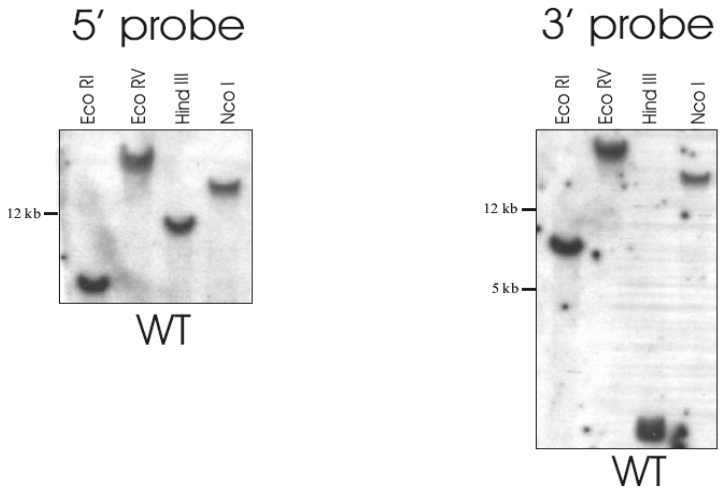

Figure 5.4: Southern blotting on wild type ES cells DNA to confirm the specificity of the probes. DNA digested by *Eco*RI, *Eco*RV, *Hind*III and *Nco*I were probed by both 5' and 3' probes. Both the probes give a expected band for the wild type DNA. The expected bands with 5' probe are, Eco*RI*: 6.8 kb, *Eco*RV: 26.4 +X, *Hind*III: 11.7 kb and *Nco*I: 16.4 kb+X and with 3' probe are 3 kb+X, *Eco*RV: 26.4+X, *Hind*III: 2 kb and *Nco*I: 16.4 kb+X. The symbol "X" indicates the unknown sequence in the genomic DNA after the 3' probe as seen in figure 5.3.

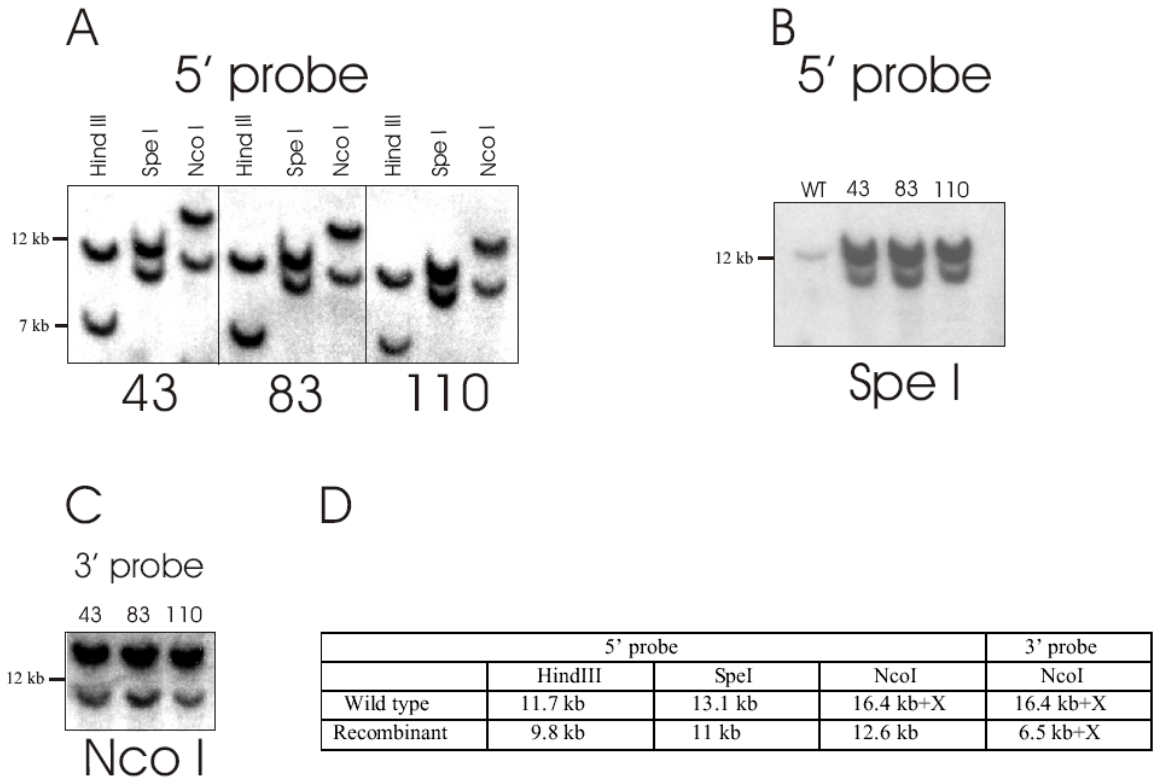

	5′ probe			3′ probe
	HindIII	SpeI	NcoI	NcoI
Wild type	11.7 kb	13.1 kb	16.4 kb+X	16.4 kb+X
Recombinant	9.8 kb	11 kb	12.6 kb	6.5 kb+X

Figure 5.5: Confirmation of recombination by southern blotting. Figures A and B show clones 43, 83 and 110 digested by H*ind*III, *Spe*I and *Nco*I and probed with 5' probe. Figure C show the same clones digested by *Nco*I and probed with 3' probe and the Figure D tables the expected wild type and recombinant bands.

Discussion

6 DISCUSSION

6.1 Enaptin, a novel NUANCE-like protein

Enaptin belongs to a novel cytolinker family of actin binding proteins, which might connect the actin cytoskeleton to the nucleus. Structurally Enaptin resembles a protein recently identified in our lab called NUANCE which is also a giant protein of molecular mass of approximately 800,000 dalton with an N-terminal actin binding domain and a C-terminal transmembrane domain separated by a stretch containing spectrin repeats (Zhen et al., 2002). The actin binding domain and transmembrane domain of Enaptin and NUANCE are closely related to each other and exhibit a high degree of homology at the amino acid level. Unlike many of the actin binding proteins of α-actinin type, the CH1 domain of Enaptin and NUANCE is separated from the CH2 domain by a serine rich stretch of 29 amino acids. The ABD domain of Enaptin is closely related to the ABDs of dystrophin, utrophin and interaptin. Dystrophin is associated with the plasma membrane of cardiac and skeletal muscle (sarcolemma) and by interacting with the integral membrane proteins (sarcoglycan, dystroglycans, syntrophin, and dystrobrevin complexes) forms a bridge between the actin cytoskeleton and the extracellular matrix (Campbell et al., 1989; Rando, 2001). This dystrophin-glycoprotein complex is thought to mechanically stabilise the sarcolemmal membrane from shear stresses imposed during eccentric muscle contraction (Petrof et al., 1993; Straub et al., 1997). Utrophin, which is highly homologous to dystrophin, binds laterally along actin filaments and can couple costameric actin with sarcolemma when overexpressed in dystrophin-deficient muscle (Rybakowa et al., 2002). The transmembrane domains of Enaptin and NUANCE are similar to the one found in the *Drosophila* Klarsicht protein, which has been shown to be important for the attachment of MTOC to the nucleus and mediate photoreceptor nuclear migration (Patterson et al., 2003). Interaptin; is the first protein characterised to be connecting the actin cytoskeleton to the nucleus, which was shown to bind actin and localise to perinuclear and golgi-like structures in *Dictyostelium discoideum* (Rivero et al., 1998*)*. The *C. elegans* orthologue of Enaptin, ANC-1 has been shown to bind actin and be involved in the positioning of nuclei and mitochondria in *C. elegans*. Unlike dystrophin and utrophin, which connect the actin cytoskeleton to the extra cellular matrix through the plasma membrane and Klarsicht, which connects the microtubule network to the nucleus, Enaptin and NUANCE along with interaptin may connect the actin cytoskeleton to the nucleus.

6.2 Isoform diversity of *Enaptin*

The *Enaptin* gene is more complex than *NUANCE* with regards to their isoform diversity. Two N-terminal and five C-terminal isoforms of *Enaptin* have been characterised so far, whereas *NUANCE* is known to have only four isoforms. Enaptin-165 identified in our lab is rather a small protein of 1,431 amino acids with a predicted molecular mass of 165 kDa. GFP-Enaptin-165 fusion protein transfected in COS7 cells largely localise to the nucleus in addition to the weak localisation along the actin stress fibers. CPG2 is another N-terminal isoform lacking the ABD domain, one of the candidate plasticity proteins found to be expressed in response to light in the adult cerebral cortex and being regulated during development (Nedivi et al., 1996).

Five C-terminal isoforms of Enaptin have been reported, human Nesprin-1α, human Nesprin-1β, mouse Syne-1A, Syne-1B and human Myne-1 (Apel et al., 2000; Mislow et al., 2000; Zhang et al., 2000). All these isoforms lack the N-terminal ABD domain but harbor the C-terminal transmembrane domain with different numbers of spectrin repeats. *Nesprin* was identified as one of the two genes encoding members of a new family of type II integral membrane proteins in a search for vascular smooth muscle differentiation markers. Human Nesprin-1β is a 3,321 amino acids protein with a predicted molecular mass of 380,000 dalton. The protein includes 21 spectrin repeats and a C-terminal transmembrane domain and was found to localise to the nuclear membrane (Zhang et al., 2001). Recent experiments showed that the third spectrin repeat of another small spliced isoform, Nesprin-1α interacted with the fifth spectrin repeat thus mediating self-association. The carboxy terminal half binds to lamin A and Nesprin-1α dimers associate with emerin, an inner nuclear membrane protein (Mislow et al., 2002).

Another C-terminal isoform of Enaptin, mouse Syne-1B, was identified as a protein which interacts with MuSK (Muscle specific tyrosine kinase), a component of the agrin receptor concentrated in the post-synaptic membrane. The agrin receptor is the receptor for the extracellular matrix molecule agrin, which mediates the motor neuron induced accumulation of acetylcholine receptors (AChR) at the neuromuscular junction and is required for all aspects of postsynaptic differentiation including transcriptional specialisation of synaptic nuclei (McMahan et al., 1990; Gautam et al., 1996; Burgess et al., 1999; Valenzuela et al., 1995). In adult skeletal muscle fibers, levels of Syne-1 are highest in the nuclei that lie beneath the postsynaptic membrane at the neuromuscular junction. These nuclei are transcriptionally specialised, expressing genes for synaptic components at higher levels than extrasynaptic nuclei in the same cytoplasm (Apel et al., 2000). Syne-1 was also identified as a

component of the golgi apparatus (Gough et al., 2003) and was shown to be involved in cytokinesis (Fan and Beck., 2004).

A further C-terminal isoform of Enaptin, Myne-1 (Myocyte nuclear envelope) was identified as a protein expressed upon early muscle differentiation in multiple intranuclear foci concomitant with lamin A/C expression and was found to be interacting with lamin A/C. It is a small protein with 1,139 amino acids with a predicted molecular weight of 131 kDa. Myne-1 has 7 putative spectrin repeats and a C-terminal transmembrane domain (Mislow et al., 2002). The high complexity of *Enaptin* gene associated with its isoform diversity suggests multiple functions for this gene. When the full length Enaptin protein is most likely involved in tethering the nucleus to the actin cytoskeleton, the C-terminal isoforms lacking the ABD have been implicated to have functions like muscle differentiation and some unknown function at the neuro-muscular junction. Though Enaptin was shown to have a role also in cytokinesis, the domain architecture of the isoform involved in this function is not known. In addition, the presence of Enaptin-165 isoform predominantly in the cell nucleus provides a basis to speculate transcriptional, chromosomal condensational and other nuclear related functions for this isoform in the nucleus.

6.3 Subcellular localisation of Enaptin

Cell fractionation studies show the presence of this protein in the nuclear fraction in addition to the cytosolic fraction. It may be that there are two pools of 400 kDa alternatively spliced Enaptin isoforms, one lacking the most of the middle rod domain but with both the ABD and transmembrane domain, which is supported by the presence of a 400 kDa in the nuclear fraction. The cytosolic fraction of the protein may be due to another alternatively spliced isoform containing the beginning of the gene with a short C-terminus without the transmembrane domain. This hypothesis is supported by the presence of the EST clone CA425673 which after 3600 amino acids of transcription, prematurely jumps to another exon which has a stop codon and 3' untranslated region giving rise to a protein the size approximately of 400 kDa.

The subcellular localisation of Enaptin was characterised by immunofluorescence studies using the polyclonal antibody and two different GFP constructs. Immunofluorescence analysis in COS7 cells gave a very bright nuclear staining and in some cells the actin cytoskeleton was also stained. C3H/10T1/2 and C2F3 cell lines give a staining of the nuclear membrane and also a staining of focal contacts, which are perfectly colocalising with α-

actinin. The protein stained in the nuclear membrane might be the biggest isoform of Enaptin containing the transmembrane domain, which was so far not identified in western blotting experiments. Our failure to detect the protein might be due to several reasons such as protein degradation during the preparation of the homogenate as large proteins of this magnitude are prone to degradation. Alternatively, the giant Enaptin transcript may also be developmentally regulated or enriched in cell lines that have not been included in the present study. Poor transfer and also low expression of this protein could contribute to the fact that we did not identify it in western blots. The staining in the focal contacts could correspond to the 400 kDa band observed. It is likely that this 400 kDa isoform does not have a transmembrane domain and could therefore have functions in the focal contacts. Two different GFP constructs were used for the elucidation of the localisation of the ABD of Enaptin and of the small N-terminal isoform Enaptin-165. The GFP tagged ABD colocalises with the actin cytoskeleton in COS7 cells and in C3H/10T1/2 cells and in focal contacts in C3H/10T1/2 cells as shown by its colocalisation with α-actinin. The protein is also very prominently localised in the nucleus in both COS7 and C3H10T1/2 cells. The GFP-Enaptin-165 protein was found at the actin cytoskeleton in COS7 cells and was also in the nucleus. The nuclear presence of this protein is not surprising owing to the fact that the ABD of Enaptin has two nuclear localisation signals and Enaptin-165 has three nuclear localisation signals. The localisation of Enaptin in the nucleus does not appear to be due to passive diffusion through the nuclear pore as the proteins are fairly large. The relevance of the nuclear localisation of these fusion proteins and the significance of the predicted NLS in this function can further be explored by site directed mutagenesis targeting the amino acids predicted to be required for nuclear localisation. While NUANCE is exclusively found in the nucleus and nuclear envelope (Zhen et al., 2002), Enaptin is found in two different compartments of the cell, at the nuclear envelope and at actin rich structures in the cytosol. It is unclear at present whether this provides evidence of an Enaptin isoform lacking the transmembrane domain, as the antibodies used throughout this study were raised against this protein's ABD. The nuclear envelope staining however implies that the labelled protein harbours the C-terminal transmembrane domain.

6.4 Tissue distribution of Enaptin

Polyclonal antibodies raised against the ABD region of Enaptin were used for western blotting and immunohistochemistry in order to find out the expression pattern of Enaptin in different tissues and also the differential expression of isoforms in various cell lines and tissues. Western blot analysis with the polyclonal antibodies identified a 165 kDa band in the

mouse brain tissue and a band corresponing to 400 kDa in the COS7, C3H/10T1/2, A431 and C2F3 cell lines. The 165 kDa protein in brain could well correspond to the N-terminal small isoform Enaptin-165 cloned in our lab from mouse brain cDNA. Enaptin stained the I-band surrounding the Z-line in the muscle sarcomere. It is possible that Enaptin is bound to the actin, which is normally present in the I-band. The presence of Enaptin in the I-band apposed to the Z-line is tempting to speculate that Enaptin probably has a role in the attachment of the I-band to the Z-line. Enaptin stained as a double layer around the periphery of the cells present in the epidermis of human skin in contrast to the nuclear envelope staining of NUANCE. This double layer staining didn't colocalise with the actin cytoskeleton when costained with phalloidin. The absence of NE staining in muscle and skin could be due to the fact that these tissues do not express the full length Enaptin but alternatively spliced isoforms without the transmembrane domain

6.5 Sun1 is a novel nuclear envelope protein and binds to Enaptin

Sun1 is a novel mouse protein with structural features to be residing in nuclear membrane with three transmembrane domains in the middle dividing the protein into an N- and C-terminal segment suggesting that both N- and C-termini are found in the opposite side of the membrane. The C-terminus of Sun1 was found to be homologous with the SUN domain. The SUN domain derives its name from the homology with the stretch of amino acids homologous between UNC-84, the *C. elegans* orthologue of Sun1 and Sad1, an *S. pombe* protein found to be associated with spindle pole body. Two nuclear migrations that occur during *C. elegans* development require the function of the unc-84 gene. Unc-84 mutants are also defective in the anchoring of nuclei within the hypodermal syncytium and in the migrations of the two distal tip cells of the gonad (Malone et al., 1999). The localisation of UNC-84 to the nuclear envelope was found to be dependent of Ce-lamin (Lee at al., 2002). Sad1 was found to be associated with the spindle pole body in *S. pombe* and was shown to be necessary for spindle formation in the yeast nucleus (Hagan and Yanagida, 1995). *C. elegans* has another SUN domain containing protein SUN1 though its SUN domain is more homologous to *S. pombe* Sad1 than to *C. elegans* UNC-84. SUN1 has been shown to play a role in the attachment of the centrosomes to the nucleus in a complex formation with a hook protein called Zyg-12 (Malone et al., 2003). Human and mouse have two proteins containing the SUN domain. The SUN domain of C. *elegans* UNC-84 is more closely related to the mammalian Sun1 than that of Sun2. Sun2 was identified as a novel type II transmembrane domain protein present in the inner membrane of the nuclear envelope (Hodzic et al., 2004).

Discussion

Sun1 was also identified as one of four proteins, AKAP9, MEA-2, TXI1 and Sun1 interacting with translin associated factor X (TRAX) in yeast two hybrid experiments (Bray et al., 2002). TRAX was identified as a protein-binding partner of unknown function of TB-RBP in a yeast two hybrid screen (Aoki et al., 1997). TB-RBP has been shown to bind translationally suppressed mRNAs to microtubules in testis and brain extracts (Han et al., 1995). This is an unusual finding, which could implicate additional function for Sun1 in relation to translational regulation.

The C-terminal 30 amino acids of Enaptin after the transmembrane domain are highly conserved across many species from *C. elegans* until humans. This highly conserved region of Enaptin binds to the C-terminus of Sun1 both *in vivo* in yeast two hybrid assay and *in vitro* in GST-pull down experiments. The closely related mammalian protein NUANCE was also shown to bind to Sun1 *in vitro* (Libotte, 2004). The interaction between Sun1 and Enaptin is in consistent with the earlier observation that the NE localisation of ANC-1 (*C. elegans* orthologue of Enaptin) was UNC-84 (*C. elegans* orthologue of mammalian Sun1) dependent (Starr and Han, 2002). It would be interesting to know if the mammalian Sun2 also associates with Enaptin. However, the SUN domain of Sun1 was not required for this interaction as shown in yeast two hybrid experiments. The development of a mild blue colour in X-gal assay in yeast cells cotransformed with BD-PNE and AD-SUN could be due to the fact that a few amino acids from the SUN domain is also involved in the interaction. The noninvolvement of SUN domain of Sun1 in its association with Enaptin and NUANCE suggests additional function for this domain. The SUN domain of *C. elegans* UNC-84 has been shown to bind to UNC-83 *in vitro* and recruit UNC-83 to the nuclear envelope. Mutations in unc-83 disrupt nuclear migration in migrating P cells, hyp7 precursors and the intestinal primordium, but have no obvious defects in the association of centrosomes with nuclei or the structure of the nuclear lamina of migrating nuclei (Starr et al., 2001). However, there are so far no proteins homologous to UNC-83 reported in mammals. It is interesting to note that the few amino acids after the transmembrane domain of Enaptin and UNC-83 are reasonably homologous (Figure 6.1).

```
                1       10        20        30
                |-------+---------+---------|
UNC-83          LAALAAIFYYHVFGKPFGPHVTYVNGPPPV
Enaptin         SEEDYSCALSNNFARSFHPMLRYTNGPPPL
Consensus       laadaacalsnnFarpFgPhlrYtNGPPPl
```

Figure 6.1: Alignment between the last 30 amino acids of *C. elegans* UNC-83 (Q23064, residues 1012-1031) and human Enaptin (AAN03486, residues 8720-8749).

Discussion

These observations can serve to classify the SUN domain containing proteins into two groups with regards to their function. *C. elegans* UNC-84, mammalian Sun1 and may be Sun2 fall in the first group connecting the actin cytoskeleton to the nucleus through associations with Enaptin/NUANCE/ANC-1. The next group of proteins, *S. pombe* Sad1 and *C. elegans* SUN1 are involved in the attachment of the centrosomes to the nucleus (Figure 6.1).

SUN domain containing proteins	**Function**
C. elegans UNC-84, mammalian Sun1 and may be Sun2	Connect the nuclear envelope to the actin cytoskeleton
S. pombe Sad1 and *C. elegans* SUN1	Connect the nuclear envelope to the centrosomes

Figure 6.2: A table showing a classification of SUN domain containing proteins into two groups.

6.6 The N- and C-termini of Sun1 localise to the nuclear envelope independently

The full length Sun1 localised to the nuclear envelope when fused to the GFP. Polyclonal antibodies raised against the N- and C-termini of Sun1 also stained the nuclear envelope. Both N- and C- termini of Sun1 with the transmembrane domains fused to GFP and overexpressed in COS7 cells, localised to the nuclear envelope. However in 70 to 80% of the cells transfected with GFP-CT+3TM, the nuclear envelope localisation was discontinuous and also formed aggregates in the endoplasmic reticulum, which was proved by its colocalisation with anti-protein disulufide isomerase antibodies. This localisation of N- and C-termini of Sun1 independently to the nuclear envelope is most likely because they might bind to different proteins on both the side of the nuclear envelope. The unexpected NE localisation C-terminus is most likely due to the dimerisation of ΔSUN domain with the endogenous Sun1. The C-terminus of Sun1 when expressed without the transmembrane domains failed to localise to the nuclear envelope implying the significance of the transmembrane domains in the NE localisation. Though these experiments prove that the C-terminus of Sun1 is in the perinuclear space, they do not provide any evidence in ascertaining the topology of the N-terminus.

6.7 Sun1 is essential for the NE localisation Enaptin and NUANCE

The GFP-CT+3TM fusion protein overexpressed cells stained negative for Sun1, NUANCE and emerin. This displacement effect is apparently due to a dominant negative effect by this overexpressed protein, which displaces the endogenous Sun1 by a mechanism, which is not clearly understood. The displacement of NUANCE from the nuclear membrane indicates that the binding of Enaptin and NUANCE to Sun1 is crucial for their retention to the nuclear envelope. It was also observed that NUANCE was displaced only from the cells where the dominant negative fusion protein formed discontinuous pattern around the nucleus and aggregates in the ER. The cells where GFP-CT+3TM formed normal rim around the nucleus stained positive for NUANCE. The emerin displacement is in consistent with the previous finding where emerin was mislocalised in cells where NUANCE was knocked down by RNAi and displaced by a dominant negative construct (Libotte, 2004). This interesting finding of displacement of emerin from the NE with the knock down of NUANCE suggests a scaffolding function for Enaptin and NUANCE in the nuclear envelope in addition to tethering the nuclei to the actin cytoskeleton.

6.8 Sun1 dimerises *in vivo*

ΔSUN domain of Sun1 dimerises *in vivo* in yeast two hybrid experiments. This was not unexpected of a domain with two coiled coil domains since these are known dimerisation domains. The ΔSUN domain of Sun1 with the three transmembrane domains fused to GFP and expressed in COS7 cells localised to the nuclear envelope. It is interesting to speculate that the NE retention of GFP-ΔSUN+3TM is possibly due to its dimerisation with the endogenous Sun1 indicating that the SUN domain of Sun1 is not required for the NE localisation Sun1. This question can further be addressed by a GFP fusion protein containing the transmembrane domains and the SUN domain but without the ΔSUN domain. GFP-ΔSUN fusion protein failed to localise to the nuclear envelope apparently due to the absence of the transmembrane domains. This data exemplifies a typical NE protein, which requires two important features for its NE localisation, transmembrane domains and NE retention signal and the signal in this case being the dimerisation. This observed dimerisation is consistent with genetic evidences, which hypothesised a possible dimerisation of *C. elegans* UNC-84 (Malone et al., 1999).

6.9 Sun1 is an element of inner nuclear envelope and its localisation is lamin A/C dependent

Digitonin experimints prove that Sun1 is present in the inner membrane of the nuclear envelope like lamin A/C. This proves that the N-terminus of Sun1 is facing the nucleoplasm. The mislocalisation of Sun1 in lamin A/C knockout fibroblasts indicates that the NE localisation of Sun1 is lamin A/C dependent. This finding is in consistent with the results, which postulated an association between UNC-84 and lamins in *C. elegans* (Lee et al., 2002). However, the inability to detect a direct interaction between the N-terminus of Sun1 and lamin A/C in yeast two hybrid experiments could be due to several reasons. This can very well be a "false negative" result as yeast two hybrid experiments produce a considerable amount of these types of results due to various reasons. On the other hand, the interaction between lamin A/C and Sun1 can be indirect through some uncharacterised protein. The presence of a Zn-H2 domain in the N-terminus of Sun1 signals that it also interacts with DNA. However, this is very unlikely since Sun1 localisation has already been shown to be lamin A/C dependent. The N-terminus of Sun1 is most likely involved in a direct or indirect association with lamin A/C, which is yet to be characterised by additional binding assays.

6.10 Enaptin, NUANCE, Sun1 and laminopathies

Laminopathies represent a group of human hereditary diseases that arise through defects in genes that encode nuclear lamina and lamin-associated proteins like emerin. Emery-Dreifuss muscular dystrophy (EDMD) is caused by mutations in the gene *emerin* (Bione et al., 1994). Mutations in the lamin A/C has been found to cause autosomal dominant Emery-Dreifuss muscular dystrophy (Bonne et al., 1999). Missense mutations in the rod domain of the lamin A/C cause dilated cardiomyopathy and conduction-system disease (Fatkin et al., 1999). The *LMNA* gene, which encodes the lamin A/C protein has been found to be mutated in partial lipodystrophy (Schackleton et al., 2000). Impaired A-type-lamin function has recently been linked to an autosomal-recessive axonal neuropathy that is also known as Charcot-Marie-Tooth disorder type 2 (CMT2) (De Sandre-Giovannoli et al., 2002).

One of the C-terminal isoforms of Enaptin, Nesprin 1α, has been found to associate directly with emerin and lamin A in vitro (Mislow et al., 2002). Another small C-terminal isoform of Enaptin, Myne-1 was found to colocalise with lamin A/C in mature muscle cells (Mislow et al., 2002). Enaptin and emerin showed aberrant localisation in the endoplasmic reticulum in type 1B muscular dystrophy patients (LGMD1B) carrying nonsense Y259X nonsense heterozygous or homozygous mutation in lamin A/C gene (Muchir et al., 2003). The possible

involvement of *Enaptin* in muscular dystrophy will well be addressed in the future by analysis of patient material and by the transgenic mouse deficient in *Enaptin* gene or the mouse knockout targeting the transmembrane domain which are already underway in our lab.

6.11 A model depicting the various interactions and findings

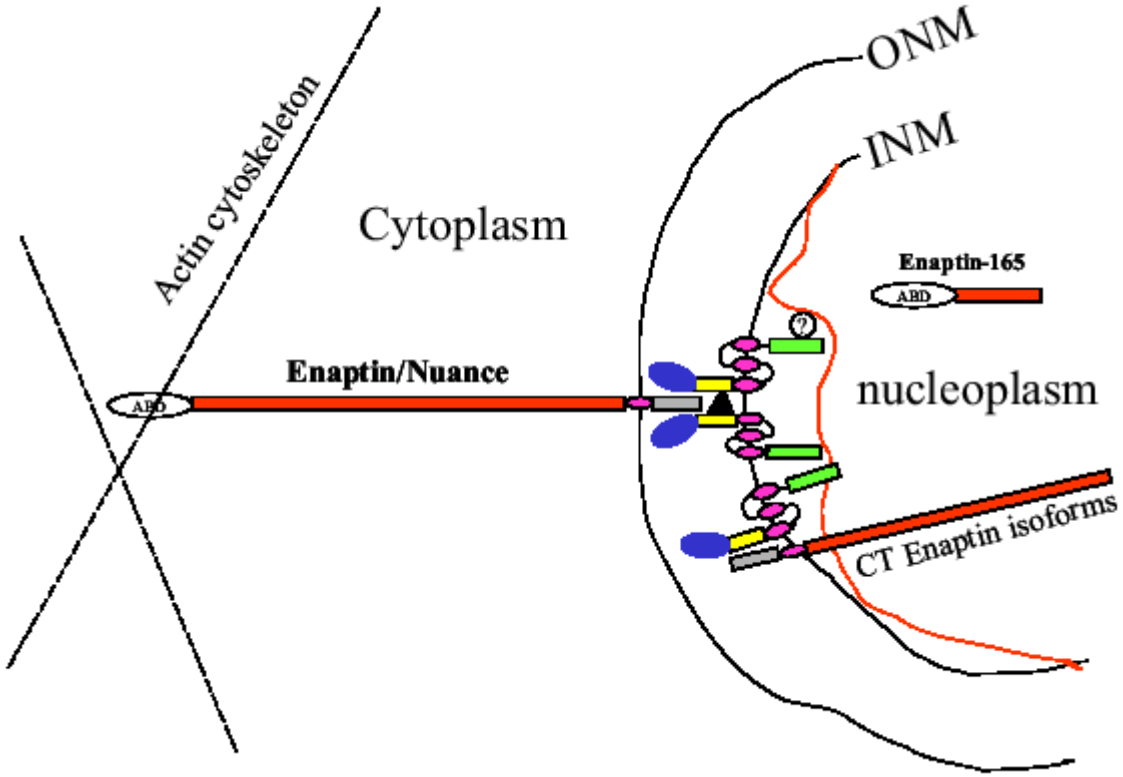

Figure 6.3: A simple model depicting the various interactions characterised in the study. ONM indicates the outer nuclear membrane and INM indicates the inner nuclear membrane.

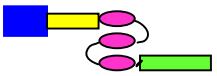

: Sun1 protein

: SUN domain

: ΔSUN domain

: NT of Sun1

: Transmembrane domain

: A type lamins

: dimerisation

6.12 A hypothetical model depicting the involvement of Enaptin, NUANCE and Sun1 in nuclear positioning and migration

The earlier finding that ΔSUN also binds to Enaptin and NUANCE in addition to dimerisation needs a clarification of the exact region of this domain, which is involved in these two different types of interactions. Based on the facts and findings from the experiments, it is appropriate to suggest that the dimerisation region of Sun1 is between amino acids 432-632 and Enaptin and NUANCE binding region is probably between 632 and 750 amino acids.

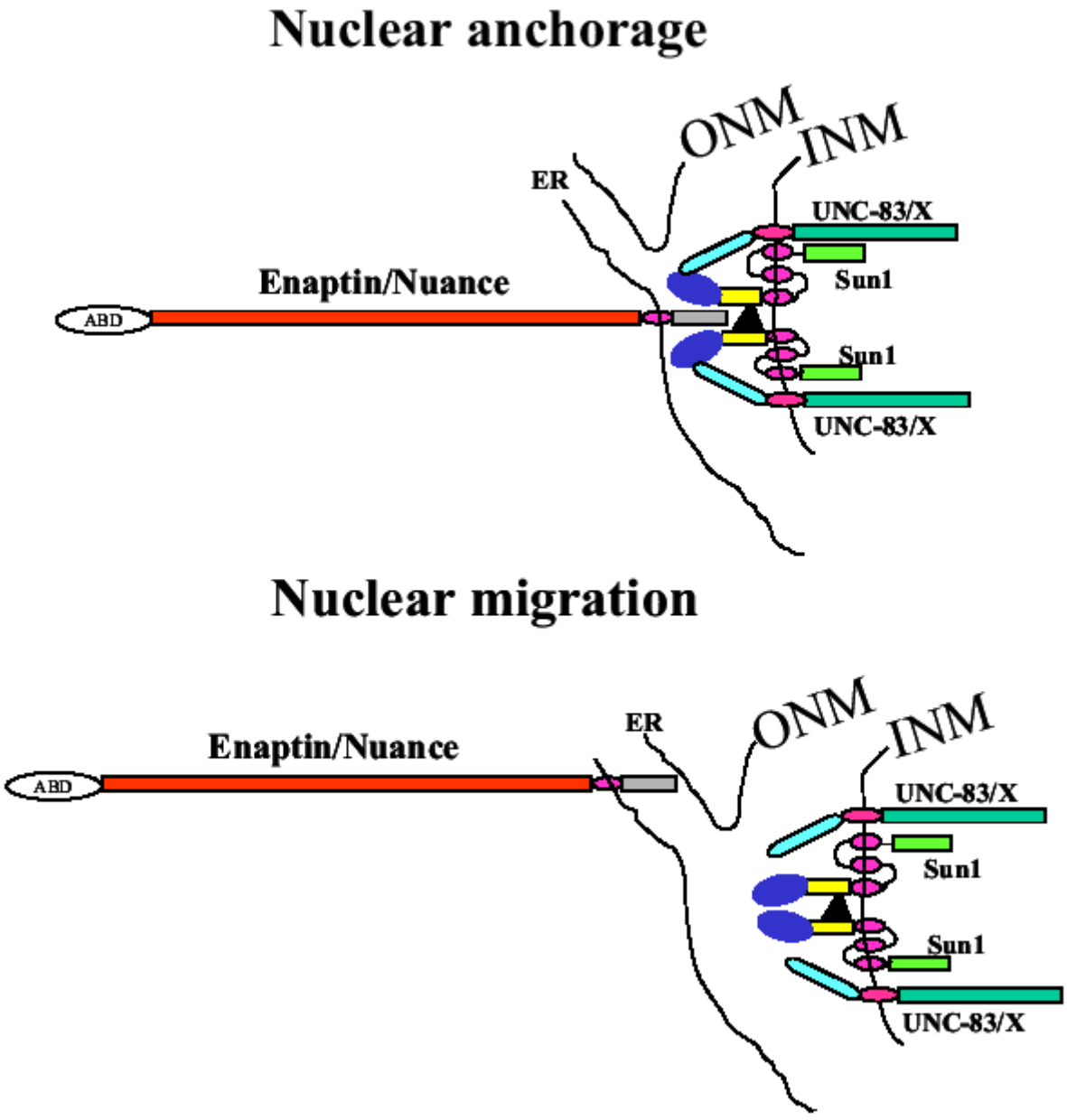

Figure 6.4: A hypothetical model based on the molecular interactions known so far to demonstrate a possible switch between nuclear migration and anchorage. ONM indicates the outer nuclear membrane, INM, the inner nuclear membrane and ER, endoplasmic reticulum.

It is already known that *C. elegans* UNC-83 and UNC-84 are important for proper nuclear migration and the SUN domain of UNC-84 binds to UNC-83 (Malone et al., 1999; Starr et al., 2001). The current study in the lab establishes two different interactions Sun1 is involved, dimerisation and direct binding with Enaptin and NUANCE. The *C. elegans* orthologue of Enaptin, ANC-1, also has been shown to be involved in nuclear positioning (Starr and Han, 2002). The fact that these molecules are involved in nuclear migration and positioning and the various interactions among them with some imagination offer enough evidence to speculate a model by which all these molecules can take part in the nuclear anchorage and migration processes. In a normal interphase nucleus, two molecules of Sun1 are located very closely to each other in the inner nuclear envelope by the dimerisation of ΔSUN domain. Two molecules of UNC-83 or the mammalian orthologue bind to the SUN domain of Sun1 and this binding, which pulls the SUN domain away from the ΔSUN domain gives space for the perinuclear region of Enaptin to bind to the ΔSUN domain making an indirect contact between the actin cytoskeleton and the nucleus, which in effect keeps the nucleus positioned in a place. On the other hand, when the nucleus has to migrate, the UNC-83 molecules are released from the SUN domain by some complex molecular interactions and the SUN domain closes the gap between the two Sun1 molecules disrupting the Enaptin/NUANCE from ΔSUN domain, which in turn releases the nucleus from the actin cytoskeleton and the nucleus migrates. This theory is entirely hypothetical and many more additional experiments have to be done to substantiate this. Though the interaction between the SUN domain of UNC-84 and UNC-83 is already known, the exact region of UNC-83 in the participation of these interactions is not yet experimentally proved. It was only logical though entirely hypothetical to assume it is the region after the transmembrane domain, which is involved in the binding.

6.13 Future perspectives

The discovery that Enaptin and NUANCE bind to and also need Sun1 for its NE localisation paves the way for more interesting experiments in the lab. Though our experiments unravelled many exciting characteristics of this nuclear envelope protein Sun1, there are still fairly a large amount of unanswered questions. The role of the conserved domain SUN and its interaction with other proteins might shed more light in understanding the mechanisms by which these proteins supposedly carry out the processes of nuclear migration and anchorage. It would also be interesting to know if the other mouse SUN domain containing protein, Sun2 also interact with Enaptin and NUANCE. In addition, the knockout mouse expressing Enaptin

without the transmembrane domain would give additional insight into understanding the complex function of these proteins.

Summary/Zusammenfassung

SUMMARY

The nucleus is a highly dynamic organelle showing migratory events during various developmental and cellular processes. These are made possible by its association with the microtubule network and, as shown recently, with the microfilament network. We have characterised Enaptin, a giant protein located at the nuclear membrane, which may provide a link to the actin cytoskeleton. Enaptin has an actin binding domain at the N-terminus with which it binds to the actin cytoskeleton and a transmembrane domain at the C-terminus, which tethers it to the nuclear envelope (NE). Western blotting experiments with antibodies specific to the ABD of Enaptin detect a 400 kDa protein in various cell lines and a 165 kDa protein in mouse brain tissue.

We concentrated on the properties of the very C-terminus composed of the last 30 amino acids after the transmembrane domain of Enaptin. A similar stretch of amino acids is found in the related NUANCE and is also highly conserved in proteins of the NE across different species from *C. elegans* to humans. We show that the conserved amino acids in Enaptin and NUANCE bind to the C-terminus of Sun1 in yeast two hybrid and GST pull down experiments. Sun1 is a novel NE protein with three transmembrane domains in the middle. The C-terminal end of Sun1 is homologous to the SUN domain, which derives its name from its homology between Sad1 (*S. pombe* protein associated with the spindle pole body) (Iain and Mitsuhiro, 1995) and UNC-84 (*C. elegans* orthologue of Sun1) (Malone et al., 1999). The SUN domain of Sun1 is however not engaged in the binding of Enaptin. Instead, the interaction site is located in a region neighboring the SUN domain.

A dominant negative version of Sun1 (GFP-CT+3TM), which displaces endogenous Sun1 from the NE also displaces NUANCE and emerin, a protein located in the inner nuclear membrane, underlining the fact that NUANCE localisation to the NE is also Sun1 dependent. Further experiments were directed at the identification of the site of location of Sun1 employing expression of GFP-tagged Sun1 as well as antibodies generated against the N- and C-terminus of Sun1. Immunofluorescence studies performed after digitonin permeabilisation finally located the protein at the inner nuclear membrane. In further experiments we analysed the requirements for the nuclear envelope localisation of Sun1. The results point to interactions with different proteins of the NE and also to the importance of the coiled coil domain.

ZUSAMMENFASSUNG

Der Zellkern ist beweglich innerhalb einer Zelle und Kernbewegungsprozesse sind essentielle Ereignisse sowohl in Entwicklungsprozssen als auch im normalen Leben einer Zelle. Diese Beweglichkeit wird ermöglicht durch das Mikrotubuli- und, wie neuere Ergebnisse zeigen, auch durch das Aktin-Netzwerk. Wir haben mit Enaptin ein neuartiges Protein beschrieben, das eine Verbindung zwischen Zellkern und Aktinnetzwerk herstellen kann. Enaptin, ein Protein mit einem Molekulargewicht von bis zu 1.000.000 D, besitzt eine Aktinbindedomäne, einen langen helikalen Bereich und eine C-terminale Transmembrandomäne, mit der es in der Kernmembran verankert ist. In Westernblotexperimenten konnte ein 400.000 D Protein in Zellinien nachgewiesen werden und ein 165.000 D Protein in Maushirn.

Unsere weiteren Untersuchungen haben sich auf Bedeutung der C-terminalen 30 Aminosäuren für die Lokalisation konzentriert, die der Transmembrandomäne folgen. Ein ähnlicher Bereich ist im verwandten Kernmembranprotein NUANCE vorhanden sowie in weiteren Proteinen der Kernmembran, die in verschiedenen Organismen identifiziert wurden. Diese Aminosäuren sind für die Bindung an den C-Terminus des Sun1-Proteins verantwortlich. Sun1 ist ein neuartiges Kernmembranprotein, das drei in der Mitte des Proteins liegende Transmembrandomänen besitzt. Der C-Terminus von Sun1 ist homolog zur SUN-Domäne, die ihren Namen auf Grund der Homologie zu Sad1 (*S. pombe* protein associated with the spindle pole body, Iain and Mitsuhiro, 1995) und UNC-84 (*C. elegans* orthologue of Sun1, Malone et al., 1999) erhalten hat. Die SUN-Domäne ist jedoch nicht in die Bindung von Enaptin involviert, sondern eine benachbarte Region.

In weiteren Untersuchungen wurde mit Hilfe von GFP-Fusionsproteinen und mit Immunfluoreszenzanalysen die Lokalisation von Sun1 in der Kernmembran analysiert. Die Ergebnisse verweisen auf die Bedeutung des helikalen Bereichs und auf die Assoziation mit weiteren Proteinen und deuten auf komplexe Interaktionen in derKernmembran.

Bibliography

7 BIBLIOGRAPHY

Ahn, A.H. and Kunkel, L.M. (1993) The structural and functional diversity of dystrophin. *Nat. Genet.* **3**, 283-291.

Andrä, K., Lassmann, H., Bittner, R., Shorny, S., Fassler, R., Propst, F. and Wiche, G. (1997) Targeted inactivation of plectin reveals essential function in maintaining the integrity of skin, muscle, and heart cytoarchitecture. *Genes Dev.* **11**, 3143-3156.

Aoki, K., Ishida, R. and Kasai, M. (1997) Isolation and characterization of a cDNA encoding a Translin-like protein, TRAX. *FEBS Lett*. 401, 109-112.
Apel, E,D., Lewis, R.M., Grady, R.M. and Sanes, J.R. (2000) Syne-1, a dystrophin- and Klarsicht-related protein associated with synaptic nuclei at the neuromuscular junction. *J. Biol. Chem.* 275, 31986-31995.

Bachs, O., Lanini, L., Serratosa, J, Coll, M.J., Bastos R., Aligue, R., Rius, E., and Carafoli, E. (1990) Calmodulin-binding proteins in the nuclei of quiescent and proliferatively activated rat liver cells. *J .Biol. Chem.* **265,** 18595-18600.

Berger, R., Theodor, L., Shoham, J., Gokkel, E., Brok-Simoni, F., Avraham, K.B., Copeland, N.G., Jenkins, N.A., Rechavi, G. and Simon, A.J. (1996) The characterization and localization of the mouse thymopoietin/lamina-associated polypeptide 2 gene and its alternatively spliced products. *Genome Res.* **6,** 361-370.

Bernier, G., De Repentigny, Y., Mathieu, M., David, S. and Kothary, R. (1998) Dystonin is an essential component of the Schwann cell cytoskeleton at the time of myelination. *Development.* **125,** 2135-2148.

Bione, S., Maestrini, E., Rivella, S., Mancini, M., Regis, S., Romeo, G. and Toniolo, D. (1994) Identification of a novel X-linked gene responsible for Emery-Dreifuss muscular dystrophy. *Nat. Genet.* 8, 323-327.

Bloom, K. (2001) Nuclear migration: cortical anchors for cytoplasmic dynein. *Curr. Biol.* **11,** R326 -R329.

Bray, J.D., Chennathukuzhi, V.M. and Hecht, N.B. (2002) Identification and characterization of cDNAs encoding four novel proteins that interact with translin associated factor-X. *Genomics.* **79,** 799-808.

Brown, A., Bernier, G., Mathieu, M., Rossant, J. and Kothary, R. (1995) The mouse dystonia musculorum gene is a neural isoform of bullous pemphigoid antigen 1. *Nat. Genet*. **10**, 301-306.

Burgess, R.W., Nguyen, Q.T., Son, Y.J., Lichtman, J.W. and Sanes, J.R. (1999) Alternatively spliced isoforms of nerve- and muscle-derived agrin: their roles at the neuromuscular junction. *Neuron.* **23,** 33-44.

Campbell, K.P. and Kahl, S.D. Association of dystrophin and an integral membrane glycoprotein. *Nature.* **338,** 259-262.

Castresana, J. and Saraste, M. (1995) Does Vav bind to F-actin through a CH domain? *FEBS Lett.* **374,** 149-151.

Chytilova, E., Macas, J., Sliwinska, E., Rafelski, S.M., Lambert, G.M. and Galbraith, D.W. (2000) Nuclear dynamics in Arabidopsis thaliana. *Mol. Biol. Cell.* **11,** 2733 –11,2741.

Clements, L., Manilal, S., Love, D.R. and Morris, G.E. (2000) Direct interaction between emerin and lamin A. *Biochem. Biophys. Res. Commun.* **267,** 709-714.

Cohen, M., Lee, K.K., Wilson, K.L. and Gruenbaum, Y. (2001) Transcriptional repression, apoptosis, human disease and the functional evolution of the nuclear lamina. *Trends Biochem. Sci.* **26,** 41-47.

Corpet, F. (1988) Multiple sequence alignment with hierarchical clustering. *Nucl. Acids. Res.* **16,** 10881-10890.

Correas, I. (1991) Characterization of isoforms of protein 4.1 present in the nucleus. *Biochem. J.* **279,** 581-585.

Dalpe, G., Leclerc, N., Vallee, A., Messer, A., Mathieu, M., De Repentigny, Y. and Kothary, R. (1998) Dystonin is essential for eaintaining neuronal cytoskeleton organization. *Mol. Cell. Neurosci.* **10,** 243-257.

Davis, S., Lu, M.L., Lo, S.H., Lin, S., Butler, J.A., Drucker, B.J., Roberts, T.M., An, Q. and Chen,L.B. (1991) Presence of an SH2 domain in the actin-binding protein tensin. *Science.* **252,** 712-715.

De Carcer, G., Lallena, M.J. and Correas, I. (1995) Protein 4.1 is a component of the nuclear matrix of mammalian cells. *Biochem. J.* **312,** 871-877.

De Sandre-Giovannoli, A., Chaouch, M., Kozlov, S., Vallat, J.M., Tazir, M., Kassouri, N., Szepetowski, P., Hammadouche, T., Vandenberghe, A., Stewart, C.L., Grid, D. and Levy N. (2002) Homozygous defects in LMNA, encoding lamin A/C nuclear-envelope proteins, cause autosomal recessive axonal neuropathy in human (Charcot-Marie-Tooth disorder type 2) and mouse. *Am. J. Hum .Genet.* **70,** 726-736.

Dechat, T., Vlcek, S. and Foisner, R. (2000) Review: lamina-associated polypeptide 2 isoforms and related proteins in cell cycle-dependent nuclear structure dynamics. *J. Struct. Biol.* **129**, 335-345.

Dechat, T., Korbei, B., Vaughan, O.A., Vlcek, S., Hutchison, C.J. and Foisner, R. (2000) Lamina-associated polypeptide 2alpha binds intranuclear A-type lamins. *J. Cell Sci.* **113,** 3473-3484.

Demma, M., Warren, V., Hock, R., Dharmawardhane, S. and Condeelis, Y. (1990) Isolation of an abundant 50,000-Dalton actin filament bundling protein from *Dictyostelium* amoebae. *J. Biol. Chem.* **265**, 2286-2291.

Djinovic-Carugo, K., Gautel, M., Ylanne, J. and Young P. (2002) The spectrin repeat: a structural platform for cytoskeletal protein assemblies. *FEBS Lett.* **513,** 119-123.

Fan, J. and Beck, K.A. (2004) A role for the spectrin superfamily member Syne-1 and kinesin II in cytokinesis. *J. Cell Sci*. **117**, 619-629.

Fatkin, D., MacRae, C., Sasaki, T., Wolff, M.R., Porcu, M., Frenneaux, M., Atherton, J., Vidaillet, H.J. Jr., Spudich, S., De Girolami, U., Seidman, J.G., Seidman, C., Muntoni, F., Muehle, G., Johnson, W. and McDonough B. (1999) Missense mutations in the rod domain of the lamin A/C gene as causes of dilated cardiomyopathy and conduction-system disease. *N. Engl. J. Med.* **341,** 1715-1724.

Fisher, D.Z., Chaudhary, N. and Blobel, G. (1986) cDNA sequencing of nuclear lamins A and C reveals primary and secondary structural homology to intermediate filament proteins. *Proc. Natl. Acad. Sci.* U S A. **83,** 6450-6454.

Foisner, R. and Gerace, L. (1993) Integral membrane proteins of the nuclear envelope interact with lamins and chromosomes, and binding is modulated by mitotic phosphorylation. *Cell.* **73,** 1267-1279.

Fowler, V.M., Sussman, M.A., Miller, P.G., Flucher, B.E. and Daniels, M.P. (1993) Tropomodulin is associated with the free (pointed) ends of the thin filaments in rat skeletal muscle. *J. Cell Biol.* **120,** 411-420.

Funayama, N., Nagafuchi, A., Sato, N., Tsukita, S. and Tsukita, S. (1991) Radixin is a novel member of the band 4.1 family. *J. Cell Biol.* **115,** 1039-1048.

Furukawa, K. and Hotta, Y. (1993) cDNA cloning of a germ cell specific lamin B3 from mouse spermatocytes and analysis of its function by ectopic expression in somatic cells. *EMBO J.* **12,** 97-106.

Furukawa, K., Pante, N., Aebi, U. and Gerace, L. (1995) Cloning of a cDNA for lamina-associated polypeptide 2 (LAP2) and identification of regions that specify targeting to the nuclear envelope. *EMBO J.* **14,** 1626-1636.

Furukawa, K., Fritze, C.E. and Gerace, L. (1998) The major nuclear envelope targeting domain of LAP2 coincides with its lamin binding region but is distinct from its chromatin interaction domain. *J. Biol. Chem.* **273,** 4213-4219.

Gant, T.M., Harris, C.A. and Wilson, K.L. (1999) Roles of LAP2 proteins in nuclear assembly and DNA replication: truncated LAP2beta proteins alter lamina assembly, envelope formation, nuclear size, and DNA replication efficiency in Xenopus laevis extracts. *J. Cell Biol.* **144,** 1083-1096.

Gautam, M., Noakes, P.G., Moscoso, L., Rupp, F, Scheller, R.H., Merlie, J.P. and Sanes, J.R. (1996) Defective neuromuscular synaptogenesis in agrin-deficient mutant mice. *Cell.* **85,** 525-535.

Gimona, M. and Winder, S.J. (1998) Single calponin homology domains are not actin-binding domains. *Curr. Biol.* **8,** R674-R675.

Gough, L.L., Fan, J., Chu S., Winnick, S. and Beck, K.A. (2003) Golgi localization of Syne-1. *Mol. Biol. Cell.* **14**, 2410-2424.

Greenfield, N.J., Swapna, G.V., Huang, Y., Palm, T., Graboski, S., Montelione, G.T. and Hitchcock-DeGregori, S.E. (2003) The structure of the carboxyl terminus of striated alpha-tropomyosin in solution reveals an unusual parallel arrangement of interacting alpha-helices. *Biochemistry.* **42,** 614-619.

Guild, G.M., Connelly, P.S., Shaw, M.K. and Tilney, L.G. (1997) Actin filament cables in *Drosophila* nurse cells are composed of modules that slide passively past one another during dumping. *J. Cell Biol.* **138,** 783 -797.

H., Brabant, G., Kumar, S., Durrington, P.N., Gregory, S., O'Rahilly, S. and Trembath RC. (2000) LMNA, encoding lamin A/C, is mutated in partial lipodystrophy. *Nat. Genet*. **24,** 153-156.

Hagan, I. and Yanagida, M. (1995) The product of the spindle formation gene sad1+ associates with the fission yeast spindle pole body and is essential for viability. *J. Cell Biol.* **129,** 1033-1047.

Han, J.R., Yiu, G.K. and Hecht, N.B. (1995) Testis/brain RNA-binding protein attaches translationally repressed and transported mRNAs to microtubules. *Proc. Natl. Acad. Sci*. USA. **92**, 9550-9554.

Harborth, J., Weber, K. and Osborn, M. (2000) GAS41, a highly conserved protein in eukaryotic nuclei, binds to NuMA. *J. Biol. Chem.* **275,** 31979-31985.

Harriman, D.G.F. and Millar, J.H.D. (1955) Progressive familial myoclonic epilepsy in 3 families: its clinical features and pathological basis. *Brain.* **78**, 325-349.

Harris, C.A., Andryuk, P.J., Cline, S., Chan, H.K., Natarajan, A., Siekierka, J.J. and Goldstein, G. (1994) Three distinct human thymopoietins are derived from alternatively spliced mRNAs. *Proc. Natl. Acad. Sci.* U S A. **91**, 6283-6287.

Hepler,P.K., Vidali,L. and Cheung,A.Y. (2001) Polarized cell growth in higher plants. Annu. Rev. Cell Dev. Biol. 17, 159 -187.

Hinshaw, J.E., Carragher, B.O. and Milligan, R.A. (1992) Architecture and design of the nuclear pore complex. *Cell.* **69,** 1133-1141.

Hodzic, D.M., Yeater, D.B., Bengtsson, L., Otto, H. and Stahl, P.D. (2004) Sun2 is a novel mammalian inner nuclear membrane protein. *J. Biol. Chem.* Apr 12 [Epub ahead of print]

Höger, T.H., Krohne, G. and Franke, W.W. (1988) Amino acid sequence and molecular characterization of murine lamin B as deduced from cDNA clones. *Eur. J. Cell Biol.* **47**, 283-290.

Höger, T.H., Zatloukal, K., Waizenegger, I. and Krohne, G. (1990) Characterization of a second highly conserved B-type lamin present in cells previously thought to contain only a single B-type lamin. *Chromosoma.* **99**, 379-390.

Bibliography

Hutchison, C.J., Alvarez-Reyes, M. and Vaughan, O.A. (2001) Lamins in disease: why do ubiquitously expressed nuclear envelope proteins give rise to tissue-specific disease phenotypes? *J. Cell Sci.* **114,** 9-19.
Izumi, M., Vaughan, O.A., Hutchison, C.J. and Gilbert, D.M. (2000) Head and/or CaaX domain deletions of lamin proteins disrupt preformed lamin A and C but not lamin B structure in mammalian cells. *Mol. Biol. Cell*. **11,** 4323-4337.

Jackle, H. and Jahn, R. (1998) Vesicle transport: klarsicht clears up the matter. *Curr. Biol.* **8,** R542-R544.

Kozak, M. (1986) Point mutations define a sequence flanking the AUG initiator codon that modulates translation by eukaryotic ribosomes. *Cell.* **44,** 283-292.

Lallena, M.J., Martinez, C., Valcarcel, J. and Correas, I. (1998) Functional association of nuclear protein 4.1 with pre-mRNA splicing factors. *J. Cell Sci.* **111,** 1963-1971.

Lambert de Rouvroit, C. and Goffinet, A.M. (2001) Neuronal migration. *Mech. Dev.* **105**, 47-56.

Lang, C., Paulin-Levasseur, M., Gajewski, A., Alsheimer, M., Benavente, R. and Krohne, G. (1999) Molecular characterization and developmentally regulated expression of Xenopus lamina-associated polypeptide 2 (XLAP2). *J. Cell Sci.* **112**, 749-759.

Lee, K.K., Starr, D., Cohen, M., Liu, J., Han, M., Wilson, K.L. and Gruenbaum, Y. (2002) Lamin-dependent localization of UNC-84, a protein required for nuclear migration in Caenorhabditis elegans. Mol. Biol. *Cell.* **13,** 892-901

Leung, C.L., Sun, D., Zheng, M., Knowles, D.R. and Liem, R.K. (1999) Microtubule actin cross-linking factor (MACF): a hybrid of dystonin and dystrophin that can interact with the actin and microtubule cytoskeletons. *J. Cell Biol.* **147,** 1275-1286.

Lin, F., Blake, D.L., Callebaut, I., Skerjanc,I .S., Holmer, L., McBurney, M.W., Paulin-Levasseur, M. and Worman, H.J. (2000) MAN1, an inner nuclear membrane protein that shares the LEM domain with lamina-associated polypeptide 2 and emerin. *J. Biol. Chem.* **275**, 4840-4847.

Liu, X., Ouyang, Q., Huang, L., Ma, H., Hu, R. and Zhang, Y. (2000) Isolation and phenotypic analysis of lamina propria mononuclear cells from colonoscopic biopsy specimens. *Hua Xi Yi Ke Da Xue Xue Bao*. **31,** 116-8.

Malnasi-Csizmadia, A., Shimony, E., Hegyi, G., Szent-Gyorgyi, A.G. and Nyitray, L. (1998) Dimerization of the head-rod junction of scallop myosin. *Biochem. Biophys. Res. Commun.* **252,**595-601.

Malone, C.J., Fixsen, W.D., Horvitz, H.R. and Han, M. (1999) UNC-84 localizes to the nuclear envelope and is required for nuclear migration and anchoring during C. elegans development. *Development.* **126**, 3171-3181.

Malone,C.J., Misner,L., Le Bot,N., Tsai,M.C., Campbell,J.M., Ahringer,J. and White JG. (2003) The C. elegans hook protein, ZYG-12, mediates the essential attachment between the centrosome and nucleus. Cell. 115, 825-836.

Manilal, S., Nguyen, T.M., Sewry, C.A. and Morris, G.E. (1996) The Emery-Dreifuss muscular dystrophy protein, emerin, is a nuclear membrane protein. *Hum. Mol. Genet.* **5,** 801-808.

Martin, L., Crimaudo, C. and Gerace, L. (1995) cDNA cloning and characterization of lamina-associated polypeptide 1C (LAP1C), an integral protein of the inner nuclear membrane. *J. Biol. Chem.* **270**, 8822-8828.

Matsudaira, P. (1991) Modular organization of actin crosslinking proteins. *Trends Biochem. Sci.* **16,** 87-92.

McLean, W.H., Pulkkinen, L., Smith, F.J., Rugg, E.L., Lane, E.B., Bullrich, F., Burgeson, R.E., Amano,S., Hudson, D.L., Owaribe, K., McGrath, J.A., McMillan, J.R., Eady, R.A., Leigh, I.M., Christiano, A.M. and Uitto, J. (1996) Loss of plectin causes epidermolysis bullosa with muscular dystrophy: cDNA cloning and genomic organization. *Genes.Dev.* **10,** 1724-1735.

McMahan, U.J. (1990) The agrin hypothesis. Cold. Spring. *Harb. Symp. Quant. Biol.* **55,** 407-418.

McMahan, U.J. (1990) The agrin hypothesis. *Cold Spring Harb. Symp. Quant. Biol.* **55,** 407-418.

Mislow, J.M., Holaska, J.M., Kim, M.S., Lee, K.K., Segura-Totten, M., Wilson, K.L. and McNally, EM. (2002) Nesprin-1alpha self-associates and binds directly to emerin and lamin A in vitro. *FEBS Lett.* **525,** 135-140.

Mislow, J.M., Kim, M.S., Davis, D.B. and McNally, E.M. (2002) Myne-1, a spectrin repeat transmembrane protein of the myocyte inner nuclear membrane, interacts with lamin A/C. *J. Cell Sci.* **115**, 61-70.

Moir, R.D., Spann, T.P. and Goldman, R.D. (1995) The dynamic properties and possible functions of nuclear lamins. *Int. Rev. Cytol.* **162**, 141-182.

Morris, N.R. (2000) Nuclear migration. From fungi to the mammalian brain. *J. Cell Biol.* **148**, 1097 -1101.

Moser, H. (1984) Duchenne muscular dystrophy: pathogenetic aspects and genetic prevention. *Hum. Genet.* **66**, 17-40.

Mosley-Bishop, K.L., Li, Q., Patterson, L. and Fischer, J.A. (1999) Molecular analysis of the klarsicht gene and its role in nuclear migration within differentiating cells of the Drosophila eye. *Curr. Biol*. **9,** 1211-1220.

Muchir, A., van Engelen, B.G., Lammens, M., Mislow, J.M., McNally, E., Schwartz, K. and Bonne, G. Nuclear envelope alterations in fibroblasts from LGMD1B patients carrying nonsense Y259X heterozygous or homozygous mutation in lamin A/C gene. *Exp. Cell. Res.* **291**, 352-362.

Bibliography

Namba, Y., Ito, M., Shigesada, K. and Maruyama, K. (1992) Human T-cell L-plastin bundles actin filaments in a calcium-dependent manner. *J. Biochem.* **112,** 503-507.
Nedivi, E., Fieldust, S., Theill, L.E. and Hevron, D. (1996) A set of genes expressed in response to light in the adult cerebral cortex and regulated during development. *Proc. Natl. Acad. Sci.* **93,** 2048-2053.

Palek, J. (1987) Hereditary elliptocytosis, spherocytosis and related disorders: consequences of a deficiency or a mutation of membrane skeletal proteins. *Blood Rev.* **1,** 147-168.

Palmer, R.E., Sullivan, D.S., Huffaker, T. and Koshland, D. (1992) Role of astral microtubules and actin in spindle orientation and migration in the budding yeast, *Saccharomyces cerevisiae. J. Cell Biol.* **119**, 583 –593.

Patterson, K., Molofsky, A.B., Robinson, C., Acosta, S., Cater, C. and Fischer, J.A. (2004) The functions of Klarsicht and nuclear lamin in developmentally regulated nuclear migrations of photoreceptor cells in the Drosophila eye. *Mol. Biol. Cell.* **15,** 600-610.

Peter, M., Kitten, G.T., Lehner, C.F., Vorburger, K., Bailer, S.M., Maridor, G. and Nigg, E.A. (1989) Cloning and sequencing of cDNA clones encoding chicken lamins A and B1 and comparison of the primary structures of vertebrate A- and B-type lamins. *J. Mol. Biol.* **208,** 393-404.

Petrof, B.J., Shrager, J.B., Stedman, H.H., Kelly, A.M. and Sweeney, H.L. (1993) Dystrophin protects the sarcolemma from stresses developed during muscle contraction. *Proc. Natl. Acad. Sci.* U S A. **90**, 3710-3714.

Podolski, J.L. and Steck, T.L. (1988) Association of deoxyribonuclease I with the pointed ends of actin filaments in human red blood cell membrane skeletons. *J. Biol. Chem.* **263,** 638.645.

Powell, L. and Burke, B. (1990) Internuclear exchange of an inner nuclear membrane protein (p55) in heterokaryons: in vivo evidence for the interaction of p55 with the nuclear lamina. *J. Cell Biol.* **111,** 2225-2234.

Rando, T.A. (2001) The dystrophin-glycoprotein complex, cellular signaling, and the regulation of cell survival in the muscular dystrophies. *Muscle Nerve.* **24,** 1575-1594.

Rivero, F., Kuspa, A., Brokamp, R., Matzner, M. and Noegel, A.A. (1998) Interaptin, an actin-binding protein of the alpha-actinin superfamily in Dictyostelium discoideum, is developmentally and cAMP-regulated and associates with intracellular membrane compartments. *J. Cell Biol*. **142,** 735-750.

Ruhrberg, C. and Watt, F.M. (1997) The plakin family: versatile organizers of cytoskeletal architecture. *Curr. Opin. Genet. Dev*. **7,** 392-397.

Rybakova, I.N., Patel, J.R., Davies, K.E., Yurchenco, P.D. and Ervasti, J.M. (2002) Utrophin binds laterally along actin filaments and can couple costameric actin with sarcolemma when overexpressed in dystrophin-deficient muscle. *Mol. Biol. Cell*. **13,** 1512-1521.

Shackleton, S., Lloyd, D.J., Jackson, S.N., Evans, R., Niermeijer, M.F., Singh, B.M., Schmidt, H., Brabant, G., Kumar, S., Durrington, P.N., Gregory, S., O'Rahilly, S. and

Trembath, R.C. (2000) LMNA, encoding lamin A/C, is mutated in partial lipodystrophy. *Nat. Genet*. **24,** 153-156.

Southwick, F.S. and Young, C.L. (1990) The actin released from profilin-actin complexes is insufficient to account for the increase in F-actin in chemoattractant-stimulated polymorphonuclear leukocytes. *J. Cell Biol.* **110,** 1965-1973.

Shumaker, D.K., Lee, K.K., Tanhehco, Y.C., Craigie, R. and Wilson, K.L. (2001) LAP2 binds to BAF.DNA complexes: requirement for the LEM domain and modulation by variable regions. *EMBO J.* **20,** 1754-1764.

Simos, G. and Georgatos, S.D. (1992) The inner nuclear membrane protein p58 associates in vivo with a p58 kinase and the nuclear lamins. *EMBO J.* **11**, 4027-4036.

Starr, D.A., Hermann, G.J., Malone, C.J., Fixsen, W., Priess, J.R., Horvitz, H.R. and Han, M. (2001) unc-83 encodes a novel component of the nuclear envelope and is essential for proper nuclear migration. *Development.* **128,** 5039-5050.

Starr, D.A. and Han, M. (2001) Role of ANC-1 in tethering nuclei to the actin cytoskeleton. *Science*. **298,** 406-409.

Straub, V. and Campbell, K.P. (1997) Muscular dystrophies and the dystrophin-glycoprotein complex. *Curr. Opin. Neurol.* **10,** 168-175.

Stuurman, N., Heins, S. and Aebi, U. (1998) Nuclear lamins: their structure, assembly, and interactions. *J. Struct. Biol*. **122**, 42-66.

Sullivan, T., Escalante-Alcalde, D., Bhatt, H., Anver, M., Bhat, N., Nagashima, K., Stewart, C.L. and Burke, B. (1999) Loss of A-type lamin expression compromises nuclear envelope integrity leading to muscular dystrophy. *J. Cell Biol*. **147,** 913-920.

Sulston, J.E., Schierenberg, E., White, J.G. and Thomson, J.N. (1983) The embryonic cell lineage of the nematode *Caenorhabditis elegans. Dev. Biol.* **100**, 64 -119.

Südhof, T.C., Czernik, A.J., Kao, H.T., Takei, K., Johnston, P.A., Horiuchi, A., kanazir, S.D., Wagner, M.A., Perin, M.S., De Camilli, P. and Greengard, P. (1989) Synapsins: Mosaics of shared and individual domains in a family of synaptic vesicle phosphoproteins. *Science.* **245,** 1474-1480.

Tran, P.T., Marsh, L., Doye, V., Inoue, S. and Chang, F. (2001) A mechanism for nuclear positioning in fission yeast based on microtubule pushing. *J. Cell Biol.* **153,** 397 -411

Valenzuela, D.M., Stitt, T.N., DiStefano, P.S., Rojas, E., Mattsson, K., Compton, D.L., Nunez, L., Park, J.S., Stark, J.L., Gies, D.R., et al. (1995) Receptor tyrosine kinase specific for the skeletal muscle lineage: expression in embryonic muscle, at the neuromuscular junction, and after injury. *Neuron.* **15,** 573-584.

van der Flier, A. and Sonnenberg, A. (2001) Function and interactions of integrins. *Cell Tissue Res.* **305**, 285-298.

Vandekerckhove, J. and Weber, K. (1979) The complete amino acid sequence of actins from

bovine aorta, bovine heart, bovine fast skeletal muscle, and rabbit slow skeletal muscle. A protein-chemical analysis of muscle actin differentiation. *Differentiation.* **14**, 123-133.

Van Etten, R.A., Jackson, P.K., Baltimore, D., Sanders, M.C., Matsudaira, P.T. and Janmey, P.A. (1994) The COOH terminus of the c-Abl tyrosine kinase contains distinct F- and G-actin binding domains with bundling activity. *J. Cell Biol*. **124**, 325-340.

Vigers, G.P. and Lohka, M.J. (1991) A distinct vesicle population targets membranes and pore complexes to the nuclear envelope in Xenopus eggs. *J.Cell Biol.* **112**, 545-556.

Vlcek, S., Dechat, T. and Foisner, R. (2001) Nuclear envelope and nuclear matrix: interactions and dynamics. Cell. Mol. Life Sci. 58, 1758-1765.

Vorburger., K, Lehner, C.F., Kitten, G.T., Eppenberger, H.M. and Nigg, E.A. (1989) A second higher vertebrate B-type lamin. cDNA sequence determination and in vitro processing of chicken lamin B2. *J. Mol. Biol.* **208,** 405-415.

Way, M., Pope, B. and Weeds, A.G. (1992) Evidence for functional homology in the F-actin binding domains of gelsolin and alpha-actinin: implications for the requirements of severing and capping. *J. Cell. Biol.* **119**, 835-842.

Way, M., Pope, B., Cross, R.A., Kendrick-Jones, J. and Weeds, A.G. (1992) Expression of the N-terminal domain of dystrophin in E. coli and demonstration of binding to F-actin. *FEBS Lett.* **301,** 243-245.

Weeds, A.G. and Maciver, S.K. (1993) F-actin capping proteins. *Curr. Oppin. Cell Biol.* **5,** 63-69.

Wiche, G. (1998) Role of plectin in cytoskeleton organization and dynamics. *J. Cell Sci.* **111,** 2477-2486.

Wilson, K.L., Zastrow, M.S. and Lee, K.K. (2001) Lamins and disease: insights into nuclear infrastructure. *Cell.* **104,** 647-650.

Winder, S.J., Hemmings, L., Maciver, S.K., Bolton, S.J., Tinsley, J.M., Davies, K.E., Critchley, D.R. and Kendrick-Jones, J. (1995) Utrophin actin binding domain: analysis of actin binding and cellular targeting. *J. Cell Sci.* **108,** 63-71.

Wolf, E., Kim, P.S. and Berger, B. (1997) MultiCoil: a program for predicting two- and three-stranded coiled coils. *Protein Sci*. **6,** 1179-1189.

Worman, H.J. and Courvalin, J.C. (2000) The inner nuclear membrane. *J. Membr. Biol.* **177,** 1-11.

Worman, H.J., Evans, C.D. and Blobel, G. (1990) The lamin B receptor of the nuclear envelope inner membrane: a polytopic protein with eight potential transmembrane domains. *J. Cell Biol.* **111,** 1535-1542.

Ye, Q. and Worman, H.J. (1994) Primary structure analysis and lamin B and DNA binding of human LBR, an integral protein of the nuclear envelope inner membrane. *J. Biol. Chem*. **269,** 11306-11311.

Yin, H.L. (1988) Gelsolin: Calcium and polyphosphoinositide-regulated actin modulating protein. *Bioessays.* **7,** 176-179.

Zhang, Q., Ragnauth, C., Greener, M.J., Shanahan, C.M. and Roberts, R.G. (2002) The nesprins are giant actin-binding proteins, orthologous to Drosophila melanogaster muscle protein MSP-300. *Genomics.* **80,** 473-481.

Zhang, Q., Skepper, J.N., Yang, F., Davies, J.D., Hegyi. L., Roberts, R.G., Weissberg, P.L., Ellis, J.A. and Shanahan, CM. (2001) Nesprins: a novel family of spectrin-repeat-containing proteins that localize to the nuclear membrane in multiple tissues. *J. Cell Sci.* **114,** 4485-4498.

Zhen, Y.Y., Libotte, T., Munck, M., Noegel, A.A. and Korenbaum, E. (2002) NUANCE, a giant protein connecting the nucleus and actin cytoskeleton. *J. Cell Sci.* **115,** 3207-3222.

Erklärung

Ich versichere, dass ich die von mir vorgelegte Dissertation selbständig angefertigt, die benutzten Quellen und Hilfsmittel vollständig angegeben und die Stellen der Arbeit- einschließlich Tabellen und Abbildungen-, die anderen Werke im Wortlaut oder dem Sinn nach entnommen sind, in jedem Einzelfall als Entlehnung kenntlich gemacht habe; dass diese Dissertation noch keiner anderen Fakultät oder Universität zur Prüfung vorgelegen hat; dass sie- abgesehen von unten angegebenen beantragten Teilpublikationen- noch nicht veröffentlicht ist, sowie, dass ich eine Veröffentlichung vor Abschluss des Promotionsverfahrens nicht vornehmen werde. Die Bestimmungen dieser Promotionsordnung sind mir bekannt. Die von mir vorgelegte Dissertation ist von Frau Prof. Dr. Angelika A. Noegel betreut worden.

Köln den

Padmakumar V.C.

Teilpublicatione:

Padmakumar, V.C, Abraham, S, Braune, S, Noegel, A.A, Tunggal, B, Karakesisoglou, I. and Korenbaum, E. (2004) Enaptin, a giant actin-binding protein, is an element of the nuclear membrane and the actin cytoskeleton. *Exp. Cell Res.* **295 (2):** 330-339.

Curriculum Vitae

Name	:	Padmakumar Velayuthan Chellammal
Address	:	Luxemburger Str, 124-136, Unicenter, Et-Zi:12-23, 50939, Köln, Deutschland.
Home address	:	III/31, Christopher Nagar, Nagercoil, India, 629 201. E-mail: vcpadmakumar@rediffmail.com
Date of Birth	:	31.07.1977
Nationality	:	Indian

School studies

1982-1990	:	Government High School, Chothavilai, India.
1990-1994	:	SMRV Higher Secondary School, Nagercoil, India.

University studies

1994-1997	:	Bachelor of Science (Biochemistry), Vel's College of Science, Chennai, India.
1997-1999	:	Master of Science (Biochemistry) Department of Biochemistry and Molecular Biology, University of Madras, Chennai, India.

Doctoral studies

08.2001-07.2004	:	Faculty of Mathematics and Natural Science, University of Cologne, Supervisor: Prof. Dr. Angelika A. Noegel, Group leader: Dr. Iakowos Karakesisoglou, Institure for Biochemistry I, Medical Faculty, University of Cologne, Cologne, Germany.

LEBENSLAUF

Name	:	Padmakumar Velayuthan Chellammal
Addresse	:	Luxemburger Str, 124-136, Unicenter, Et-Zi:12-23, 50939, Köln, Deutschland.
Heimataddresse	:	III/31, Christopher Nagar, Nagercoil, India, 629 201. E-mail: vcpadmakumar@rediffmail.com
Geburtsdatum	:	31.07.1977
Staatsangehörigkeit	:	Indisch

Schulausbildung

1982-1990	:	Government High School, Chothavilai, Indien.
1990-1994	:	SMRV Higher Secondary School, Nagercoil, Indien.

Universität Studium

1994-1997	:	Bachelor of Science (Biochemistry) Vel's College of Science, Chennai, Indien.
1997-1999	:	Master of Science (Biochemistry) Department of Biochemistry and Molecular Biology, University of Madras, Chennai, Indien.

Promotions Studium

08.2001-07.2004	:	Mathematisch-Naturwissenschaftliche Fakultat, Universität zu Köln, Betreurin: Prof. Dr. Angelika A. Noegel, Group leader: Dr. Iakowos Karakesisoglou, Institüt Für Biochemie I, Medizinische Fakultät, Universität zu Köln, Köln, Deutschland